New methodology to generate Floor Design Spectra (FDS) directly from Uniform Hazard Spectra (UHS) for seismic assessment of Non-structural Components (NSCs) of buildings

by

Amin Asgarian

December 2017

Department of Civil Engineering and Applied Mechanics

McGill University, Montreal

A thesis submitted to McGill University in partial fulfillment of the requirements of the degree of Doctor of Philosophy in Engineering

Abstract

Achieving global good seismic performance of a building as required in modern building codes is contingent upon maintaining the integrity and functionality of its structural system as well as its Non-Structural Components (NSCs). Experience of past earthquakes has shown that many buildings have suffered from the failure of NSCs which caused life safety hazards, costly property damages, and significantly impacted the building functionality while their structural systems have performed satisfactorily. Avoiding these undesired consequences is of tremendous importance particularly in post-disaster buildings that must remain operational during and after earthquakes. That is why the rational assessment of seismic performance of NSCs has been the focus of many researchers during the last few decades with a focus on performance. Most recent editions of building codes incorporate empirical equations for seismic design of NSCs which are, for the most part, based on past experience and engineering judgment, rather than on objective experimental and analytical results. The lack of significant advances in design code provisions may be attributed partly to the fact that the previously developed analytical methods are too cumbersome to be employed in the design of ordinary NSCs (and their connections) housed in conventional buildings.

As an effective solution to these problems, an original approach is developed and introduced in this thesis to generate Floor Design Spectra (FDS) directly from Uniform Hazard Spectra (UHS) specified in building codes. Generated FDS play the same role as UHS for structural components and can be used as a simple, fast, and reliable tool for seismic assessment and analysis of NSCs particularly in existing post-critical buildings. To develop and validate the proposed method, Ambient Vibration Measurements (AVM) data pertaining to 27 existing

Reinforced Concrete (RC) buildings in have been collected and studied. The procedure has been coded in MATLAB to generate elastic Floor Response Spectrum (FRS) and inter-story drift curves at every floor of the building in both orthogonal horizontal (X and Y) directions, and considering NSCs with several damping ratios (2, 5, 10, and 20 % of critical viscous damping) having a fundamental period range of [0-4] seconds with intervals of 0.02 s. (damping ratios, period range, and intervals are user-defined in the code). The validation of the proposed method has been done through the case-study of one building from a pediatric hospital campus located in Montréal, Canada. Employing the proposed method over the entire 27-building database, approximately 132,000 FRS curves have been generated. In the first phase of the study, the generated FRS for the roof level and 5% NSC damping (ξ_{NSC}=5%) have been statistically analyzed and compared with the 5% damped UHS and a method has been proposed to generate an FDS for roof level and ξ_{NSC}=5% directly from the UHS. In the second phase of the study, the effects of the NSCs damping ratio and NSC location along the building height on the FDS have been statistically studied to extend the application of the methodology. As a result, two sets of modification factors were introduced that account for NSC damping and location effects. The extended methodology is able to produce FDS directly from UHS at any selected floor and any NSC damping ratio of interest. The methodology has been formulated for RC low and medium rise buildings and a set of equations have been recommended for each building category. When compared to the conventional FRS approach and current building code recommendations, the proposed method offers several advantages and improvements including capturing the effects of: 1- dynamic interaction between supporting system and NSCs, 2- higher and torsional modes of the building structure, 3- NSC damping . The method enables the generation of an exclusive FDS for each existing building taking its dynamic characteristics into account (as extracted from AVM records) and the acceleration design spectrum for the site. The generated FDS is a practical, accurate, and fast tool for seismic assessment and design of acceleration-sensitive NSCs particularly in post-critical buildings.

Sommaire

Les codes du bâtiment modernes comportent des exigences spécifiques quant à la résistance et à la fonctionnalité des systèmes structuraux et des éléments non-structuraux. L'expérience a démontré que plusieurs bâtiments dont la charpente a bien résisté aux séismes ont subi des dommages importants aux éléments non structuraux avec des conséquences néfastes quant à la sécurité des occupants, la valeur des pertes économiques encourues, et la non-fonctionnalité des bâtiments. Il est impératif de limiter ces conséquences néfastes en particulier pour les bâtiments désignés postcritiques (écoles, établissements hospitaliers, bâtiments de protection civile, etc.) qui doivent demeurer fonctionnels et opérationnels durant et après un séisme majeur. C'est ce qui explique en partie l'emphase sur la conception, l'évaluation et la réhabilitation parasismique des éléments non structuraux des bâtiments ces dernières décennies.

La plupart des codes du bâtiment récents proposent des équations empiriques pour le calcul des charges sismiques sur les éléments non-structuraux, basées sur la pratique et le jugement d'experts plutôt que l'étude objective des observations expérimentales et des analyses. Le manque d'avancées significatives dans les codes pour la conception parasismique des éléments non-structuraux est également en partie attribuable à la complexité des méthodes analytiques développées lesquelles ne sont pas adaptées au contexte de conception des bâtiments conventionnels.

Cette thèse propose une nouvelle approche de conception pour pallier ces problèmes avec une méthode qui permet de générer des spectres de réponse de planchers directement à partir des spectres uniformes d'aléas sismiques prescrits dans les codes du bâtiment. En fait,

ces spectres de planchers sont les outils de base pour l'analyse sismique des éléments non-structuraux au même titre que les spectres d'aléas sismiques le sont pour la structure des bâtiments. Les spectres de planchers sont un outil d'analyse simple, rapide et efficace pour évaluer la performance des éléments non-structuraux, en particulier dans les bâtiments postcritiques. La méthode proposée pour générer ces spectres de réponse est basée sur des mesures de vibrations ambiantes dont l'analyse permet d'extraire les caractéristiques dynamiques essentielles des bâtiments. Dans cette étude, 27 bâtiments à ossature en béton armé situés à Montréal ont été instrumentés et étudiés pour élaborer et valider la méthode. La procédure a été codée dans une application MATLAB qui génère les spectres de réponse élastique des planchers du bâtiment de même que les courbes de déplacements inter-étages pour chaque étage et selon deux directions horizontales principales (orthogonales). L'outil inclut également différents niveaux d'amortissement des éléments non-structuraux (2, 5, 10, et 20 % d'amortissement visqueux critique) dans la gamme de périodes naturelles variant de [0-4] secondes à intervalle de 0.02 s. La méthode est validée en détail à l'aide d'une étude de cas de un bâtiments faisant partie d'un campus hospitalier situé à Montréal, Canada.

L'application de la méthode à la base de données de mesures ambiantes des 27 bâtiments en béton armé a permis de générer un ensemble d'environ 132,000 spectres de planchers. Dans une première étape, les spectres de réponse ont été générés pour le toit du bâtiment (en fait le plancher structural le plus élevé) avec un amortissement interne du composant non-structural, ξ_{NSC}=5%. Ces spectres de réponse ont été analysés statistiquement et comparés aux spectres d'aléa sismique pour le site désigné avec amortissement structural de 5% (standard spécifié aux normes parasismiques pour les bâtiments). Dans une deuxième étape, l'analyse statistique des spectres en considérant l'effet de l'amortissement des éléments non-structuraux ainsi que leur emplacement selon les étages du bâtiment a permis d'étendre l'application de la méthode à tous les planchers du bâtiment considéré, au moyen de deux coefficients qui ajustent les valeurs du spectre du plancher le plus élevé avec amortissement de 5% aux valeurs appropriées pour l'étage et l'amortissement spécifique cu composant. Ainsi, la méthode permet de produire des spectres de réponse de planchers pour la conception parasismique des éléments non-structuraux directement à partir des spectres d'aléas sismiques spécifiés par les codes pour le site du bâtiment.

Il convient de préciser que la méthode a été développée sur la base de mesures faites sur des bâtiments à ossature en béton armé de faible et moyenne hauteur, et deux formulations sont proposées séparément pour ces deux catégories.

La méthode proposée offre plusieurs avantages techniques importants lorsque comparée aux méthodes empiriques des codes actuels. Étant basée sur la mesure de vibrations ambiantes dans les bâtiments, elle permet de tenir compte de plusieurs facteurs ignorés jusqu'à présent dans les normes, à savoir: 1- l'interaction dynamique entre la structure du bâtiment et les éléments non-structuraux; 2- l'effet des modes de vibration de plus haute fréquence, y inclus les modes de vibration en torsion du bâtiment; et 3- l'effet de l'amortissement interne des éléments non-structuraux. La méthode permet de générer des spectres de conception exclusifs pour chaque plancher d'un bâtiment existant pour lequel des mesures de vibration ambiantes ont permis d'extraire les caractéristiques dynamiques de base, et ce directement à partir du spectre d'aléa sismique spécifié au site du bâtiment. Les spectres de planchers générés constituent un outil pratique, précis et rapide pour l'évaluation et la conception parasismique d'éléments non-structuraux sensibles aux effets d’accélération, en particulier pour les bâtiments postcritiques, alors que les courbes de déplacement inter-étages conviennent particulièrement aux éléments sensibles aux déformations du bâtiment.

Statement of original contributions

To the author's best knowledge, the original contributions of this research include:

1- Developing an original method to generate Floor Design Spectra (FDS) directly from Uniform Hazard Spectra (UHS) using experimental data and Ambient Vibration Measurements (AVM) in buildings. The proposed method improves the code provisions for NSCs and the conventional analytical Floor Response Spectrum (FRS) approach by considering the effects of: 1- dynamic interaction between the building structure and NSCs on NSCs response, 2- higher frequency and torsional modes of the supporting system on NSCs response, and 3- NSCs internal damping. The proposed FDS are generated exclusively for each building taking its dynamic characteristics into account.

2- Formulating the methodology for reinforce concrete low and medium rise buildings and recommending a set of FDS equations for each building category.

3- Developing the FRS and inter-story drift curves using the experimental data recorded through ambient vibration measurements.

4- Implementation of the proposed methodology in MATLAB code for automatic generation of FRS, Inter-story drift, and FDS curves.

5- Collecting an inclusive database of the permanently-instrumented buildings comprising the results of 56 buildings and proposing a set of modification factors to modify AVM-extracted modal parameters of buildings for higher-amplitude ground motions typical of design earthquakes.

6- Collecting a database of 156 buildings, all located in Montreal and tested by AVM, from which a subset of 27 RC buildings comprising 12 low-rise, 10 medium-rise, and 5 high-rise buildings were used for the detailed study presented here.

Acknowledgments

I am grateful for the financial support provided by McGill International Doctoral Award (MIDA) and Natural Sciences and Engineering Research Council of Canada through strategic grant project STPGP-396464.

I would like to express my profound and sincere gratitude to my research advisor, Professor Ghyslaine McClure, for her continuous help and support, constant encouragement, and skilful guidance throughout this research. I am so glad to have had the opportunity to work with her.

I would like to thanks my fellow graduate students who helped me throughout the course of my graduate studies specially my colleague Dr. Farshad Mirshafiei whose helps are deeply appreciated.

At last but certainly not the least, my deepest gratitude goes to my beloved family (my spouse, Mehrnoosh, my father, Mohammad Hossein, my mother, Zahra, my brother, Ali, and my sister, Azin) for their invaluable and irreplaceable love, constant support, and all the difficulties through which they have put themselves during these years to reach me to this stage. They have been always on my side and they are the reason for who I am today and will be tomorrow.

Contribution of authors

Please note that this is a manuscript-based thesis consisting of one report, one published conference paper, and three journal manuscripts submitted to peer-reviewed journals. These papers were written in collaboration with other authors. The title of the articles, name of the authors, and the related conference papers are listed below. The author of this thesis is the sole student, among the co-authors, who was responsible for conducting the research, the in-situ inspection and AVM experiments, analyzing the data, developing the methodology, preparing the draft manuscripts and presenting the research at conferences. The author's supervisor, Prof. Ghyslaine McClure, provided invaluable guidance and editorial revisions throughout the entire process.

This thesis is comprised of the following five publications:

A. Asgarian, G. McClure. State-of-the-art review: Seismic response analysis of Operational and Functional Components (OFCs) in buildings. Montreal, Canada: McGill University; 2013. 41 p.

A. Asgarian, G. McClure. Generation of experimental floor response spectra for seismic assessment of Non-Structural Components (NSCs) based on ambient vibration measurements. Submitted to Earthquake Engineering and Structural Dynamics, EQE-18-0086 (Manuscript under review). 22 p.

A. Asgarian, F. Mirshafiei, G. McClure. Experimental floor response spectra for seismic evaluation of operational and functional components of building. Proceedings of the CSCE 2014, 4th International Structural Specialty Conference. Halifax, NS, May 28 to 312014. 10 p.

Asgarian A, McClure G. Direct generation of Floor Design Spectra (FDS) from Uniform Hazard Spectra (UHS) - Part I: Formulation of the method. Submitted to Canadian Journal of Civil Engineering, cjce-2018-0146 (Manuscript under review). 19 p.

Asgarian A, McClure G. Direct generation of Floor Design Spectra (FDS) from Uniform Hazard Spectra (UHS) - Pat II: Extension and Application of the method. Submitted to Canadian Journal of Civil Engineering, cjce-2018-0151 (Manuscript under review). 20 p.

Table of Contents

List of Figures

List of Tables

1 Introduction

1.1 Research motivations

Building components can be classified into two main types: 1- Structural components, which comprise the main load-resisting system of the building and are also called “primary system” or “supporting structure”, and 2- Non-Structural Components (NSCs), which are usually not intended to be part of the load-carrying system of the building and, hence, are called “secondary systems”. NSCs are also termed as Operational and Functional Components of buildings in Canadian Standard Association CSA-S832 [1], a more inclusive terminology that emphasizes the fact that NSCs’ damage can limit the functionality of the buildings significantly following moderate to severe seismic events. According to their main function, NSCs can be categorized into the following three sub-groups: Architectural components, Building services (mechanical, electrical, and telecommunication equipment), and Building contents (common and specialized) [1, 2]. Another classification of NSCs can be made in accordance with the nature of their seismic response sensitivity: 1- Inter-storey-drift-sensitive components, 2- Floor-acceleration-sensitive components, and 3- both inter-storey-drift- and floor-acceleration-sensitive components [3].

As mentioned above, the functionality and performance of NSCs during and after an earthquake are of great importance especially in post-disaster facilities such as hospitals, emergency shelters, for example, since their failure can considerably impair the overall building functionality, and cause risk to life safety and property damage even if the structural system has performed well during an earthquake. Indeed, the good seismic performance of NSCs is essential to achieve the life-safety performance objective that is mandatory for all buildings in Canada [4] and elsewhere. Possible adverse consequences caused by failure of NSCs during an earthquake can be associated with:

1- Life safety: Movement or failure of NSCs can become a safety hazard, directly threaten the life of building occupants or passers-by, hamper the safe movement of occupants evacuating buildings, or of rescue workers entering buildings.

2- Building functionality: Induced seismic failure or malfunction of some critical NSCs can seriously impair the continuous functionality of post-disaster buildings such as hospitals, emergency shelters, etc. that should be guaranteed by design according to building codes.

3- Property protection: The financial investment in NSCs is far greater than the value of the building structure. As illustrated in Figure 1.1, NSCs represent a large portion of the total cost of buildings (e.g. 65 % to 85% of the total cost depending on their use and occupancy), and their damage can result in important economic losses [1, 3].

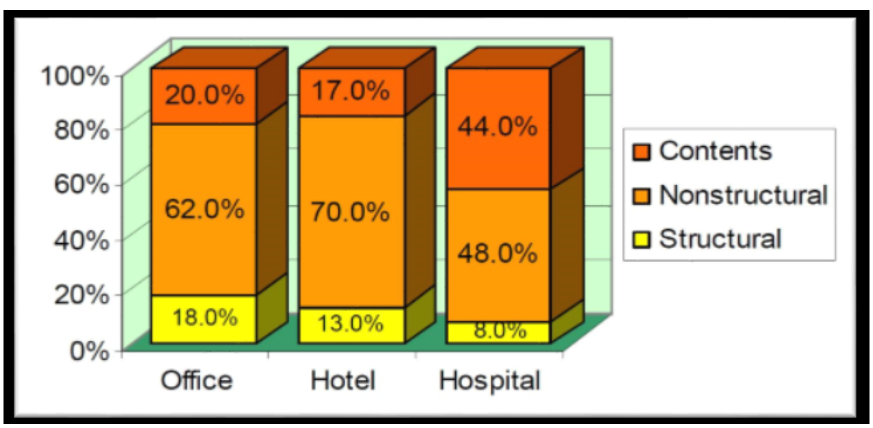

Figure 1.1- Typical investments in building construction according to main occupancy [3, 5]

Experiences from past earthquakes and current understanding of the seismic behaviour of building structures indicate that NSCs require rational seismic design and analysis procedures to guarantee their good performance under seismically induced forces and displacements.

Predicting the seismic response of NSCs has been the focus of many researchers during the past four decades and several analytical approaches have been developed which can be categorized into two general groups: 1- Floor Response Spectrum (FRS) approach, and 2- Combined Primary-Secondary system (CPSS) approach. In addition to these analytical approaches, recent building codes and standards include several recommendations and provisions for seismic risk assessment and mitigation of NSCs in existing buildings, and empirical equations for seismic design and analysis of NSCs. In Canada, a set of recommendations and guidelines is presented in the National Building Code (NBCC) [4] and in CSA S832-14 [1]. The current NBCC edition includes two types of seismic requirements for NSCs design: 1-Seismic force requirement in which the lateral equivalent static force required for design of the components and their anchoring connections is calculated using an empirical equation based on the Uniform Hazard Spectrum (UHS) approach that is used for the design of building structures, 2-Seismic displacement requirements in terms of building inter-story drift limits. However, in spite of all the efforts devoted to this subject, researchers have not yet reached a consensus on a generally accepted approach and the modern building codes and standards still do not reflect the current level of understanding of the seismic behaviour of NSCs and do not incorporate the developed techniques available.

The above mentioned issues are the main motivations for this research to attempt to develop an analysis method that is rational and reasonably accurate on the one hand, and simple enough to be employed in seismic assessment and design of NSCs on the other hand, while reflecting the real building dynamic characteristics.

1.2 Research goal and methodology

The main goal of this research is to propose a new methodology to generate FDS directly from UHS, making use of experimental data obtained from Ambient Vibration Measurements (AVM) on existing buildings. These floor design spectra can then be used to assess the seismic response of acceleration-sensitive NSCs.

A database of 27 RC buildings in which AVM was conducted has been collected and studied. A MATLAB [6] code has been written to generate FRS and inter-story drift curves for every floor of the buildings considering four different NSC damping ratios. The accuracy of the generated FRS and inter-story drift curves has been validated through a case study of a paediatric hospital located in Montreal, Canada. For the sake of validation, the FRS and inter-story drift curves generated by the code have been compared to those derived from a detailed linear finite element model of the hospital building. The generated FRS have been statistically analysed and at the first step, a methodology proposed to derive FDS for roof and 5% NSC equivalent internal damping. At the second step, the effects of NSCs location in the building and their damping ratios have been quantified using statistical analysis and the methodology has been extended to cover different floor levels and various NSCs damping ratios.

The more specific research steps are summarized as follows:

1. To collect an inclusive database of real RC buildings properly covering different height levels (i.e. low, medium, and high-rise buildings) in which AVM testing has

been conducted. To analyze the recorded AVM data and extract the modal properties of the building. To estimate the mass and in-plane rotary inertia of every building floor according to the collected architectural and structural drawings.

2. To provide an ensemble of twenty ground accelerograms compatible with UHS of NBCC 2015 [4] for Montreal and to be used as input excitations for dynamic analysis.
3. To collect an inclusive database of the evaluated permanently-instrumented buildings for the sake of proposing a set of modification factors to modify AVM-extracted modal parameters of buildings for higher-amplitude ground motions typical of earthquakes.
4. To write a MATLAB code that generates FRS curves in terms of velocity and acceleration and inter-story drift curves for every building floor in two main orthogonal horizontal directions (i.e. X and Y) and for different NSC damping ratios.
5. To validate the proposed method through a case-study of a paediatric hospital building located in Montreal, Canada by comparing the results of the detailed dynamic linear finite element analysis of the hospital building with the corresponding MATLAB routine outputs.
6. To employ the routine over the entire database and generate FRS for every building.
7. To do statistical analysis on the derived Pseudo Acceleration FRS (PA-FRS) and develop the new methodology to generate FDS for roof level and 5% NSC damping directly from the 5% damped UHS of the building.
8. To study and quantify the effect of NSCs damping ratio and their location along the height of the building on the generated PA-FRS through statistical analysis.

9. To extend the proposed methodology to generate FDS directly from UHS for any floor level and NSCs damping ratio.
10. To formulate the proposed methodology for RC low and medium rise buildings and to recommend a set of equations for each category.
11. To implement the whole procedure in MATLAB program and employ it over the entire database.

1.3 Thesis organization

This thesis is manuscript-based and divided into the following chapters:

Chapter 1 includes a general introduction to the research motivations, research objectives, and organization of the dissertation.

Chapter 2 includes the literature review report: “A. Asgarian and G. McClure, State-of-the-art review: Seismic response analysis of Operational and Functional Components (OFCs) in buildings, in STENG-2013-02. 2013, McGill University: Montreal, Canada. 41 p.” [7]. This internal report presents the literature review and background materials on the following topics relevant to this research: description and classification of NSCs, physical properties of NSCs, detailed explanations of different analytical methods for seismic analysis of NSCs, Building code and standard requirements for NSCs, experimental modal analysis and ambient vibration measurements (AVM). It should be noted that the literature review, first published in 2013, has been extensively updated on the above-mentioned subjects as well as on the several new subjects through the course of the research. These additional parts are covered in the conference and journal papers brought in Chapters 3-6 and are not included in this chapter solely to prevent repetitions. Hence, the readers are referred to Chapters 3-6 for the literature review updates.

Chapter 3 includes the journal paper manuscript: "A. Asgarian and G. McClure, *Generation of experimental floor response spectra for seismic assessment of Non-Structural Components (NSCs) based on ambient vibration measurements.* Manuscript under review, 2017: 22 p." [8]. This chapter contains the detailed description of: 1-the collected RC building database and their extracted modal properties from AVM; 2- the adopted procedure for selection and scaling of the input earthquake excitation; 3- the characteristics of the twenty scaled ground accelerograms used in this study; 4- the extensive literature review and collection of the data recorded in all permanently instrumented buildings during past earthquakes and proposition of an appropriate set of modification factors to modify AVM-extracted modal properties of the building for higher amplitude excitations; 5- the development of the methodology to generate FRS and inter-story drift curves for the building floors and implementation of the method in MTALAB program [6]; and 6- the application of the method over the building database (detailed presentation of Building#15 results).

Chapter 4 includes the conference paper "A. Asgarian, F. Mirshafiei, and G. McClure, *Experimental floor response spectra for seismic evaluation of operational and functional components of building*, in Proceedings of the CSCE 2014, 4th International Structural Specialty Conference. 2014: Halifax, NS, May 28 to 31. 10 p." [9]. This chapter covers the validation of the proposed methodology and results of the written MATLAB code through a case-study of a paediatric hospital building located in Montreal, Canada.

Chapter 5 includes the journal paper manuscript "*Direct generation of Floor Design Spectra (FDS) from Uniform Hazard Spectra (UHS) - Part I: Formulation of the method*. Manuscript under review, 2017: 19 p.." [10]. In this chapter the PA-FRS curves generated for the building database using the method proposed in chapter 3 are used to discuss the effect of key parameters (i.e. Tuning, elevation of NSCs, damping of NSCs) on the acceleration response of NSCs. The new method is developed and presented to generate FDS for the roof level and 5% NSC damping directly from 5% damped UHS. The proposed method is formulated for RC low and medium rise buildings and a set of equations is recommended for each building type. The FDS curves derived for the building database are presented and compared with the provision of three well-known international building codes: NBCC 2015 [4], ASCE SEI-7-16 [11], and Eurocode 8 [12].

Chapter 6 includes the journal paper manuscript "Asgarian, A. and G. McClure, *Direct generation of Floor Design Spectra (FDS) from Uniform Hazard Spectra (UHS) - Part II: Extension and Application of the method.* Manuscript under review, 2017: 20 p. [13]. This chapter presents the extension of the previously proposed approach in Chapter 5 to generate FDS directly from UHS but for any selected floor level and NSC damping ratio. The detail statistical analysis of the generated PA-FRS curves has been done to quantify the effects of NSCs elevation and damping ratios on FDS. The extended methodology is formulated and a set of complete equations are recommended. The extended method is implemented in MATLAB and employed over the entire building database. The derived FDS for one low-rise (Building#4) and one medium-rise (Building#18) building are presented to show the application of the extended proposed approach.

Although specific discussion and conclusions are presented at the end of each chapter, the general conclusions of this study and suggestions for future work are presented in **Chapter 7**.

1.4 References

1. Canadian Standard Association (CSA) *CAN/CSA-S832-06: Guidline for seismic risk reduction of operational and functional components (OFCs) of buildings*. 2006: Rexdale, ON, Canada.
2. Villaverde, R., *Fundamental concepts of earthquake engineering*. 2009, Boca Raton, FL: Taylor & Francis Group.
3. Taghavi, S., *Response Assessment of Nonstructural Building Elements*, in *Department of Civil and Environmental Engineering*. 2003, Stanford University: Stanford, California. p. 96.
4. National Research Council of Canada (NRC), Institute for Research in Construction (IRC), *National Building Code of Canada (NBCC)*. 2015: Ottawa, ON, Canada.
5. Soong, T. and D. Lopez Garcia. *Seismic Vulnerability and Protection of Nonstructural Components*. in *Proc. Joint NCREE/JRC workshop on International collaboration on earthquake disaster mitigation research*. 2003. Taipei, Taiwan.
6. The MathWorks Inc., *MATLAB*. 2014: Natick, MA.
7. A. Asgarian and G. McClure, *State-of-the-art review: Seismic response analysis of Operational and Functional Components (OFCs) in buildings*, in *STENG-2013-02*. 2013, McGill University: Montreal, Canada. p. 41.
8. A. Asgarian and G. McClure, *Generation of experimental floor response spectra for seismic assessment of Non-Structural Components (NSCs) based on ambient vibration measurements.* Manuscript submitted for publication, 2017: p. 22.
9. A. Asgarian, F. Mirshafiei, and G. McClure, *Experimental floor response spectra for seismic evaluation of operational and functional components of building*, in *CSCE 2014, 4th International Structural Specialty Conference*. 2014: Halifax, NS, May 28 to 31. p. 10.
10. Asgarian, A. and G. McClure, *Direct generation of Floor Design Spectra (FDS) from Uniform Hazard Spectra (UHS) - Part I: Formulation of the method.* Manuscript submitted for publication, 2017: p. 19.
11. American Society of Civil Engineers, *ASCE Standard 7-16: Minimum Design Loads for Buildings and Other Structures*. 2016, American Society of Civil Engineers: Reston, VA.
12. Comite Europeen de Normalization, *Eurocode 8–Design of Structures for earthquake resistance–Part 1: General rules, seismic actions and rules for buildings*, in *EN-1998-1*. 2004: Brussels, Belgium.
13. Asgarian, A. and G. McClure, *Direct generation of Floor Design Spectra (FDS) from Uniform Hazard Spectra (UHS) - Pat II: Extension and Application of the method.* Manuscript submitted for publication, 2017: p. 20.

2 State-of-the-art review: Seismic response analysis of Operational and Functional Components (OFCs) in buildings

A. Asgarian and G. McClure, McGill University, Canada

2.1 Introduction

A building is composed of two main types of components: structural components (see Figure 2.1) and non-structural components (NSCs) also called operational and functional components (OFCs) (see Figure 2.2). NSCs are those components or systems housed or mounted in the buildings which are not part of the main or intended load-resisting system of the structure. Therefore, the building structure is commonly called "primary structure" or "supporting structure" and NSCs are also known by alternative names such as "non-structural elements", "building attachments", "architectural, mechanical, and electrical elements", "secondary systems", and "secondary structural elements".

Figure 2.1 - Structural Components (taken from http://openbuildings.com/buildings/the-yellow-building-profile4695/media)

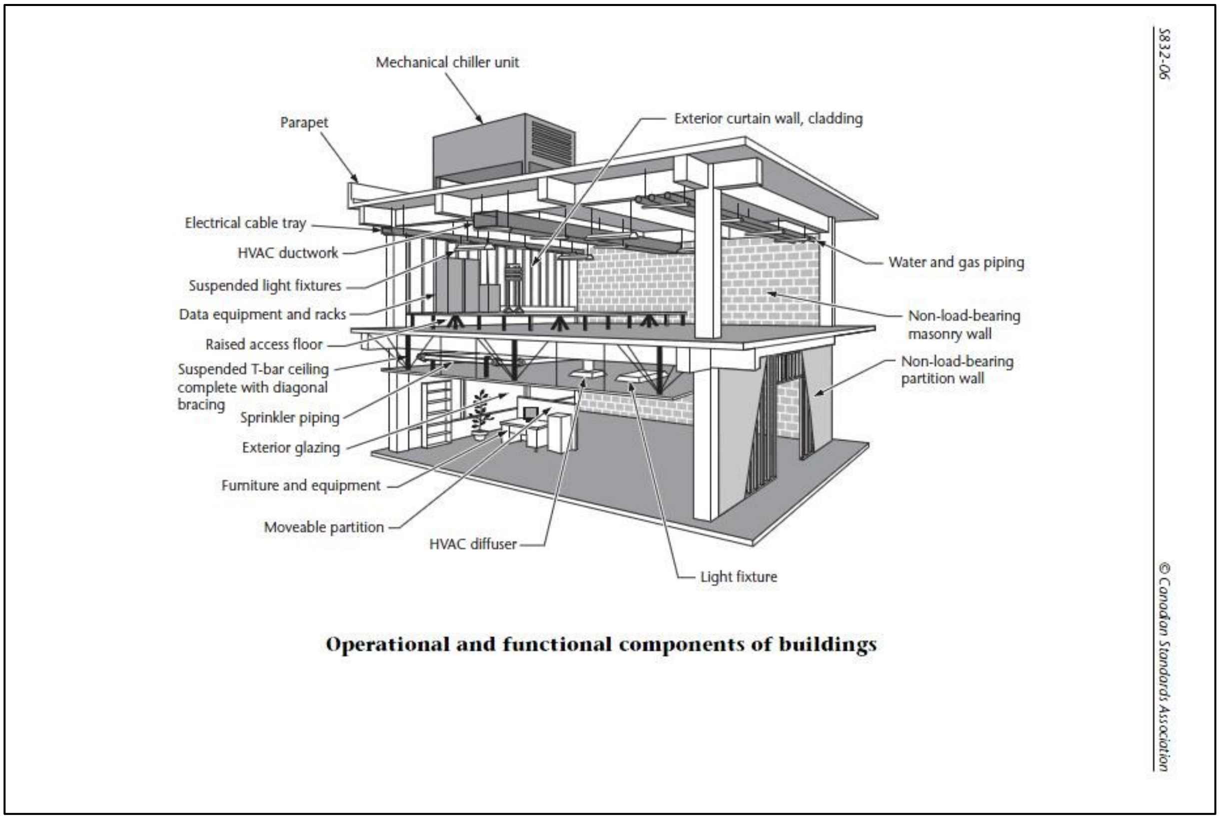

Figure 2.2 - Operational and functional components of buildings [1]

According to CSA S832-06(R11), NSCs can be categorized into three sub-groups according to their function: Architectural (external or internal), Building services (mechanical, electrical, and telecommunication), and Building contents (common and specialized) [2, 3]. They can also be classified into three categories according to the nature of their seismic response sensitivity: 1- Inter-storey-drift-sensitive components, 2- Floor-acceleration-sensitive components, and 3- both Inter-storey-drift- and floor-acceleration-sensitive components. Based on their intrinsic stiffness and the stiffness of their anchoring system to the building structure, they can be grouped as rigid, flexible and hanging type components. A component (considered here with its anchoring system) is defined as rigid if its fundamental sway period is less than or equal to 0.06 sec (frequency above 16 Hz) [4]: such components are expected to follow floor/roof building motions without further dynamic amplification. As such, the dynamic properties of rigid components depend primarily on the stiffness of its anchors to the supporting structure. Flexible components are those that have inherent flexibility due to their configuration (pipes, racks, etc.) and/or otherwise rigid components connected with flexible anchors. Such components are prone to dynamic amplification of the floor/roof motions and should be analysed accordingly. Distributed components can be modeled as multi-degree-of-freedom (MDOF) systems or continuous systems with distributed mass and stiffness. They are typically connected by multiple attachments to the buildings (e.g. pipes, cable trays). For the third category of systems hanging from the ceiling (ex. Suspended ceilings, lighting fixtures, other components located in the ceiling plenum) the best way to model them is by single (or distributed) mass pendulum [5, 6].

Although NSCs are called secondary systems, they are far from being secondary in importance in terms of functionality and economical value. Their functionality and performance during and after an earthquake is of great significance especially in post-disaster structures such as hospitals, emergency shelters, power stations, etc. As a matter of fact, the good seismic performance of NSCs is essential to achieve the life-safety performance objective that is mandatory for all buildings in Canada [7].

The failure of NSCs during an earthquake can directly threaten the life of building occupants or passersby and impair safe egress procedures. In addition, the failure of some critical NSCs can seriously impair the functionality of post-disaster buildings that should be guaranteed by design. For examples, hospitals should resist design earthquakes without the need for their evacuation. This was an issue with several major hospitals following the 1994 Northridge earthquake in Los Angeles, California (magnitude of 6.7), which had to be evacuated not because of structural damage but due to (a) the failure of water lines and water supply tank; and (b) the failure of emergency power systems and heating, ventilation, and air-conditioning units [8] (See Figure 2.3).

a)

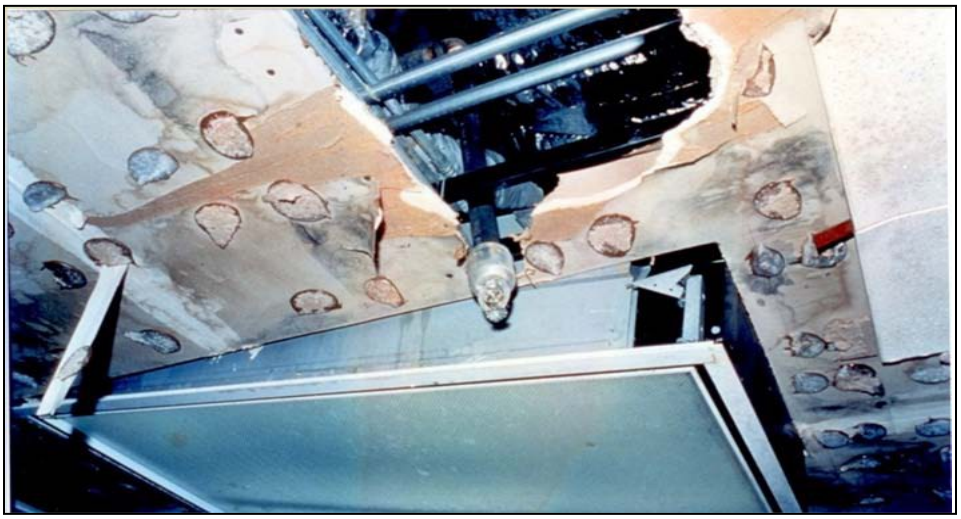

b)

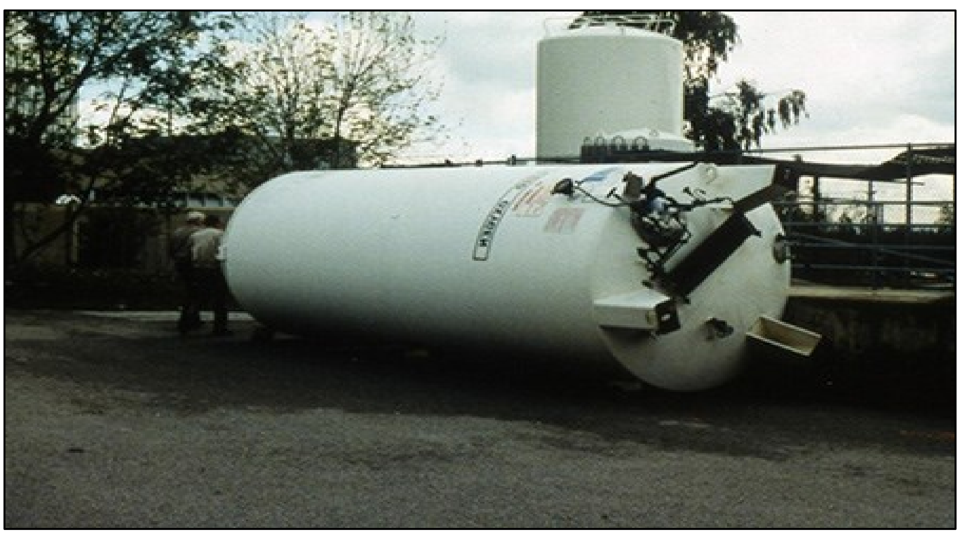

Figure 2.3 - NSCs damage during the 1994 Northridge Earthquake, California: a) Broken sprinkler pipe; b) Vertical tank at hospital overturned due to inadequate anchorage [9].

Life-threatening hazards may result from the collapse of suspended ceiling systems, lighting fixtures, fall of heavy partition walls, collapse of heavy equipment, bookshelves, etc. Exterior components like parapets, signboards, and facade panels may also fall off the building and can cause serious threats to injury or death. An unfortunate example of this type is the death of a student who was struck by a falling precast panel during 1987 Whittier Narrows earthquake with magnitude of 5.9 [10](See Figure 2.4).

a)

b)

Figure 2.4 - a) Failure of office partitions, ceilings, and light fixtures in the 1994 Northridge Earthquake; b) Failure of precast panel at parking garage that resulted in fatality in the 1987 Whittier, California earthquake [9].

Lastly, as NSCs represent a large portion of the total cost of the building (e.g. 65 % to 85% of the total cost depending on their use and occupancy), their damage can result in important economic losses (See Figure 2.5). The financial impact arising from NSCs damage can be divided into direct and indirect economic losses; direct losses are the costs associated with replacing or repairing the failed NSCs, while indirect losses result from business interruption [3, 5].

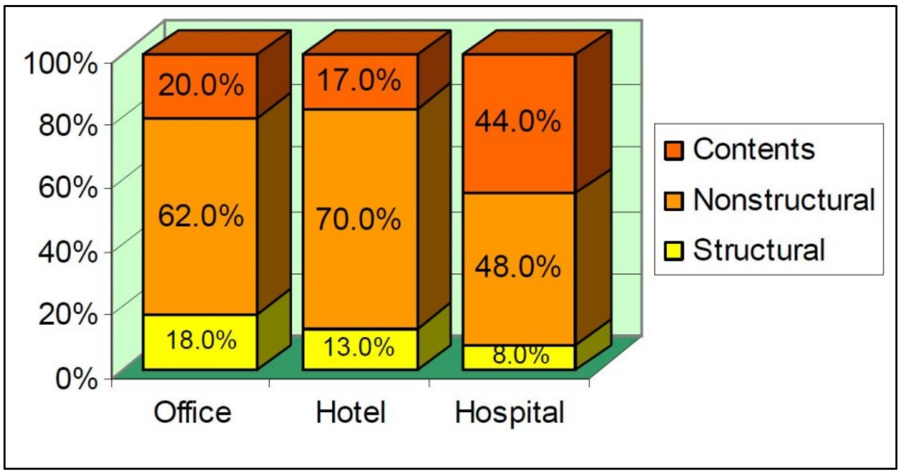

Figure 2.5 - Typical investments in building construction [11].

Experience and observations from past earthquakes and current understanding of the seismic behaviour of building structures indicate that NSCs are exposed to large seismic forces during an earthquake and they deserve rational and careful seismic design and analysis procedures of their own.

2.2 **Physical properties of NSCs**

NSCs possess several physical characteristic which increase seismic risk and vulnerability associated with them. These characteristics are as follows [2, 5]:

1- In medium- to high-rise buildings, some functional components related to building services are usually located at the higher elevation of the building which makes them exposed to amplified seismic displacements and accelerations compared to ground motion. The amplification of floor accelerations is typically three times the ground acceleration at the upper roof level, and it saturates rapidly above the lower few levels.

2- In general, the stiffness and weight of isolated components are both much lower than those of the supporting structure. As a result, their natural frequencies might be close to one of the natural frequencies of the supporting structure which causes resonant NSCs motions.

3- Apart from architectural components, NSCs have typically low damping ratios compared to the building structure. Consequently, they cannot benefit from the fast damping of the effects of strong motions.

4- Architectural components and distributed NSCs are usually multiply-supported, which means that they are attached to the building framework (walls or floors) at different points. Thus, they are subjected to differential motions at their supports and are affected by distortions.

5- NSCs supports are mainly designed for purposes other than resisting forces which makes them more vulnerable to even low level seismic motions. This means that damage to non-structural components is normally triggered at levels of deformation and/or acceleration much smaller than those required to initiate structural damage.

2.3 Important factors in seismic response of NSCs

As mentioned in the preceding section, the physical properties of NSCs make them respond to earthquake ground motions differently from the building structure. Thus, to evaluate the seismic response of NSCs, one needs to account for some parameters that are specifically associated to NSCs. They are including [12, 13]:

1- The *dynamic response of the building structure.* As NSCs are attached to or supported by the building, they are directly subjected to the in-building seismic response (floor response) instead of the earthquake ground motion. Such in-building response is typically amplified and filtered according to the dynamic properties of the building lateral load resisting system.
2- *The* NSCs *location along the height of the building*. Owing to different floor responses, two identical components positioned at two different floors in the building will respond differently.

3- *Possible dynamic interaction between NSCs and the building structure.* As mentioned previously, in certain "quasi-resonant" conditions, both the structure and NSCs can interact dynamically and mutually affect or modify each other's seismic response. Well-known rational dynamic analysis techniques are available to consider this effect, where primary (structural) and secondary (NSCs) systems are considered as a coupled system.

4- *Low damping of NSCs*. As mentioned earlier, NSCs normally possess a damping ratio which is much lower than that of the building. This difference in damping ratios of the primary and secondary systems causes the combined system to have non-classical damping and natural frequencies and modes shapes are complex.

5- *Multiple-support excitations.* Multi-supported NSCs are subjected to different and out-of-phase seismic excitations which are exerted at different support locations.

6- *Nonlinear response*. The response of NSCs can be quite affected by the nonlinear behaviour of both the primary and secondary structures.

2.4 **Methods of seismic analysis of NSCs**

The seismic response of NSCs is a challenging problem which attracted the attention of many researchers during the past four decades. Attempts have been made to develop rational yet practical methods to analyse the seismic response of NSCs, but researchers have not yet reached a consensus on a generally accepted method to evaluate NSCs' seismic behaviour. This difficulty arises from dynamic characteristics of NSCs that increase the complexity of the problem compared to structural building response such as [2, 13-15]:

1- *Large number of degrees of freedom (DOFs):* When both the primary and secondary systems are Multi- Degree-Of-Freedom (MDOF) systems, the combined system includes a large number of DOFs which makes the analysis less amenable to simple procedures.

2- *Tuning*: The natural frequencies of NSCs may be close to those of the primary system and this matter causes resonance. Hence, the response of NSCs can be controlled by two or more dominant modes of vibration.

3- *Support configurations*: Multiple supports and various attachment configurations of secondary systems can be quite complicated to analyse (e.g. piping systems).

4- *Non-classical damping*: The presence of non-classical damping in combined systems mandates working with complex natural frequencies and mode shapes and increases the level of complexity of analysis.

5- *Nonlinearity*: The building structure is designed to undergo some inelastic deformations during a severe design earthquake. NSCs themselves might also show some inelastic behaviour in their response which have to be considered as well.

6- *Diversity of NSCs*: There exists a vast variety of NSCs each having different shapes, materials, functions, weight, sensitivity to response parameters of buildings, connections to building, etc.

Despite of all these difficulties, many attempts have been made to develop accurate methods for seismic design and analysis of NSCs and to assure their seismic safety and integrity during earthquakes. These efforts were first initiated by research projects focusing on critical equipment mounted in nuclear power plants such as piping and control systems. In general, the available methods of analysis of NSCs can be categorized into two general groups: 1) Floor Response Spectrum (FRS) approach, and 2) Combined Primary-Secondary (P-S) system approach.

2.5 **Floor response spectrum (FRS) approach**

2.5.1 Review of early work

One of the first methods developed for analysis of NSCs is the Floor Response Spectrum (FRS) in which the primary and secondary systems are decoupled (i.e. no dynamic interaction between them is considered) and analysed individually. This method is also known by alternative names such as “systems-in-cascade”; or “in-structure response spectrum” [16]. The available technique to determine the FRS can be divided into two general categories: 1- deterministic methods which utilize the time histories compatible with the design response spectra and time-history analysis, and 2- probabilistic methods that use random vibration analysis for determination of FRS from a target Power Spectral Density Function (PSDF) without using time history analysis. The latter properly accounts for the uncertainties associated with soil response, materials and inherent uncertainties in seismic motions [17].

In the deterministic approach, the response acceleration time history of the primary system at the support locations of NSCs is firstly determined by using the direct time-step integration method given a compatible set of ground accelerograms. This floor acceleration time-history is then utilized as the base-excitation for NSCs to generate a floor response spectrum using either time-domain direct integration analysis or modal superposition [18] (See Figure 2.6).

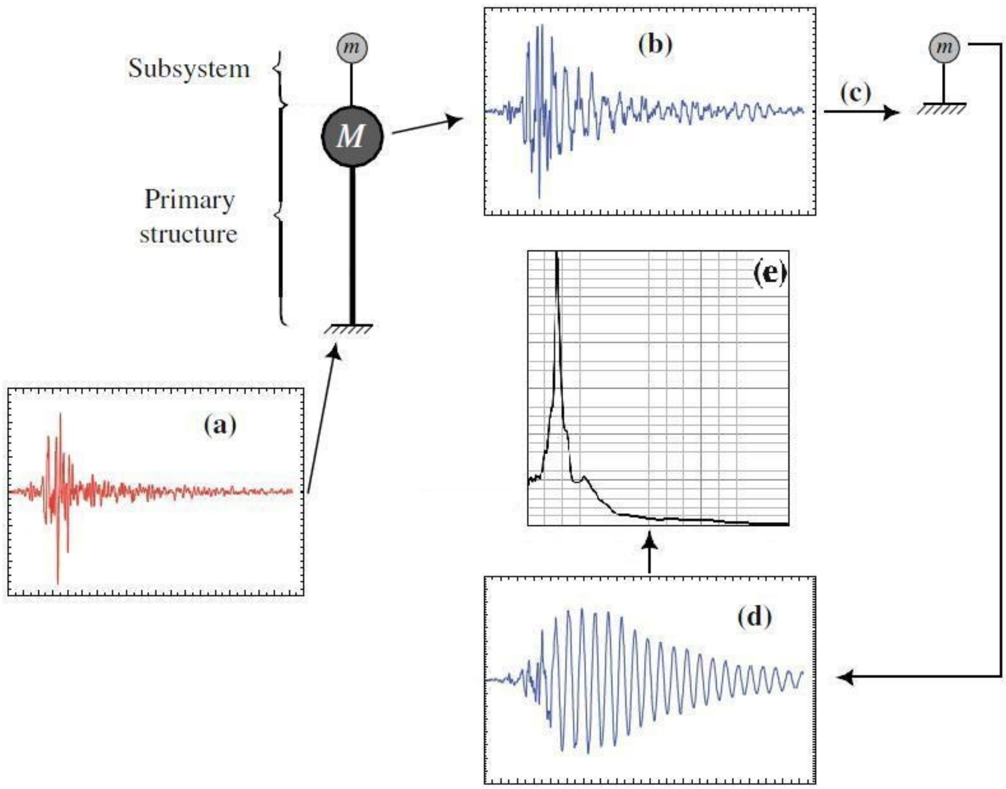

Figure 2.6 - Floor response spectrum approach: a)-Ground acceleration time history as an input for primary structure, b)-Acceleration response-history of the primary structure, c)-Using the acceleration response-history of primary system as the input for secondary

The generated FRS is expected to have peaks at frequencies corresponding to the peaks of the ground motion spectrum and/or at the fundamental dominant natural frequencies of the primary system. For design purposes, FRS peaks are typically broadened to account for the variability in structural frequencies caused by uncertainties in ground motion spectrum, damping, material properties of structure and soil, as well as inaccuracies in the approximation techniques used for modeling and computation in dynamic analysis [17]. For instance, as described in the USNRC code [19] in order to determine the amount of peak widening, the sensitivities of structural natural frequencies to each important factor are evaluated first. Then, the expected value of the variation in structural frequency, Δf_j, for each fundamental frequency, f_j, is calculated by taking the Square Root of the Sum of Squares

(SRSS) of a minimum variation, 0.05 f_j, and the individual frequency variations, Δf_{jn}, as follows:

$$\Delta f_j = \left[(0.05 f_j)^2 + \sum_{n=1}^{p} (\Delta f_{jn})^2\right]^{1/2} \nless 0.1 f_j \qquad \textit{Equation 2.1}$$

where Δf_{jn} denotes the variation in the j^{th} mode frequency, f_j, due to variation in parameter number n, and P is the number of significant parameters considered. A value of $0.1f_j$ should be used if the actual computed value of Δf_j is less than $0.1f_j$. If the above procedure is not used, Δf_j should be taken as $0.15f_j$ [19] (See Figure 2.7).

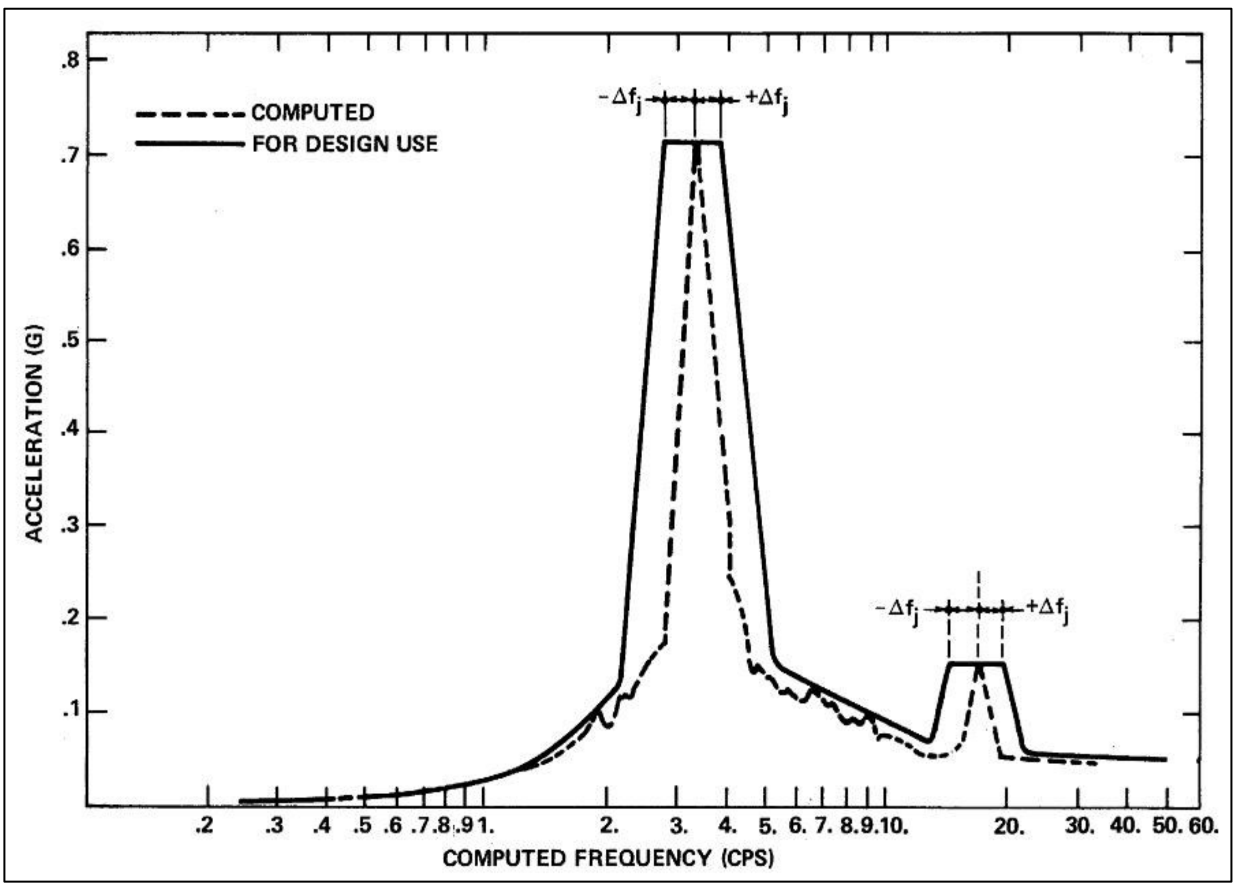

Figure 2.7 - Response spectrum peak broadening and Smoothing [19]

The response of the primary structure at a NSCs support location may have components in three orthogonal directions, which may also come from three-directional excitations (i.e. two horizontal and one vertical in the usual Cartesian system of coordinates). Considering each excitation component, the FRS can be generated at the same location and in the same direction. These individual FRSs can be combined using SSRS technique to derive the total FRS for the given location and given direction [13].

Concerning multi-supported components, an upper-bound envelope of all individual FRSs at support locations can be used to estimate the conservative maximum acceleration response.

Although the method explained above is analytically accurate, the results from a single ground motion time-history are not reliable for design purposes since one ground motion accelerograms cannot represent the characteristics of a possible future earthquake appropriately. So one should consider an ensemble of ground motion inputs and use the average of or envelope to all determined FRSs for NSCs design. This series of analytical runs are time-consuming, analytically expensive, and economically unwise. As a result, an alternative approach was introduced to tackle this issue which is called "Spectrum-Consistent Time-History" (SCTH). A spectrum-consistent time-history is an artificially generated ground acceleration time-history whose response spectrum closely envelops the prescribed ground design spectrum and it is used as the excitation input for the primary structure to generate the FRS. Several techniques have been suggested to obtain the SCTH [20-23]. However, it was observed that different SCTHs that all envelop the target design spectrum in the same manner, can result in quite different FRS [24, 25], which means that the artificial time-histories are not uniquely defined. Thus, to generate an appropriate FRS for NSC design, one should carry out the analysis for a set of SCTHs and utilize the average of or envelope to all derived FRSs, which is also a time-consuming process.

To overcome these problems and also avoid time-history analysis altogether, great research efforts have been made to develop alternative approaches that can derive the FRS directly from the design spectrum without generating any intermediary input such as the floor response time-history. The result of these efforts is what is named as "Direct methods". These methods generate the FRS directly based on the design spectrum and the dominant modal properties of the primary structure. These methods are applicable to linear building structures. Examples of works done in the 1970s are [26-32], some of which are briefly explained below.

Biggs and Rosset (1990) were among the first to propose the direct method. They suggested the derivation of magnification curves which were obtained from the observed response of secondary systems subjected to a set of recorded seismic ground motions. Their method is semi-empirical and gives conservative results. They divided the equipment into two groups: rigid equipment whose maximum acceleration is the same as that of the supporting point on the structure and very flexible equipment which behave as though supported directly on the ground, as they mentioned. Between these two extreme cases, there exist a wide range of dynamic interactions and resonant effects between the two systems. It is assumed in their study that the structure and equipment will behave elastically. Using the suggested magnification curves, one can simply calculate the maximum modal acceleration response of the equipment directly from the ground motion response spectrum and combining these maximums will give the maximum acceleration response of NSCs.

Singh (1975) also proposed a direct method to obtain the FRS, based on the assumption that the earthquake motions can be modeled as homogeneous stationary Gaussian random processes. Having a Gaussian seismic input, the response of a linear structure will be also Gaussian. Only two factors are required to define a Gaussian process: its mean value and correlation function. Thus, the method is developed to calculate these factors using the PSDF of the input ground motion and the dynamic characteristics (lower natural frequencies) of the structure. Knowing these two factors, one can determine the PSDF of the floor acceleration. The variance of the absolute acceleration of the oscillator connected to the floor is determined using another formula developed in the study. Then, the maximum response of the oscillator is equal to the amplified standard deviation by an appropriate factor. Hence, only the dynamic characteristics of the structure and the prescribed ground motion are required for this procedure. The main limitation of this method is that the structure should behave linearly. In addition, this approach cannot be used when the NSCs is tuned with one of the fundamental frequency of structure where the FRS usually shows the highest peaks. Supplementary work was done by Singh in 1980 which extends the developed method to the cases in which the NSCs are tuned with the primary structure but still for linear structures only.

Some other direct approaches are based on random vibration analysis in which a MDOF structural system is subjected to a stationary random excitation. Knowing the dynamic properties of primary system, the PSDF of structural floor can be directly derived from that of the ground accelerograms. Then this floor PSDF is used as input to generate the floor response spectrum. Examples of this method are works by Singh 1975; Vahi 1975; Vanmarke 1977.

Vanmarke (1977) proposed a procedure to obtain the response of a secondary system directly from specified ground response spectra. In his method, the maximum acceleration of a single DOF secondary system is presented as the square root of a sum of contributions which depend on two factors: 1- pseudo-acceleration response spectrum (ground) for the period and damping of the primary system, and 2- the pseudo-acceleration response spectrum (ground) for the equipment period and damping. The Spectral Density Function (SDF) of the absolute acceleration response of the structure at the support point of the secondary system is derived using the dynamic properties of the structure and SDF of ground motion. Then, this absolute acceleration SDF of the primary system is used as input for the random vibration analysis of the secondary system. The SDF of the secondary system response is calculated directly using this input and transfer function/frequency response function of the secondary system. Using the random vibration analysis and SDF of the secondary system response, a formula is suggested to derive the maximum acceleration response of a secondary system directly from specified ground response spectra.

2.5.2 Advantages of FRS approach

The FRS approach is a simple analysis method which allows uncoupling the primary and secondary systems and evaluating their response independently. In comparison with the Combined Primary-Secondary System (CPSS) model, the FRS method is faster, more economic in terms of analysis time and computational costs. It avoids the numerical complexities that could be encountered in the CPSS models due the large number of DOFs and considerable differences in terms of the damping ratios, stiffness, and mass of primary and secondary systems. Furthermore, once the floor response spectra are specified, the method then allows the analyst to work on the secondary system independently of the primary system characteristics.

2.5.3 Disadvantages of FRS approach

Despite its simplicity, the FRS method has been proven to be reasonably precise when considering the NSCs that are quite lighter than the primary system and that have natural frequencies not close to those of the supporting structure. When these conditions are not satisfied, however, the FRS method can lead to some gross error or over conservative results in seismic response analysis of NSCs.

As instances, some researchers have recommended that the decoupling the primary and secondary systems is acceptable when the mass of the NSC is less than 1% of the total mass of the supporting structure [19, 31]. Some shortcomings of the FRS approach which are as follows:

1- As mentioned earlier, no <u>dynamic interaction</u> is considered between the primary and secondary systems in FRS as they are decoupled and analysed independently. When this assumption is not correct, the motion of NSCs may modify the motion of the primary system which in turn affects the response of NSCs [33]. Though neglecting dynamic interaction is usually on the conservative side for acceleration-sensitive components, in some cases it may be grossly conservative and uneconomical [2].

2- FRS cannot take into account the effect of large differences existing between the damping ratios of NSCs and their primary system (i.e. non-classical damping effects), which makes them vibrate out-of-phase. Non-classical damping effects can be significant when the non-structural to structural mass ratio is small and when the NSC is tuned with the supporting structure [12].

3- Cross-correlation between the support excitations of multi-connected NSCs is addressed improperly or completely ignored in the FRS method [34]. Several empirical techniques have been proposed to account for this problem. As such, Thailer [35] suggested to obtain the response of the primary structure at different support locations. Then each of these acceleration time-histories are utilized as input for the secondary system to calculate a set of floor response spectra. These FRSs are then combined according to an empirical procedure to estimate the true maximum response of NSCs. A common procedure is to pick the largest of the maximum response estimates (i.e. FRS) or to combine them using SRSS. Alternative techniques generate a spectrum enveloping the FRSs corresponding to each support point. However, these methods normally result in overly conservative response predictions for acceleration-sensitive equipment, which is not economically justifiable.

4- It is cumbersome to take into account the torsional response of the structure on the seismic response of NSCs.

5- The other difficulty is to take into consideration the eventual nonlinear response of either or both the primary and secondary structures. In this regard, NSCs with natural frequencies higher than the fundamental natural frequency of the primary structure, generally experience response reductions due to: 1-increased damping of the primary structure when it undergoes inelastic deformations (hysteretic damping) and 2- shift of the fundamental natural frequency of the primary structure away from the natural frequencies of the NSCs. The reason for the shift is the period elongation of the supporting structure caused by inelastic behaviour which decreases the total stiffness of the building. On the other hand, some of the NSCs themselves may have ductile anchors with some post-elastic capacity, which can cause further reductions in their response. One approach to account for nonlinear response is to predict the inelastic response of NSCs from their elastic response using response amplification factors; this technique will be further explained later in section2.7.

2.6 **Combined Primary-Secondary System (CPSS) approach**

2.6.1 Review of early work

The aforementioned deficiencies of the FRS method have led to the development of other analysis approaches which can overcome these problems. One solution is to consider the primary and secondary systems together as a coupled system. This is called “Combined Primary-Secondary (CPSS) system approach”. In this approach the secondary system is assumed as an integral part of the combined primary-secondary system. Both modal analysis and time history integration can be performed in this approach. Two examples of studies regarding combined P-S systems are described next.

Igusa and Der Kiureghian [18] have suggested a method for response analysis of multi-supported MDOF secondary systems that is capable of considering the effects of tuning, dynamic interactions, non-classical damping and cross-correlation of support motions. The method proceeds in two steps: 1- determining the modal properties of combined P-S system using the known properties of individual subsystems (i.e. modal synthesis which is discussed in details in 2.7) and 2- modal superposition analysis of the combined system to obtain the response of the secondary system. Considering that the secondary system is much lighter than the primary system, perturbation theory is used to solve the eigenvalue problem of the combined system in the first step to gain its modal properties, based on the modal properties of the primary system.

Villaverde [36] also proposed a simplified approximate method to predict the seismic response of a multi-supported MDOF secondary system mounted on a nonlinear primary structure. The procedure first calculates the modal properties of the combined system using the independent dynamic properties of the two systems. Then the maximum response of the equipment is predicted using nonlinear FRS and modal combination techniques. This approach accounts for the interaction and non-classical damping effects completely; however, it is limited in terms of application to the buildings with elastoplastic load-deformation behaviour and also to low-mass components. Villaverde classified the modes of combined systems into two types, resonant and non-resonant. A resonant mode is obtained if the natural frequency of both primary and secondary systems is coinciding. The same method was applied to linear systems in a later study [37].

2.6.2 Advantages of CPSS approach

Considering the primary and secondary systems as a whole, one can incorporate the following parameters into the analysis:

1- Dynamic interactions between the primary and secondary systems. This effect was first studied by Newmark [38] who used a modal superposition approach on the combined P-S system.

2- Different values of mass, stiffness, and damping ratio for the primary and secondary systems.

3- Cross-correlation between the motions of various supports of multi-supported NSCs [39].

4- Non-linearity of the primary and secondary systems.

2.6.3 Disadvantages of CPSS approach

Although the CPSS approach resolves many of the problems associated with the FRS method, establishing a combined P-S system normally results in a coupled system with an excessive number of DOFs, with drastic differences existing between the masses, stiffness, and damping ratios of the two systems. These conditions render any conventional methods of analysis costly, imprecise and inefficient.

Also, adopting this method for NCS analysis means that every time a change is made in the NSCs' parameters, the whole coupled structure needs to be reanalysed which is not practical, considering that the design of these two systems is conducted by different teams (structural/mechanical/architectural) and at different times.

2.7 Modal Synthesis (MS) approach

In view of the shortcomings of the FRS approach and the impracticality associated with direct analysis of a combined complex P-S system, several methods have been developed that, while considering the interaction between two systems by analysing them as a coupled system, do not involve the difficulties pertaining to direct dynamic analysis of coupled mechanical systems. One such methods is "Modal Synthesis approach" (MS) that can be thought of as a sub-category of the CPSS method. In the MS approach, as it can be inferred from its name, the response of NSCs is determined based on the modal superposition analysis of the combined system. But it is different from CPSS in view of the fact that in MS approach, the dynamic properties of the combined system are determined using those characteristics of its individual components when considered independently and not directly from analysis of the whole system. For instance, if using the conventional response spectrum method in this approach, the different steps involved can be summarised as follows:

1- Determination of ground response spectrum or prescribed design spectrum.

2- Calculation of dynamic properties of combined system – natural frequencies, mode shapes, damping ratios, and participation factors- using the dynamic properties of its individual components.

3- Computation of maximum modal NSC response in terms of the given response spectrum and calculated dynamic properties of combined system.

4- Combination of these maximum modal responses using one of the classical modal combination rules such as SRSS, CQC, etc.

Since in this method the primary and secondary systems are considered as a coupled unit, the deficiencies inherent to the FRS such as neglecting dynamic interactions and variable out-of-phase support motions are eliminated here. Formulating the analysis according to dynamic properties of the independent subsystems can resolve the computational difficulties concerning conventional P-S methods. Furthermore, the need to generate response history of each floor as an intermediary input and also the necessity of reanalysing the structure by every change made in NSCs are not concerns any more. Examples of proposed methods using this MS approach are those by Gupta (1984)[40]; Newmark and Villaverde [41]; Newmark (1972) [38]; Villaverde (1987) [36]; Villaverde (1991) [37]. Works by Villaverde are explained earlier in section 2.6. Newmark and Villaverde (1980) [41] proposed a similar approach which is limited to linear elastic primary and secondary systems and also to secondary systems that are connected to the primary system at no more than two points.

As observed in the studies by Aziz and Ghobarah (1988) [42]; Sewell, et al. (1989) [43]; Singh, et al. (1993) [44], nonlinear behaviour of the primary and/or secondary systems may noticeably affect the force response of the latter. Thus, a simple approximate way to account for this effect is using force response reduction factors to modify the linear response of NSCs in much the same way as is done with ductility ratios for buildings. The essential difference is that for NSCs, the total force reduction factor is equal to the product of the reduction factors of both the primary and secondary systems. Suggested methods to calculate these force reduction factors are, for examples, by Newmark and Hall (1982)[45] and more recently by Miranda and Bertero (1994)[46]. It should be noted that in some cases, NSCs might show response amplifications instead of reduction, in terms of response acceleration, which usually occurred when fundamental natural frequency of NSC is tuned with one of the higher natural frequencies of the supporting structure and the NSC is located at lower levels of the building. It is important to mention that despite a reduction in the acceleration response, the displacement response will be increased in presence of non-linear behaviour which can be crucial regarding drift-sensitive components. Several studies have been done to determine the response modification factor and the effect of various parameters on this factor such as the level of inelasticity of the supporting structure, the NSC location in the building, the fundamental period of the component and supporting building, their damping ratios, etc. Examples of these works are those by Lepage, et al. (2012) [47]; Medina, et al. (2006) [48]; Sankaranarayanan (2007)[6]; Sankaranarayanan and Medina (2007)[49].

Medina et al. (2006) [48] evaluated the dependence of peak component acceleration demand on different parameters such as NSC location and damping ratio, and properties of the primary system including modal periods, height, stiffness distribution, and level of inelasticity in the building. The analytical study covered a variety of stiff and flexible, and elastic and inelastic regular moment-resisting frames subjected to a set of 40 ground motions. Based on the results, some recommendations were made for values of modification factors to obtain the acceleration response of elastic NSCs mounted on inelastic structure, from their response when mounted on elastic structure. Herein, NSCs are represented by linear elastic SDOF systems and no dynamic interactions are considered.

Sankaranarayanan et al. (2007) [49] did a similar study to evaluate the main factors that affect the amplification or decrease of acceleration FRS values caused by inelasticity in the primary structure. Three distinct spectral regions were defined namely long-period, fundamental-period, and short-period regions according to the ratio of T_c/T_s (component period to fundamental period of the building) and the effective acceleration modification factors are defined in each region separately.

Lepage et al. (2012) [47] proposed a simple method for determining the horizontal peak acceleration of NSC in terms of the peak ground acceleration. The results of shake-table tests performed on the floor diaphragms of 30 small-scale reinforced concrete structures have been used to develop the model in which the effect of inelastic response of the supporting structure is taken into account. The method was validated using the data measured in seven instrumented buildings during strong seismic motions and also verified analytically performing non-linear dynamic analysis of 6- and 12-storey reinforced concrete frames subjected to a set of 10 ground motions. The ground motions were scaled to three intensity levels to assess the effect of various level of inelasticity developed in the structure on the response of NSCs.

2.8 Experimental studies

Beside the numerical studies described above, some experimental studies on NSCs have been performed to qualify equipment, to investigate their seismic response when mounted on the building, and to verify some analytical studies. In general, experimental works can be categorized into two groups of tests. The first group refers to testing of secondary systems mounted on the primary system. This means the experiment is conducted on the integrated combined P-S system (See Figure 2.8). The second group relates to the testing of individual NSCs to evaluate their dynamic properties and load capacity. A few examples of experimental studies are works done by Craig and Goodno (1981) [50]; Kelly and Tsai (1985) [51]; Marsantyo, et al. (2000) [52]; Schneider, et al. (1982) [53].

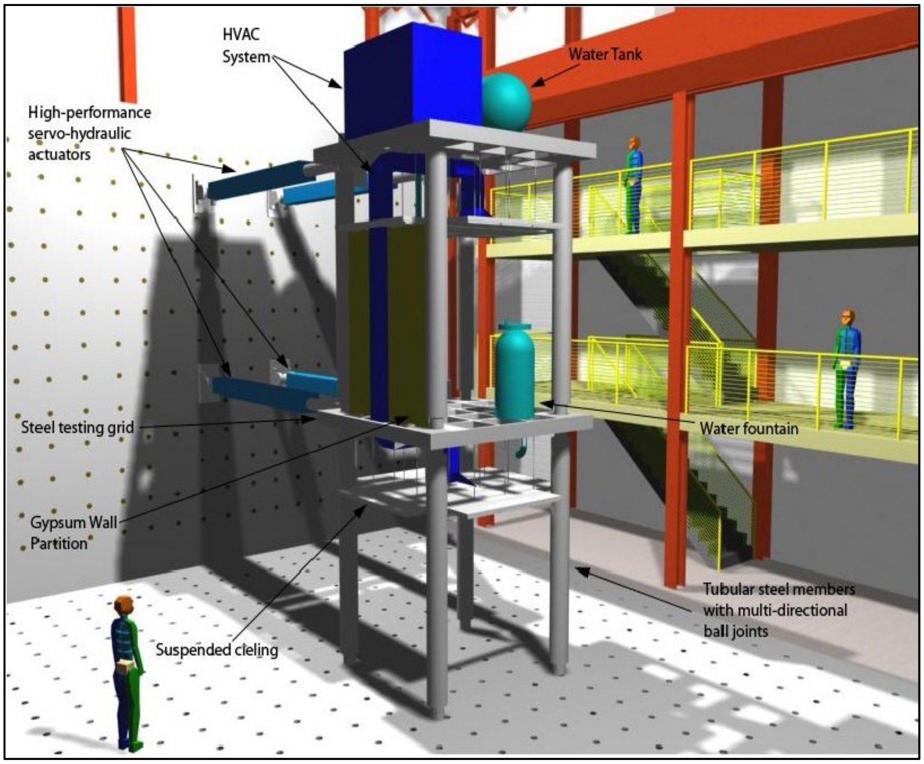

Figure 2.8 - Testing the integrated combined P-S system [54]

Craig and Goodno (1981) [50] conducted a series of experiments on full-scale glass cladding panels to measure their natural frequencies, mode shapes, and damping ratios. Their specimens consisted of a single-story section of a cladding system and included the mullions, spandrel framing, glazing materials, and four double-pane vision lights (2.51 x 1.45 x 0.0254 m).

Schneider et al. (1982) [53] performed shake-table tests on one-half scale piping system models typically used in nuclear reactor power plants and mounted on a three-storey steel frame. The experimental investigation addressed both simple and complex piping systems. The piping system was tested in its original design configuration using mechanical shock arrestors (snubbers), and in a revised configuration using ductile steel energy absorbers.

The effects of the snubbers and various energy absorbers on the dynamic response of the piping system were studied. The response of the structure was investigated under all three Cartesian components of ground motions. More than 100 tests were conducted in which four artificial earthquakes and sinusoidal excitations were used as inputs. The study addressed the damping behaviour, frequency spectra, and hysteresis loops for both shock arrestors and energy absorbers.

Kelly and Tsai (1985) [51] investigated the response of light equipment in structures isolated using rubber bearings, and compared it with the equipment's response in a fixed-base system. The test setup comprised three oscillators, representing light equipment, attached to the fifth floor of a 1/3 scale five-story frame mounted on four rubber, or lead-rubber, isolators. The total mass of the structure was 36,320 kg. Three isolators were used that weighted 36, 18, and 9 kg. The isolators were tuned to the fundamental natural frequency of the fixed frame, the second natural frequency of the base-isolated frame, and the third natural frequency of the base-isolated frame, respectively. The dynamic response of the equipment was studied in terms of the influence of fixed-base and isolated-base structure.

In the study by Marsantyo (2000) [52], the maximum acceleration amplification factor of NSCs mounted on a building floor was assessed through shake-table tests on two types of acceleration-sensitive components including building equipment and building contents. Four recorded strong earthquake motions were utilized as inputs. Various types of connections of NSCs to the floor were considered. Moreover, the effects of seismic base isolation in reducing the response of NSCs were evaluated.

2.9 **Building code and standards requirements for seismic design of NSCs**

2.9.1 General

Recent building codes address the seismic design of NSCs in new buildings. Some examples in the United States are the Uniform Building Code (UBC) [55], the National Earthquake Hazard Reduction Program (NEHRP) provisions [56], ASCE/SEI 7-10 [57], the Recommended Lateral Force Requirements and Commentary [58], and the American Society of Mechanical Engineers (ASME) boiler and pressure vessel code [59]. Examples of Canadian codes in this regard are CSAS832-06(R11) [60] and the National Building Code of Canada 2010 [61]. The older versions of NBCC also contained some provisions regarding the seismic design of NSCs in terms of the seismic force and inter-storey drift demand requirements [62].

Common limitations which can be pointed out concerning the recommendations of international codes for seismic design of NSCs are: 1- most of them neglect the effect of NSCs damping when estimating the acceleration demand, 2- They usually do not consider the effect of higher building modes in their NSCs force calculations although this can become important when dealing with high-rise buildings [63]. Some of these standards provisions for NSCs seismic design are discussed below.

2.9.2 Uniform Building Code

Since its inception in 1935, the UBC [55] of the United States has required the element of structures (e.g. infill walls and etc.), permanent NSCs, and their attachments (e.g. anchors and connections) to be designed for the lateral seismic force, F_p, calculated according to the following formula:

$$F_p = ZI_pC_pW_p$$ *Equation 2.2*

Where

Z = zone factor representing the expected peak ground acceleration with return period of 475 years.
I_p = Importance factor of NSCs, which is set equal to 1.0 and 1.5 for ordinary and critical components, respectively.
C_p= coefficient specified by the code, having a value ranging from 0.75 to 2.0 depending on the type of component or equipment.
W_p = total weight of the component.

C_p is intended to account for the dynamic amplification of the ground motion by the building for items located above grade. This equation is intended to be used in conjunction working stress design principles which are no longer in use in Canada. The suggested formula by UBC is mainly derived empirically and not based on structural dynamics principles. Hence, it does account for some important factors such as: 1- dynamic interaction; 2- the location of NSCs along the height of structure; 3- attachment configuration and the way the component is connected to the building; 4- tuning or detuning of NSCs with the primary structure ; 5- Cross-correlation and distortion between supports of multi-supported components; 6- Nonlinearity.

2.9.3 NEHRP Provisions (1994)

Similar to UBC, the United States NEHRP provisions [56] also provide minimum requirements for seismic design of NSCs and permanent components attached to the building and are intended to use in conjunction with ultimate stress design approach. The requirements are composed of two parts: a minimum required equivalent static force, F_p, and minimum relative displacement demand, D_p, for multiple-supported components. For static force calculations, two formulas are suggested: the first one is conservative and straightforward:

$$F_p = 4.0C_aI_pW_p \qquad \textit{Equation 2.3}$$

The second one is more comprehensive as it includes the effects of more parameters and generally yields lower forces than Equation 2.3

$$F_p = \frac{a_pA_pI_pW_p}{R_p} > 0.5C_aI_pW_p \qquad \textit{Equation 2.4}$$

Where

$$A_p = C_a + (A_r - C_a)(\frac{x}{h}) \qquad \textit{Equation 2.5}$$

and

$$A_r = (0.2A_s) \leq (4.0C_a) \qquad \textit{Equation 2.6}$$

The description of the variables of the above formulas is as follows:

F_p = seismic design force applied at the component's center of gravity.

a_p = component amplification factor specified in the provisions according to component type (varies between 1.0 and 2.5).

A_p = acceleration (expressed as a fraction of gravity) at the point of attachment to the structure.

I_p = component importance factor specified in the provisions according to component type (equal to either 1.0 or 1.5).

W_p = component operating weight.

R_p = component response modification factor specified according to component type (varies between 1.5 and 6.0).

C_a = seismic coefficient (expressed as a fraction of gravity) specified for the design of the structure (i.e. effective peak ground acceleration).

A_r = acceleration (expressed as a fraction of gravity) at the structure's roof level.

A_s = structural response acceleration coefficient (i.e. ground response spectrum ordinate), expressed as a fraction of gravity determined from equation:

$$A_s = \frac{1.2\ C_v}{T^{\frac{2}{3}}} \leq 2.5\ C_a$$

Equation 2.7

in which

C_v = velocity-related effective ground acceleration specified for structural design.

T = effective fundamental period of the structure in seconds.

The minimum relative displacement demand for multi-supported components is calculated as the minimum value of the following two recommended equations:

$$D_p = \left(\delta_{xA} - \delta_{yA}\right)$$

Equation 2.8

$$D_p = (X - Y)\ \Delta_{aA}/h_{sx}$$

Equation 2.9

where

D_p = relative seismic displacement between component supports.

δ_{xA}, δ_{yA}, δ_{xB}, δ_{yB} = deflections of building under design forces, multiplied by an amplification factor to account for inelastic deformations, at building levels x, y of buildings A, B.

X, Y = heights above grade of component supports at levels x, y.

Δ_{aA}, Δ_{aB} = allowable story drifts for buildings A, B.

h_{sx} = story height.

Comparing to the UBC recommendations, the NEHRP provisions are much improved as they take into account more effective parameters such as the amplification of ground motion at those points of the structure which are above grade, the location of NSCs along the height of building, some dynamic amplification caused by component characteristics, ductility and energy-absorption of NSCs, and also the expected performance of the components. However, this method has some limitations as well. As such, it accounts for the response amplification of NSCs using two separate amplification factors (i.e. one related to the structure and another specific to the NSCs). Hence, it is not fully accounting for the interaction between the two systems. The implication of different importance factors for the building and the NSCs is also not fully justified. The other deficiency relating to this provision is that it requires the satisfaction of both the maximum acceleration and relative displacement demands simultaneously which is overly conservative since indeed they do not happen at the same time: NSCs will typically undergo strong accelerations during the strong motion and large displacements after they have suffered some inelastic damage.

2.9.4 ASCE/SEI 7-10

In the ASCE 7-10 standards the design seismic force for NSCs is defined as:

$$F_p = \frac{0.4 a_p S_{DS} W_p}{\left(\frac{R_p}{I_p}\right)} (1 + 2\frac{z}{h})$$

Equation 2.10

F_p = seismic design force.

S_{DS} = spectral acceleration at short period (0.2 s).

A_p = component amplification factor that varies from 1.0 to 2.50.

I_p = component importance factor that can be 1.0 or 1.5 according to the type of NSCs.

W_p = component operating weight.

R_p = component response modification factor that varies from 1.0 to 12.

z = height in structure of point of attachment of component with respect to the base.

h = average roof height of structure with respect to the base.

There is also one alternative equation and recommendation for the displacement demand. The effects of seismic relative displacements shall be considered in combination with displacements caused by other loads as appropriate. Seismic relative displacements, D_{pI}, shall be determined as follows:

$$D_{pI} = D_p I_e \qquad \text{Equation 2.11}$$

where

I_e = the seismic importance factor of the building which can be 1.0, 1.25, or 1.5 according to the risk category assigned to the building.

D_p = displacement which is calculated according to two different recommendations explained below:

1- Displacements within structures: having two connection points on the same structure, for example structure A, one at a height h_x and the other at a height h_y. In this case, D_p is calculated according to this equation:

$$D_P = \Delta_{xA} - \Delta_{yA} \leq \frac{(h_x - h_y)\Delta_{aA}}{h_{sx}} \qquad \text{Equation 2.12}$$

2- Displacement between structures: having two connection points on separate structures, for example structures A and B, one at height h_x and the other at height h_y, D_p is calculated as follow:

$$D_p = |\delta_{xA}| + |\delta_{yB}| \leq \frac{h_x \Delta_{aA}}{h_{sx}} + \frac{h_y \Delta_{aB}}{h_{sx}} \qquad \textit{Equation 2.13}$$

where

D_p = relative seismic displacement that the component must be designed to accommodate

δ_{xA} = deflection at building Level x of Structure A.

δ_{yA} = deflection at building Level y of Structure A.

δ_{yB} = deflection at building Level y of Structure B.

h_x = height of Level x to which upper connection point is attached.

h_y = height of Level y to which lower connection point is attached.

Δ_{aA} = allowable story drift for Structure A as defined in the code.

Δ_{aB} = allowable story drift for Structure B as defined in the code.

h_{sx} = story height used in the definition of the allowable drift.

This ASCE standard indicates that a coupled analysis is not necessary if the NSCs mass is less than 1% of the supporting floor mass.

2.9.5 National Building Code of Canada 2010

The first edition of the NBCC in 1941 [64] contained seismic provisions in an appendix, based on concepts presented in the 1937 United States Uniform Building Code [65]. Specific provisions for seismic design of structural and non-structural components in buildings and essential facilities were first introduced only in the 1953 edition. In all editions of the NBCC, the provisions concerning the NSCs and non-structural components are given in part 4 for structural design and commentary J.

The most recent version is NBCC 2010 in which Clause 4.1.8.18 of NBC Division B Part 4 [66] covers the non-structural elements. It suggests the following equation to calculate the lateral equivalent static force, V_p, for which the components shall be designed:

$$V_p = 0.3 F_a S_a(0.2) I_E S_p W_p \qquad \textit{Equation 2.14}$$

Where

F_a = acceleration-based site coefficient of the building.

$S_a(0.2)$ = 5% damped spectral response acceleration, expressed as a ratio to gravitational acceleration, for a period of 0.2 s.

I_E = importance factor for the building.

$S_p = C_p A_r A_x / R_p$

S_p = seismic amplification factor of the component response; the maximum value of S_p shall be taken as 4.0 and the minimum value of S_p shall be taken as 0.7, where

C_p = seismic coefficient for mechanical/electrical equipment as recommended in code.

A_r = response amplification factor to account for type of attachment of mechanical/electrical equipment as recommended in code.

A_x = amplification factor at level x to account for variation of response of mechanical/electrical equipment with elevation within the building = $(1 + 2h_x / h_n)$.

R_p = element or component response modification factor.

W_p = weight of the component or element.

Regarding the displacement demand, NBCC 2010 stipulates maximum inter-story drifts at any level based on the lateral deflections obtained from linear elastic analysis. These limits are 1% for post-disaster buildings, 2% for schools and 2.5% for all other buildings. The lateral deflections obtained from an elastic analysis should be multiplied by R_dR_o/I_E to give realistic values of anticipated deflections, where R_d is the force overstrength factor and R_o represents the energy dissipation capacity of the element or its connections. I_E is the importance factor of the building. Further details about the improvement of design provisions for NSCs in Canada can be found in work by Assi [62].

2.9.6 Canadian Standard CSA-S832

CSA-S832-06 (CSA 2006) is the Canadian standard for the "Seismic risk reduction of Operational and Functional Components (OFCs) of buildings". This standard is used in conjunction with NBCC for the calculation of seismic demand parameters of NSCs of new buildings while it contains design provisions and guidelines for the seismic risk assessment and mitigation of NSCs in existing buildings. It recommends two approaches to deal with the seismic design of NSCs. They are:

1- Prescriptive approach: it provides general concepts for design and performance of NSCs and includes the application of typical details, provisions, seismic risk mitigation actions published in industry or manufacturer guidelines that describe the design concepts and construction features required to protect NSCs against seismic hazards. This approach is based on sound engineering standards and practices rather than analysis and calculations.

2- Analytical approach: it requires the seismic design of NSCs against the horizontal and vertical forces, drift ratios, and relative displacement induced by the earthquake. These seismic demand parameters can be calculated using:

a) Simplified approximate approaches based on the equivalent static force analysis method described in NBCC Division B Part 4 Clause 4.1.8.18

b) Rational refined methods which are based on engineering analysis, research, and experimentation. These methods duly account for the seismic response of the supporting buildings. They essentially include the methods described previously: floor response spectra, acceleration-time history analysis, elastic/inelastic analysis, and 2-D/3-D frame analysis. Refined methods are mandatory for NSCs with mass greater than 20% of that of the supporting floor (or structural component) or 10% of the total building mass.

2.10 **Experimental modal analysis: Ambient Vibration Measurements (AVM)**

As part of this research, experimental modal analysis is done using the AVM records collected on several post-disaster buildings located in Montreal. In AVM tests, the velocities induced by ambient excitations are recorded in two orthogonal horizontal directions and along the vertical by sensors placed at several locations (typically on floors and rooftop) in each building. Analysis of recorded data is carried out using two different operational modal analysis techniques, namely Frequency Domain Decomposition (FDD) and Enhanced Frequency Domain Decomposition (EFDD). The dynamic properties of the building including the lowest natural frequencies, corresponding mode shapes, and effective modal damping ratios, are extracted. These experimental dynamic properties accompanied with other structural parameters are then used as input to derive the response time-histories and subsequently the FRS for selected building floors under a set of synthetically generated ground accelerograms representative of the site. Further explanations concerning AVM and experimental modal analysis of buildings can be found in [67, 68].

2.11 **Literature review updates**

The literature review on the aforementioned subjects as well as the new topics related to the research study has been extensively updated through the course of the project. However as these updates will be fully described in the manuscripts included in the following chapters, they are not described here again solely to prevent any unnecessary repetitions. Hence, the readers are referred to the following chapters for the literature review updates.

2.12 **References**

1. Canadian Standard Association (CSA) *CAN/CSA-S832-06: Guidline for seismic risk reduction of operational and functional components (OFCs) of buildings*. 2006: Rexdale, ON, Canada.
2. Villaverde, R., *Fundamental concepts of earthquake engineering*. 2009, Boca Raton, FL: Taylor & Francis Group.
3. CSA, C.S.A., *Seismic risk reduction of operational and functional components (OFCs) of buildings, CAN/CSA-S832-06*. 2006.
4. BSSC, *The 2003 NEHRP Recommended Provisions For New Buildings And Other Structures Parts 1 and 2: Provisions and Commentary (FEMA 450).* ed. F.E.M. Agency. 2003, Washington DC: Building Seismic Safety Council.
5. Taghavi, S., *Response Assessment of Nonstructural Building Elements*, in *Department of Civil and Environmental Engineering*. 2003, Stanford University: Stanford, California. p. 96.
6. Sankaranarayanan, R., *Seismic response of acceleration-sensitive nonstructural components mounted on moment-resisting frame structures*, in *Department of Civil and Environmental Engineering*. 2007, University of Maryland: Maryland. p. 223.
7. National Research Council of Canada (NRC), Institute for Research in Construction (IRC), *National Building Code of Canada (NBCC)*. 2015: Ottawa, ON, Canada.
8. Hall, J., *Preliminary Reconnaissance Report, Northridge Earthquake, January 17, 1994.* Earthquake Engineering Research Institute, Oakland, Calif., Publication, 1994: p. 94-01.
9. FEMA E-74, *Reducing the Risks of Nonstructural Earthquake Damage – A Practical Guide*. 2011, FEDERAL EMERGENCY MANAGEMENT AGENCY: Washington, D.C.
10. Taly, N., *The Whittier Narrows, California Earthquake of October 1, 1987-Performance of Buildings at California State University, Los Angeles.* Earthquake Spectra, 1988. **4**(2): p. 277-317.
11. Soong, T. and D. Lopez Garcia. *Seismic Vulnerability and Protection of Nonstructural Components*. in *Proc. The Joint NCREE/JRC workshop on International collaboration on earthquake disaster mitigation research*. 2003.
12. Villaverde, R., *Seismic design of secondary structures: state of the art.* Journal of Structural Engineering, 1997. **123**(8): p. 1011-1019.
13. Chen, Y. and T. Soong, *Seismic response of secondary systems.* Engineering Structures, 1988. **10**(4): p. 218-228.
14. Villaverde, R. *Earthquake resistant design of secondary structures: a report on the state of the art*. in *Proc., 11th World Conf. on Earthquake Engineering*. 1996. Elsevier Science Ltd.
15. Singh, M., *Seismic design of secondary systems.* Probabilistic engineering mechanics, 1988. **3**(3): p. 151-158.
16. Villaverde, R., *Earthquake resistant design of secondary structures: a report on the state of the art*, in *Proc., 11th World Conf. on Earthquake Engineering*. 1996, Elsevier Science Ltd.: Acapulco, Mexico. p. 13.
17. Paskalov, A. and S. Reese, *Deterministic and probabilistic floor response spectra.* Soil Dynamics and Earthquake Engineering, 2003. **23**(7): p. 605-618.

18. Igusa, T. and A. Der Kiureghian, *Dynamic response of multiply supported secondary systems.* Journal of Engineering Mechanics, 1985. **111**(1): p. 20-41.
19. U.S. Nuclear Regulatory Commission, *Standard Review Plan*. 1975, US Nuclear Regulatory Commission, Office of Nuclear Reactor Regulation.
20. Preumont, A., *The generation of non-separable artificial earthquake accelerograms for the design of nuclear power plants.* Nuclear engineering and design, 1985. **88**(1): p. 59-67.
21. Kaul, M.K., *Spectrum-consistent time-history generation.* Journal of the Engineering Mechanics Division, 1978. **104**(4): p. 781-788.
22. Iyengar, R.N. and P.N. Rao, *Generation of spectrum compatible accelerograms.* Earthquake engineering & structural dynamics, 1979. **7**(3): p. 253-263.
23. Preumont, A., *The generation of spectrum compatible accelerograms for the design of nuclear power plants.* Earthquake engineering & structural dynamics, 1984. **12**(4): p. 481-497.
24. Singh, M., S. Singh, and S. Chu. *Stochastic concepts in seismic design of nuclear power plants*. in *Second Int. Conf. Structural Mechanics in Reactor Technology, Berlin*. 1973.
25. Singh, M. and S. Chu, *Stochastic considerations in seismic analysis of structures.* Earthquake engineering & structural dynamics, 1976. **4**(3): p. 295-307.
26. Biggs, J.M., *Seismic response spectra for equipment design in nuclear power plants*. 1971.
27. Singh, M.P., *Generation of seismic floor spectra.* Journal of the Engineering Mechanics Division, 1975. **101**(5): p. 593-607.
28. Singh, M.P., *Seismic design input for secondary systems.* Journal of the Structural Division, 1980. **106**(2): p. 505-517.
29. Kapur, K.K. and L.C. Shao. *Generation of seismic floor response spectra for equipment design*. in *Structural Design of Nuclear Plant Facilities 1973*. 1973. ASCE.
30. Biggs, J.M. and J. Roesset, *Seismic analysis of equipment mounted on a massive structure*. 1970, Massachusetts Inst. of Tech., Cambridge.
31. Amin, M., Hall, W.J., Newmark, N.M., Kassawara, R.P. *Earthquake response of multiply connected light secondary systems by spectrum methods*. in *Proceedings of the 1st ASME congress on vessels and piping, New York*. 1971.
32. Peters, K., D. Schmitz, and U. Wagner, *Determination of floor response spectra on the basis of the response spectrum method.* Nuclear engineering and design, 1977. **44**(2): p. 255-262.
33. Gupta, A.K. and J.M. Tembulkar, *Dynamic decoupling of secondary systems.* Nuclear engineering and design, 1984. **81**(3): p. 359-373.
34. Wang, Y., M. Subudhi, and P. Bezler, *Comparison Study of Time History and Response Spectrum: Responses for Multiply Supported Piping Systems*. 1983: Brookhaven National Laboratory.
35. Thailer, H., *Spectral analysis of complex systems supported at several elevations.* Journal of Pressure Vessel Technology, 1976: p. 98:162.
36. Villaverde, R., *Simplified approach for the seismic analysis of equipment attached to elastoplastic structures.* Nuclear engineering and design, 1987. **103**(3): p. 267-279.
37. Villaverde, R., *Approximate formulas to calculate the seismic response of light attachments to buildings.* Nuclear engineering and design, 1991. **128**(3): p. 349-368.

38. Newmark, N., *Earthquake response analysis of reactor structures.* Nuclear engineering and design, 1972. **20**(2): p. 303-322.
39. Asfura, A. and A.D. Kiureghian, *Floor response spectrum method for seismic analysis of multiply supported secondary systems.* Earthquake engineering & structural dynamics, 1986. **14**(2): p. 245-265.
40. Gupta, A.K., *Seismic response of multiply connected MDOF primary and MDOF secondary systems.* Nuclear engineering and design, 1984. **81**(3): p. 385-394.
41. Newmark, N.M. and R. Villaverde. *Computation of seismic response of light attachments to buildings*. in *7th World Conf. on Earthquake Engineering*. 1980. Ankara, Turkey.: Turkish Nat.
42. Aziz, T. and A. Ghobarah. *Equipment design: Future directions*. in *Proceedings 9th world conference on earthquake engineering*. 1988. Tokyo-kyoto, Japan.
43. Sewell, R.C., CA. Toro, GR. McGuire, RK. Kassawara, RP. Singh, A. Stepp, JC. *Factors influencing equipment response in linear and nonlinear structures*. in *Transactions 9th International Conference on Structural Mechanics and Reactor Technology*. 1989.
44. Singh, M.P.S., LE. Matheu, EE. Maldonado, GO., *Simplified procedures for seismic design of nonstructural components and assessment of current code provisions.* Technical Report NCEER, 1993(93-0013).
45. Newmark, N.M. and W.J. Hall, *Earthquake spectra and design*. 1982: Earthquake Engineering Research Institute.
46. Miranda, E. and V.V. Bertero, *Evaluation of strength reduction factors for earthquake-resistant design.* Earthquake Spectra, 1994. **10**(2): p. 357-379.
47. Lepage, A., J.M. Shoemaker, and A.M. Memari, *Accelerations of Nonstructural Components during Nonlinear Seismic Response of Multistory Structures.* Journal of Architectural Engineering, 2012. **18**(4): p. 285-297.
48. Medina, R.A., R. Sankaranarayanan, and K.M. Kingston, *Floor response spectra for light components mounted on regular moment-resisting frame structures.* Engineering Structures, 2006. **28**(14): p. 1927-1940.
49. Sankaranarayanan, R. and R.A. Medina, *Acceleration response modification factors for nonstructural components attached to inelastic moment-resisting frame structures.* Earthquake engineering & structural dynamics, 2007. **36**(14): p. 2189-2210.
50. Craig, J.I. and J.G. Barry, *Response measurements for glass cladding panels.* Journal of the Structural Division, 1981. **107(11)**: p.:2199-2214.
51. Kelly, J.M. and T. Hsiang-Chuan, *Seismic response of light internal equipment in base-isolated structures.* Earthquake engineering & structural dynamics 1985. **13(6)**: p. 711-732.
52. Marsantyo, R., T. Shimazu, and H. Araki. *Dynamic response of nonstructural systems mounted on floors of buildings*. in *Proceedings of the 12th World Conference on Earthquake Engineering (CD)*. January 30th to Februraruy 4th, 2000. Auckland, New Zealand.
53. Schneider, S., H.-M. Lee, and W.G. Godden, *Behavior of a piping system under seismic excitation. Experimental investigations of a spatial piping system supported by mechanical shock arrestors and steel energy absorbing devices under seismic excitation*. 1982, California Univ., Berkeley (USA). Earthquake Engineering Research Center: California, USA.

54. Mosqueda, G., et al., *EXPERIMENTAL EVALUATION OF NONSTRUCTURAL COMPONENTS UNDER FULL-SCALE FLOOR MOTIONS*, in *4th International Conference on Earthquake Engineering* 2006: Taipei, Taiwan.
55. International Conference of Building Officials, *Uniform building code*. 1997, International Conference of Building Officials: Whittier, California.
56. Building Seismic Safety Council, *NEHRP recommended provisions for seismic regulations for new buildings and other structures*. 2000, Building Seismic Safety Council.
57. American Society of Civil Engineers, *Minimum Design Loads for Buildings and Other Structures: ASCE Standard 7-10*. 2010: American Society of Civil Engineers.
58. Seismology Committee, *Recommended lateral force requirements and commentary*. 1990, Structural Engineers Association of California: San Francisco, Calif.
59. ASME boiler and pressure vessel code, *American Society of Mechanical Engineers.* New York, 1993. **10017**.
60. ASSOCIATION-CSA, C.S., *Seismic risk reduction of operational and functional components (OFCs) of buildings, CAN/CSA-S832-06*. 2006.
61. National Research Council Canada (NRC), I.f.R.i.C.I., *National Building Code of Canada (NBCC)*. 2010.
62. Assi, R., *Seismic analysis of telecommunication towers mounted on building rooftops*, in *Department of Civil Engineering and Applied Mechanics*. 2006, McGill University: Montreal. p. 348.
63. Sullivan, T.J., P.M. Calvi, and R. Nascimbene, *Towards improved floor spectra estimates for seismic design.* Earthquake and Structures, 2012.
64. National Building Code of Canada, *NRCC*. 1941, Associate Committee on the National Building Code: National Research Council of Canada, Ottawa, ON.
65. UBC, *Uniform building code*. 1935, International Conference of Building Officials (ICBO): Whittier, California.
66. National Research Council of Canada (NRC), Institute for Research in Construction (IRC), *National Building Code of Canada (NBCC)*. 2010: Ottawa, ON, Canada.
67. Brincker, R. and C. Ventura, *Introduction to operational modal analysis*. 2015: John Wiley & Sons.
68. Asgarian, A., *Impact of seismic retrofit and presence of terra cotta masonry walls on the dynamic properties of a hospital building in Montreal, Canada*, in *Department of Civil Engineering and Applied Mechanics*. 2012, McGill Univeristy: Montreal, Canada. p. 156.

Chapter 3

This chapter contains the detailed description of: 1-the collected RC buildings database and their extracted modal properties from AVM; 2- the adopted procedure for selection and scaling of the input earthquake excitation; 3- the characteristics of the twenty scaled ground accelerograms used in this study; 4- the extensive literature review and collection of the data recorded in all permanently instrumented buildings during past earthquakes and proposition of an appropriate set of modification factors to modify AVM-extracted modal properties of the building for higher amplitude excitations; 5- the development of the methodology to generate FRS and inter-story drift curves for the building floors and implementation of the method in MATLAB program [1]; and 6- the application of the method over the building database (Presentation of Building#15 results).

3 Generation of experimental floor response spectra for seismic assessment of Non-Structural Components (NSCs) using Ambient Vibration Measurements (AVM)

A. Asgarian[(1)], G. McClure[(2)]

[(1)] Ph.D. candidate, Department of Civil Engineering and Applied Mechanics, McGill University, Canada, amin.asgarian@mail.mcgill.ca

[(2)] Professor, Department of Civil Engineering and Applied Mechanics, McGill University, Canada, ghyslaine.mcclure@mcgill.ca

3.1 Abstract

Numerous experiences from past earthquakes in populated areas emphasize the necessity of a careful design and analysis of Non-Structural Components (NSCs) of buildings against seismically-induced forces and displacements. The good seismic performance of NSCs is of great importance to maintain post-earthquake functionality of post-critical buildings and to ensure life-safety protection of occupants, and also to avoid costly property damages during and after seismic events. In the last few decades, several analytical approaches have been developed for the seismic evaluation of NSCs in buildings. Moreover, most of the recent building codes and standards include some provisions and empirical seismic force equations for the seismic assessment and design of NSCs in buildings. However, these code recommendations have some shortcomings that make them either too imprecise or impractical. These shortcomings are addressed in this study and an original approach is proposed to generate experimental floor response spectrum and inter-story drift curves based on ambient vibration measurements. The proposed method improves the practicality and accuracy of seismic evaluation of NSCs in existing buildings in several ways. The method

is validated herein through a case-study of a hospital building located in Montreal, Canada, by comparing the numerical results derived from a detailed calibrated linear finite element model of the building and the experimental results produced using the proposed method. The procedure is then employed for a database comprising 27 real reinforced concrete buildings subjected to ambient vibration measurements. The methodology and the results are illustrated here in detail for one building and the effective parameters and advantages of the method are discussed.

Keywords: Operational and Functional Components (OFCs); Operational Modal Analysis (OMA); Earthquake Engineering; Seismic Assessment and Design.

3.2 **Introduction**

Observations of building damages in past earthquakes have highlighted the fact that achieving the overall good performance of buildings is contingent upon assuring the good performance of both the structural system and Non-Structural Components (NSCs) at the same time. While the structural components are designed to resist and transfer the building loads (gravity and lateral loads), the NSCs are not meant to be a part of the main load-bearing system of the building, although they may contribute in some instances (for example, masonry partitions). That is why in technical literature structural components are often referred to as "Primary system" or "Supporting structure" and NSCs as "Secondary system". NSCs can be sub-categorized according to their functions as: Architectural components, Building services (mechanical, electrical, and telecommunication equipment), and Building contents (common and specialized) [2, 3]. NSCs can also be classified into three different groups in accordance with the nature of their seismic response sensitivity as: 1- Inter-story-drift-sensitive components, 2- Floor-acceleration-sensitive components, and 3- both Inter-story-drift- and floor-acceleration-sensitive components [4].

In Canadian Standards Association CSA-S832 [2], NSCs are termed as Operational and Functional Components (OFCs) of buildings. This terminology emphasizes the fact that NSCs' damage/failure can limit the functionality of the buildings significantly following moderate to severe earthquakes. In general, the failure or malfunction of NSCs can give rise to undesired consequences that can be associated with:

1- Life safety: Collapse of NSCs can create a safety hazard and hamper the safety or the movement of passersby or building occupants as they evacuate, or of rescuers as they enter the building [5].

2- Building functionality: Seismic failure or malfunction of NSCs can severely limit the continuous functionality of critical facilities such as hospitals, emergency response and other essential facilities like those essential to telecommunications and electric power supply.

3- Property protection: NSCs represent a large portion of the total cost of buildings (e.g. 65% to 85% of the total cost depending on their use and occupancy according to [2, 4].), and their damage can result in large financial losses that can be of direct or indirect; direct losses are the costs associated with replacing or repairing the failed NSCs, while indirect losses result from business interruption.

Experiences and numerous observations from past earthquakes and current knowledge of the seismic performance of buildings indicate that NSCs are subjected to large seismically-induced forces and displacements or distortions that have to be taken care of by rational, reasonably precise, and yet practical seismic design and analysis procedures. This matter is of great importance as the performance of NSCs plays a vital role in the global seismic performance of buildings.

3.3 **Seismic design and analysis of NSCs**

3.3.1 Analytical approaches

Predicting the seismic response of NSCs is a challenging problem which has been of interest to many researchers and structural engineers of the past four decades. Although numerous efforts have been made to develop rational yet practical methods for seismic analysis of

NSCs, a consensus on a generally accepted approach has not been reached yet. The complexity of the problem arises from several factors including:1- Diverse dynamic characteristics of NSCs due to the various configurations of NSCs themselves and their anchoring systems, being single/multiple attachment point components; 2- Possible dynamic interaction between NSCs and the primary structural system; 3- Tuning effects, i.e. coincidence of the fundamental period of NSCs with one of the fundamental periods of the building causing resonance; and 4- Low internal damping of many NSCs compared to the primary system, which leads to a non-classical damping problem difficult to analyse.

The currently available approaches for seismic response analysis of OFCs can be classified in two general groups: 1- Floor Response Spectrum (FRS) approach, and 2- Combined Primary-Secondary System (CPSS) approach. The main difference between these two methods is the assumption of dynamic coupling or decoupling of the primary and secondary systems in the analysis. The FRS approach essentially assumes the primary and secondary systems as decoupled units and analyses them independently (i.e. no dynamic interaction is considered between them), while the CPSS approach analyses them as a coupled or combined unit, thus accounting for possible dynamic interactions. The FRS approach is considerably simpler, faster, and computationally more economical compared to the CPSS method since it avoids all the complexities caused by dynamic coupling. However, the FRS modeling method as currently used has the limitations of not considering: 1- Dynamic interactions between primary and secondary systems; 2- Non-classical damping effects; 3- Cross-correlation of response for multi-supported NSCs; and 4- the effects of the torsional response of the primary system on NSC response. The CPSS approach, however, will circumvent the aforementioned drawbacks of the FRS method by capturing the coupling effects and dynamic interactions between NSCs and their supporting structure but it will typically result in a coupled system with a large number of DOFs and non-classical damping problem, which has to be reanalyzed entirely every time a change is made in the NSC parameters. The use of the CPSS approach is also limited in structural engineering practice as the design of the structural (primary) system is not typically synchronized with the design of NSCs and their anchoring systems (special heavy industrial buildings and power plants are exceptions), and these two tasks may involve different teams of professionals, in most instances [3, 6, 7].

3.3.2 Building code and standard requirements

Beside the analytical approaches, recent building codes and standards also address seismic design and analysis of NSCs through recommendations and provisions for NSCs in existing buildings, and empirical force equations for seismic design of NSCs in new structures. Examples of the American codes with seismic design requirements for NSCs are the Uniform Building Code (UBC) [8], the National Earthquake Hazard Reduction Program (NEHRP) provisions [9], and ASCE/SEI 7-16[10]. Recommendations and guidelines are also presented in the National Building Code of Canada (NBCC) [11] and in CSA S832-14 [2] dedicated to operational and functional components in buildings.

In Canada, seismic design provisions for NSCs were first introduced in the 1953 edition of the NBCC [12] and afterwards, until 2015, every new edition included some improved requirements. The most recent, 2015 edition [11] classifies NSCs into 24 categories and addresses their seismic design by suggesting two sets of seismic requirements:

1. <u>Seismic force requirement:</u> An empirical equation based on the Uniform Hazard Spectrum (UHS) approach used for the design of structural components, is suggested to

calculate the minimum lateral equivalent static force for which the NSCs and their connections shall be designed [13, 14]:

$$V_p = 0.3F_aS_a(0.2)I_ES_pW_p \qquad \textit{Equation 3.1}$$

where F_a = acceleration-based site coefficient of the building, $S_a(0.2)$ = 5% damped spectral response acceleration, expressed as a ratio to gravitational acceleration, for a period of 0.2 s, I_E = importance factor for the building, $S_p = C_p A_r A_x/R_p$: S_p is a seismic amplification factor of the component response which should be in the range of 0.7 to 4.0, C_p = component factor accounting for the risk associated with the failure of the components, A_r = response amplification factor accounting for the dynamic amplification of the component relative to the position of its attachment to the building structure, A_x = amplification factor at level x to account for variation of the component response with its elevation within the building = $(1 + 2h_x/ h_n)$, R_p = component response modification factor representing the energy dissipation capability of the component and its connection to the structure; and W_p = weight of the component. The values of C_p , A_r , and R_p for each category of components are stipulated in NBCC 2015.

2. <u>Seismic displacement requirement:</u> Regarding the displacement demand, NBCC 2015 contains only requirements in terms of inter-story drift limits at any level based on the lateral deflections obtained from linear elastic analysis of the building. These limits are $0.01*h_s$ for post-disaster buildings (I_E = 1.5), $0.02*h_s$ for high-importance buildings (I_E = 1.3) and $0.025*h_s$ for all other buildings of normal importance category (I_E = 1.0).

CSA-S832 [2] “Seismic risk reduction of operational and functional components (OFCs) of buildings” is a Canadian Standards Association code that is to be used in conjunction with the NBCC seismic requirements. These codes and standards share the same limitations mentioned above for the FRS approach, namely: 1- they neglect the effect of NSC damping when estimating the acceleration demand; 2- they ignore the effect of a building's higher frequency modes, which can be of importance to assess the response of NSCs in high-rise buildings [15]; 3- they ignore the effect of the torsional motion of the building on the seismic response of NSCs, which can be of significance for those NSCs located in the periphery of irregular structures; 4- they assume a linear variation of the floor acceleration over the building height, which is rarely accurate; and 5- they calculate the NSC seismic design force based on the spectral acceleration at a fixed short period of 0.2 s, considering that most components in buildings are stiff or rigid, while a more accurate and less conservative approach is to consider the natural periods of NSCs, tuning, detuning, and resonance effects.

3.4 **Experimental modal identification using Ambient Vibration Measurements (AVM)**

The modal parameters of building structures, i.e. their natural frequencies, modal damping ratios and mode shapes, play a key role in predicting their seismic response and, subsequently, the response of their supported NSCs. Thanks to technological advances in sensing techniques, AVM has become a well-known, robust, and reliable technique to derive dynamic properties of buildings without disrupting their normal operation. During AVM tests, the velocities/accelerations induced by ambient excitations such as wind, traffic, micro tremors, etc. are recorded at several pre-selected locations (measurement points) at each or pre-selected building floors depending on the test setup arrangement using highly sensitive sensors. AVM records of motion are taken in two orthogonal horizontal directions and along the vertical. The recorded data are typically analyzed using two different operational modal analysis techniques- namely, Frequency Domain Decomposition (FDD) and Enhanced Frequency Domain Decomposition (EFDD), and the in situ dynamic properties of the building including its lowest natural frequencies, corresponding mode shapes, and effective modal damping ratios, are extracted. In this study, these experimental dynamic properties are then used as input parameters to derive the response time-history and subsequently the FRS for selected floors of the buildings. Further details pertaining to AVM and experimental modal analysis of buildings can be found in [16-19].

The extracted modal properties from AVM records are only valid strictly for a linear building response starting from its current in situ state. Such a linear response would be experienced when the building is subjected to small intensity earthquakes, or, if the building was designed as a post-critical structure or as a high importance structure, a linear response would also be expected also under moderate earthquakes. Recognizing the decrease of natural frequencies as the building suffers structural damage, some studies have proposed modification factors to translate AVM-extracted natural frequencies into frequencies more representative of damaged buildings. Using these modification factors, the proposed method is adapted to higher ground shaking levels as described in section 3.5.4.

3.5 **Methodology**

3.5.1 Description of the proposed experimentally-derived FRS method

As discussed above, in spite of the research efforts devoted to seismic analysis of NSCs, modern building codes and standards still do not reflect our current level of understanding of the seismic behavior of these components. The code provisions for seismic design and analysis of NSCs typically use empirical methods with several force modification coefficients which are, for the most part, based on past experience, engineering judgment and expert opinions, rather than on objective experimental and analytical results. The lack of significant advances in design code recommendations or guidelines may be attributed to the fact that the previously developed analytical methods are too cumbersome to be employed in the design of ordinary NSCs (and their connections) housed in conventional buildings. An effective solution to this problem is to introduce an analysis method which is rational and reasonably accurate to reflect the real building characteristics on the one hand, and simple enough to be utilized in existing buildings, on the other hand, without cumbersome modeling. Such an approach could involve the use of floor design spectra to assess the seismic performance of NSCs in existing buildings. It could also serve to derive improved design procedures for NSCs in new structures.

NBCC 2015 includes the most recent seismic hazard data for building design in the form of a Uniform Hazard Spectrum (UHS). However, floor design spectra for NSC design (NSC-FRS) compatible with the UHS of NBCC are currently not available. In this study, an original approach is proposed to fill this gap by generating the NSC-FRS of buildings based on experimental data obtained from AVM in buildings.

This research project was initiated by collecting modal data from an inclusive database of buildings in which AVM testing had been already conducted by others. Initially, it was intended to cover different types of lateral load resisting systems (LLRS) (i.e. Reinforced Concrete (RC) buildings and steel structures) but as most of the measured buildings in the database comprised RC structures, the focus was narrowed down to only RC buildings covering various height levels (low, medium, and high rise buildings) – see section 3.5.2. The AVM data recorded on the selected buildings have then been reanalyzed and the dynamic properties of the buildings have been extracted utilizing commercial software ARTeMIS Extractor™ [20]. For each building, the mass and in-plane rotary inertia of the building floors (and roof) have been estimated according to the dimensions available from structural and architectural drawings. The extracted modal properties and the estimated mass\inertia of the building floors establish the input parameters required for the 3D-SAM approach developed by Mirshafiei and McClure [21, 22]. Using this approach, the floor response histories of the building subjected to a set of twenty synthetic ground accelerograms, compatible with UHS of NBCC 2015 for Montréal, are derived in two perpendicular horizontal directions and are subsequently assumed as base excitations for NSCs to develop their FRS. The selection and scaling process of seismic inputs are explained in section 3.5.3.

The procedure has been coded in MATLAB [1] to generate the elastic FRS and inter-story drift curves at every floor of the building in both orthogonal horizontal (X and Y) directions, and considering NSCs with several damping ratios (0, 2, 5, 10, and 20 % of critical viscous damping) having a fundamental period range of [0-4] seconds with intervals of 0.02 s (damping ratios, period range, and intervals are user-defined in the program). Direct integration with Newmark's linear acceleration method was adopted to solve the equation of motion of NSCs [23], where the beta and gamma parameters of the integrator were set as 0.25 and 0.5, respectively to preserve the unconditional stability of the operator; other values can also be user-selected in the program to generate algorithmic damping. The dynamic analysis proceeds over the entire set of seismic records and the mean and mean ± standard deviation results are calculated and plotted. Another output of the program is the envelope FRS curve, constructed on the basis of the response parameters of NSCs in X and Y directions at each natural period.

The proposed method has been validated in detail with the case study of a pediatric hospital campus located in Montréal, Canada. The detailed linear elastic finite element model of one of the buildings has been generated in SAP 2000 v.14.0.0 [24]. The building has been tested by AVM and its dynamic characteristics have been extracted. The numerical building model has then been calibrated (its stiffness has been adjusted) to match the extracted dynamic properties. For validation, given the same seismic inputs, two sets of FRS and inter-story drift curves have been generated, one using the calibrated numerical model, and another using the proposed experimental AVM method. The comparison of the results from the two procedures has shown consistency; a detailed description of the validation process has been presented in [25]. The last milestone of the study is to compare the derived FRS with the corresponding UHS and develop a mathematical model to predict the FRS directly from UHS, taking into account the effect of parameters such as elevation of NSC along the height of the building, natural period and damping ratio of NSC, tuning effect, and soil site condition of the building foundation. Developed FRS can be served as a robust tool to address seismic performance of acceleration-sensitive NSCs. Consideration of nonlinear building response during earthquakes is presented in a future communication where the proposed method based on AVM data is adapted to higher forced vibration and base shaking levels.

3.5.2 Description of the building AVM database

Achieving the objectives of the study necessitates a database of buildings in which AVM is conducted. Hence, the first step of the project was to collect an inclusive database of the tested buildings covering different types of lateral load resisting systems (LLRS) and various heights in which AVM records had already been collected by other research assistants of the McGill University team. The complete database is comprised of 156 AVM-tested buildings located on the island of Montreal, Canada. From this number, a subset of 59 structures has met the initial quality and data completeness criteria required for the proposed approach, namely sufficient quality of AVM results including adequate number of extracted modes, clearly defined mode shapes and reasonable values for natural frequency and damping ratio estimates, proper AVM test-setup arrangements and adequate number of measurement points at each floor, availability of architectural and structural drawings to determine floor masses, to name the most important. Further refinements and filtering have been done on the database to select the most comprehensive and clear cases in terms of data quality. As a result, the final version of the database includes 27 RC structures including 12 low-rise, 10 medium-rise, and 5 high-rise buildings, with their AVM-extracted properties as indicated in Table 3-1.

Table 3-1 - Building characteristics and AVM results

Building category	Building #	LLRS type	Construction year	H_A / H_B (m)	N_A / N_B	Mode 1		Mode 2		Mode 3		NBCC period (s)
						Translational mode		Translational mode		Torsional mode		
						AVM Period (s)	AVM ξ (%)	AVM Period (s)	AVM ξ (%)	AVM Period (s)	AVM ξ (%)	
Low-rise buildings	1	RCSW	1969	6.5 / 1.5	1 / 1	0.15	1.15	0.13	1.81	0.12	0.16	0.20
	2	RCSW	1969	6.5 / 1.5	1 / 1	0.27	4.10	0.24	1.90	NA	NA	0.20
	3	RCMF	1957	8.6 / 6.4	2 / 1	0.15	2.90	0.12	1.40	0.10	2.40	0.38

	4	RCMF	1957	7.7 / 3.3	2 / 1	0.18	1.50	0.18	1.30	0.10	2.00	0.35
	5	RCMF	1963	7.5 / 2.7	2 / 1	0.20	1.18	0.16	1.55	0.11	0.42	0.34
	6	RCMF	1963	7.5 / 2.7	2 / 1	0.18	2.53	0.13	1.17	NA	NA	0.34
	7	RCMF	1963	7.5 / 2.7	2 / 1	0.18	3.17	0.14	2.14	0.11	0.75	0.34
	8	RCMF	1993	8.4 / 3.3	2 / 1	0.19	2.00	0.18	1.80	0.13	2.10	0.37
	9	RCMF	1961	8.4 / 4.7	2 / 1	0.23	1.70	0.21	1.70	0.16	3.30	0.37
	10	RCMF	1964	17.1 / NA	2 / 1	0.38	3.60	0.38	3.90	0.15	1.40	0.63
	11	RCMF	1975	10.8 / 2.7	3 / 1	0.15	2.00	0.13	2.30	0.11	1.60	0.45
	12	RCMF	1964	13.0 / 4.1	3 / 1	0.38	4.10	0.38	4.00	0.23	2.90	0.51
Medium-rise buildings	13	RCMF	1967	13. 0/ 2.2	4 / 1	0.22	1.44	0.19	1.08	0.11	0.67	0.51
	14	RCMF	1964	12.0 / 3.1	4 / 1	0.18	2.72	0.15	2.70	0.12	0.09	0.48
	15	RCMF	1975	18.6 / 2.4	4 / 1	0.30	2.00	0.22	2.30	0.18	1.60	0.67
	16	RCMF	1975	15.9 / 5.1	4 / 2	0.30	2.00	0.22	2.90	0.18	2.60	0.60
	17	RCMF	1969	18.1 / 0.0	5 / 0	0.29	0.81	0.29	0.39	0.16	0.20	0.66
	18	RCSW	1998	19.6 / 3.6	5 / 1	0.40	2.32	0.36	1.66	0.28	2.76	0.47
	19	RCMF	1961	20.2 / 3.1	7 / 1	0.36	1.74	0.32	1.34	0.30	1.09	0.71
	20	RCMF	1961	20.2 / 3.1	7 / 1	0.37	1.42	0.31	0.75	0.29	1.01	0.71
	21	RCMF	1962	20.2 / 3.1	7 / 1	0.37	1.63	0.31	1.41	0.28	1.07	0.71
	22	RCSW	1971	28.0 / 6.7	7 / 2	0.59	3.61	0.46	4.35	0.36	1.72	0.61
High-rise buildings	23	RCMF	1957	36.0 / 3.5	10 / 1	0.53	1.72	0.40	1.22	0.37	1.09	1.10
	24	RCMF	1965	45.6 / 7.4	13 / 2	1.30	3.70	1.03	3.3	0.96	3.70	1.32
	25	RCSW	1969	55.4 / 8.4	13 / 2	0.70	1.79	0.68	1.70	0.41	2.04	1.01
	26	RCSW	1978	51.2 / 6.3	16 / 2	0.96	1.89	0.87	1.78	0.42	1.30	0.96
	27	RCMF	1965	58.7 / 7.9	18 / NA	1.25	2.54	1.03	2.87	0.94	2.15	1.59

RCSW = Reinforced Concrete Shear Wall system, RCMF = Reinforced Concrete Moment-resisting Frame system, H_A = Height above ground level (m), H_B = Height below ground level (m), N_A = Number of floors above ground level, N_B = Number of floors below ground level, ξ = Modal damping ratio (percentage). The NBCC period is that obtained using the empirical seismic period formula prescribed in the code: $T_n = 0.075(h_n)^{3/4}$ for RCMF and $0.05(h_n)^{3/4}$ for RCSW.

3.5.3 Description of the ground motion records

In this study, the buildings are subjected to a set of 20 seismic records compatible to UHS of Montreal for site class "C" (stiff soil with average shear wave velocity of 360 m/s < $\bar{V}_{s30}$ < 760 m/s) corresponding to probability of exceedance of 2% in 50 years, as defined by NBCC 2015 [11]. The seismic inputs have been selected from the reference time-history library developed by Atkinson [26] (available from: www.seismotoolbox.ca) and have been scaled accordingly. The records are synthetically generated using the stochastic finite-fault implementation of Atkinson and Bore [27]. Ground motions for eastern Canada are simulated for moment magnitude of M6 at fault distances from 10-15 km (M6 set 1), 20-30 km (M6 set 2), and for M7 at 15-25 km (M7 set 1) and 50-100 km (M7 set 2). For each of these record sets, three random components were simulated at 15 randomly drawn locations around the fault for a total of 4 sets × 3 components × 15 realizations = 180 simulations for each site class condition. M6 events in the 10–30 km distance range match the short-period end of the UHS, whereas M7 events at a somewhat larger distance (but within the same range) match the long-period end of the UHS for eastern Canada locations in regions of moderate-to-high seismicity (such as Montreal). As NBCC [11] dynamic analysis procedure requires a minimum number of 11 ground motions to be matched with the target spectrum or UHS, 20 records comprising 5 records from each set (i.e. M6 sets 1&2 and M7 sets 1&2) have been selected and scaled as follows [26]:

1. The target UHS is defined for the appropriate locality and site conditions according to NBCC 2015 (SA_{targ}) which is the UHS of Montreal for site class C in this case.
2. The period range of interest over which the target spectrum should be matched is selected. The M6 sets (lower magnitude events) are used to match the UHS for period

range of [0.1-0.5] s, whereas the M7 (higher magnitude records) are to match the UHS over periods of [0.5-2] s. Considering these recommendations and the fundamental periods of the buildings (see Table 3-1), different scenarios of period ranges have been tested for M6 and M7 record sets and in each instance, the averaged spectrum was compared to the UHS of Montreal. The comparison showed that the period ranges of [0.15-0.4] s for M6 records and [0.5-1.32] s for M7 ones provide the best fit to the target UHS of Montreal for site class C.

3. For each record within the appropriate set, the ratio of SA_{target}/SA_{sim} is computed at every period throughout the range of interest (SA_{sim} stands for the spectrum of the simulated record).
4. The mean and standard deviation of the spectral acceleration ratios of step 3 are calculated over the corresponding period range of interest for each ground motion record.
5. The records with lowest standard deviation (best shape) and mean of SA_{target}/SA_{sim} ratios in the range of [0.5-2.0] s are selected. In this study, the 5 best-fitting records have been selected from each record set.
6. Finally, every point of the selected records is scaled by the corresponding mean SA_{target}/SA_{sim} factor.

The scaling and selection procedure have been implemented in a MATLAB code. The program takes the period ranges of interest, records sets, and number of records to be selected as the user-defined inputs and it provides the scaled records to be used in the analysis as outputs. The details of the selected records are listed in Table 3-2 and the comparison of their mean and mean ± standard deviation spectra with the target UHS of Montreal is shown in Figure 3.1.

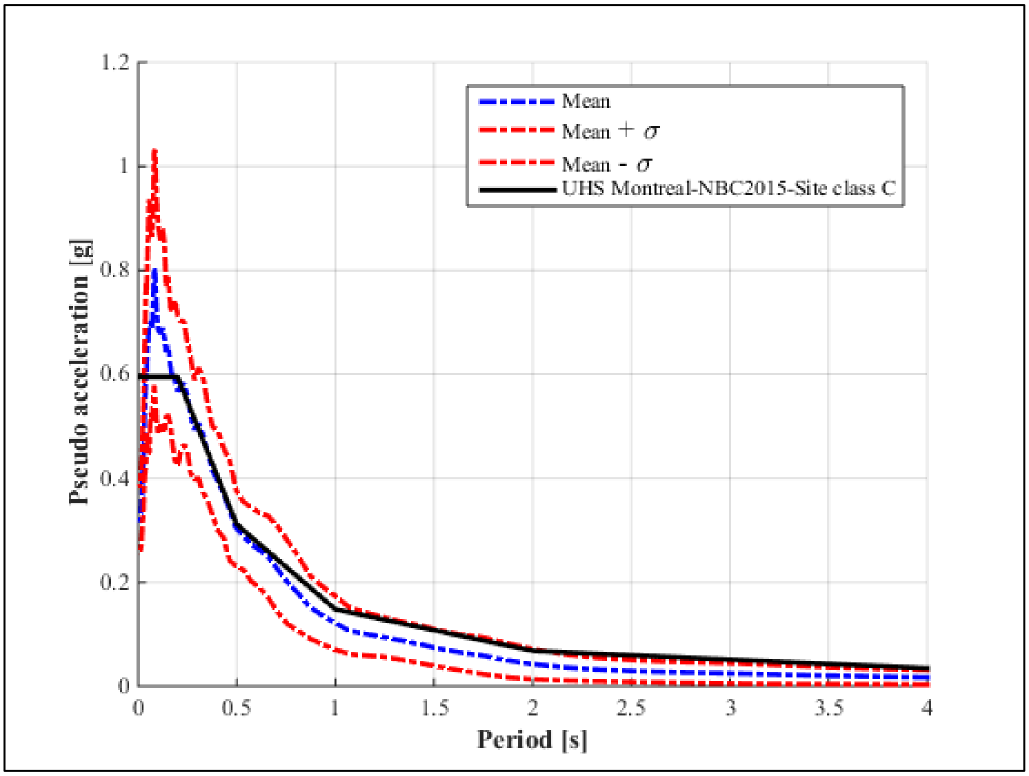

Figure 3.1 - Comparison of mean spectrum of scaled records with UHS of Montreal (Canada) for site class C.

Table 3-2- Characteristics of the scaled synthetic ground motion records

Record #	Magnitude M	Fault distance (km)	PGA (g)	PGV (cm/s)	Δt (s)	Length (s)	Return period (years)
1	6	16.6	0.47	13.59	0.002	43.598	2500
2	6	12.5	0.38	12.52	0.002	43.598	2500
3	6	10.7	0.35	11.93	0.002	43.598	2500
4	6	12.8	0.34	12.01	0.002	43.598	2500

5	6	14.4	0.32	12.07	0.002	43.598	2500
6	6	16.9	0.32	14.90	0.002	47.53	2500
7	6	26.1	0.32	10.17	0.002	47.53	2500
8	6	16.9	0.35	13.79	0.002	47.53	2500
9	6	16.9	0.28	10.78	0.002	47.53	2500
10	6	21.6	0.31	12.48	0.002	47.53	2500
11	7	25.6	0.31	17.48	0.002	51.126	2500
12	7	19.6	0.29	15.28	0.002	51.126	2500
13	7	17	0.38	15.58	0.002	51.126	2500
14	7	17	0.36	16.61	0.002	51.126	2500
15	7	25.8	0.32	18.91	0.002	51.126	2500
16	7	41.6	0.27	15.99	0.002	57.352	2500
17	7	41.6	0.29	18.49	0.002	57.352	2500
18	7	50.3	0.21	12.69	0.002	57.352	2500
19	7	95.5	0.21	15.22	0.002	57.352	2500
20	7	45.2	0.21	10.53	0.002	57.352	2500

3.5.4 Modification of building modal parameters for higher-amplitude ground motions

The modal building properties including natural frequencies, modal damping ratios and mode shapes are the most essential factors to predict the dynamic response of the building and, subsequently, that of its supported NSCs. It has been shown in several studies such as in Celebi [28-30], Todorovska *et al.* [31, 32], and Dunand *et al.* [33] to name a few, that these parameters vary with the intensity/amplitude of the input excitation. These variations are referred to as "wandering" of the natural frequencies of the structure [34]. Hence, the dynamic properties extracted from low-amplitude excitations (PGA < 10^{-5}g) such as in AVM are expected to be different from those derived from high-amplitude shaking (PGA > 0.1g) such as observed in significant earthquakes. By increasing the intensity level of seismic excitation, the natural frequencies are decreased and the modal damping ratios are increased while the mode shapes are not altered much as long as no localized collapse happens. Wandering of the natural frequencies and damping ratios can be attributed to: 1- softening of the building due to damages and non-linear behaviour of the building (e.g. micro-cracking of concrete at foundation and superstructure); 2- possible soil-structure interactions; 3- slippage of steel connections; and 4- interaction between the structural system and NSCs. Slight changes in modal parameters, in the range of 1-4 % differences, can also be caused by ambient conditions, being weather variables such as temperature, wind, rainfall, nearby traffic or normal building operations [34, 35].

Decreased building natural frequencies during the main seismic shock have been observed to increase again and being recovered partly or completely during the aftershocks; suggesting system recovery. This can be associated with: 1- changes in the bond between soil and foundation, 2- dynamic compaction of the soil and dynamic settlement, and 3- elastic recovery of the building if undamaged [32].

A simple approach to enable extrapolation of the dynamic properties of the building as extracted from AVM (low-amplitude excitation) for predicting the seismic response of the primary and secondary systems during strong shaking (high-amplitude excitation), is to develop a set of appropriate modification factors applicable to AVM-extracted results. These modification factors can be derived from the data collected in permanently instrumented buildings during earthquakes where the building has not suffered visible structural damage. The variation of the modal parameters of instrumented buildings before, during, and after earthquakes has been the subject matter of several studies, as summarized next (in chronological order):

1. Çelebi *et al.* (1993), Çelebi (1996, 2007, and 2009) [28-30, 36]: They have compared the modal properties of five buildings extracted from AVM and from strong motion records. All five buildings are located in the San Francisco Bay area, CA. The AVM tests were all conducted in September 1990 and their response during the 1989 Loma Prieta EQ had also been recorded. The selected buildings are: 1- Administration building of California State University at Hayward (CSUH), a Steel Moment Resisting Frame (SMRF) core with exterior Reinforced Concrete Moment-resisting frame (RCMF) with 13 floors and 61 m height; 2- the Santa Clara County Office Building (SCCOB), SMRF with 12 floors and 57 m height; 3- an office building in San Bruno (SBR), RCMF with 6 floors and 24 m height; 4- the Transamerica building in San Francisco (TRA), SMRF with 60 floors and 257 m height; and 5- the Pacific Park Plaza building in Emeryville (PPP), RCMF 30 floors and 94 m height. The range of variations observed during strong shaking compared to AVM tests was [13-35] % decrease in the natural frequencies and [60-500] % increase in the damping ratios.
2. Trifunac *et al.* (2001) [37]: This study has evaluated the strong motion data recorded in the Hollywood Storage Building, in Los Angeles, CA (a 14 story RCMF building constructed in 1925). This is the oldest strong motion recording building site in

California. The data reviewed in this report covers a period of 61 years of measurements, between October of 1933 and January of 1994. The comparison of the natural frequencies extracted from AVM (1938) to the ones derived during the weak-to-strong ground motions experienced by the building shows a natural frequency decrease of [15-45] % in the north-south direction (weak direction) and of [5-37] % in the east-west direction (strong direction)..

3. Hao *et al.* (2004) [38]: 13 instrumented buildings on the University Park and Health Sciences Campuses of University of Southern California, both located near downtown Los Angeles, have been investigated in this study. The results show the expected trend of decreasing building frequency with increasing amplitudes of earthquake shaking, indicating "softening" of the system. The study reports a decrease of [5-40] % in natural frequencies of the buildings during 19 seismic records.
4. Todorovska *et al.* (2004 and 2006) [31, 32]: they have studied 21 instrumented buildings in Los Angeles, CA during several earthquakes including 1994 Northridge (M_S=6.7), 1971 San Fernando (M_L=6.6), 1987 Whittier Narrows (M_L=5.9), and some of their aftershocks as well as other seismic events. The maximum and minimum values of the fundamental frequencies of the buildings were measured in two horizontal directions during the events. The general observed trend was again a decrease the building natural frequency during the main shock and recovery in the aftershocks. For most buildings of the database, the frequency decreased by approximately 25%, and the change did not exceed 30% for any of them.
5. Dunand *et al.* (2004, 2005, and 2006) [33, 39, 40]: they have studied 12 instrumented buildings located in Los Angeles, CA and in San Francisco Bay area; half of them having

a RC frame structure and the other half a steel frame. The number of stories is varying from 4 to 13 for RC buildings and from 5 to 48 for steel buildings. The observed decrease in natural frequencies during earthquakes of high intensity (PGA over 200 to 500 cm/s^2) did not exceed 40% for RC buildings and 30% for steel buildings. Damping values measured during the earthquakes are mostly larger than the ambient vibration damping values for RC buildings.

6. Clinton *et al.* (2006) [34]: In this study, two instrumented buildings of the Caltech campus in Pasadena, CA have been measured, namely the Robert A. Millikan Library and the Broad Center. The Millikan Library is a nine-story building constructed in 1967 with total height of 43.9 m above grade and 48.2 m above basement level. The structural system is RCMF and RCSW. The Broad Center is a three-story building constructed in 2002 and instrumented since February 2003. Its basements are enclosed by stiff shear walls, and the steel superstructure is braced with stiff unbounded braces in both the north–south and east–west directions. The study reports a decrease of [1-31] % in natural frequencies recorded during earthquakes compared to the ones obtained from forced-vibration tests conducted prior to seismic events.
7. Boroschek and Lazcano (2008), and Carreño and Boroschek (2011) [35, 41]: These two papers relate to the study of the Chilean Construction Chamber Building, a 22-story RCSW building located in Santiago, Chile which has been instrumented since 1995. These studies present the modal parameter variations of the building during 55 low-to-high intensity earthquakes. A decrease of [4-35] % in natural frequencies is reported for the seismic records experienced by the building during the period of

observation. Regarding the observed variations in modal damping ratios, increasing values with increasing motion-amplitude are observed - an increase of the order of 50% for the first translational modes and over 120% for the building higher modes. In the case of low-to-moderate earthquakes, these variations disappeared when the strong shaking ended suggesting system recovery. A preliminary study of the building properties during the Mw=8.8 earthquake that occurred in Maule, Chile in 2010 has also been done. During this very strong earthquake, the modal frequencies of the building decreased up to 35% for the first translational modes and after the event, 18% of permanent decrease has remained, attributed to structural damage.

8. Singh *et al.* (2014) [42]: The instrumented building in this study is the Regional Passport Office Staff Quarters (RPOSQ) building in Ahmedabad, India. The building, constructed in 1996 and completed in 2000, is a RCMF with total height of 30 m above ground and 10 stories. The strong shaking results show a 25 % decrease in natural frequencies on average and [6-360] % increase in damping ratios. The frequencies extracted from the AVM test conducted after the earthquake approach to the measured frequencies at the beginning of the earthquake, indicating almost full elastic recovery.

After a careful review of the aforementioned studies, a database of all the evaluated instrumented buildings has been collected comprising the results of 56 buildings (including RC and steel structures). As the present study is mainly focused on RC structures, only RC instrumented buildings have been considered to determine the appropriate strong shaking modification factors. Information on the instrumented RC buildings collected from the literature is summarized in Table 3-3. Due to space limitations, only the data of the first two modes are presented in the table.

Table 3-3 - Summary of recorded data in instrumented RC buildings

Building	**N_A/N_B**	**Event**	**Measurement type**	**Mode 1**			**Mode 2**			**Ref.**
				Translational mode			**Translational mode**			
				f (Hz)	**ξ (%)**	**AVG. frequency ratio**	**f (Hz)**	**ξ (%)**	**AVG. frequency ratio**	
Commercial office building	6/0	1989 Loma Prieta EQ	SMR	1.17	7.2	0.68	0.98	4.1	0.70	[28-30, 36]
		1989 Loma Prieta EQ	AVM-Post-EQ	1.72	2.2		1.41	2.3		
Pacific Park Plaza	30/1	1989 Loma Prieta EQ	SMR	0.38	11.6	0.69	0.38	15.5	0.69	
		1990 AVM	AVM	0.48	0.60		0.48	3.4		
		1985 FVM	FVM	0.59	1.7		0.6	1.8		
		1985 AVM	AVM	0.59	2.6		0.59	2.6		
Hollywood Storage Building,	14/1	1938 AVM	AVM	0.83	-	0.69	2	-	0.79	[37]
		Low-to-Moderate EQs	SMR	0.7	-		1.9	-		
		Strong EQs	SMR	0.45	-		1.25	-		
Vivaian Hall	7/1	EQs	SMR-F_{max}	1.59	-	0.82	1.65	-	0.74	[38]
		EQs	SMR-F_{min}	1.31	-		1.22	-		
Webb Tower	14/1	EQs	SMR-F_{max}	0.75	-	0.65	0.77	-	0.64	
		EQs	SMR-F_{min}	0.49	-		0.49	-		
Flour Tower	11/0	EQs	SMR-F_{max}	1.34	-	0.69	1.75	-	0.74	
		EQs	SMR-F_{min}	0.93	-		1.3	-		
Waite Phillips Hall	11/1	EQs	SMR-F_{max}	1.08	-	0.77	1.23	-	0.74	
		EQs	SMR-F_{min}	0.83	-		0.91	-		
Pardee Tower	8/0	EQs	SMR-F_{max}	3.05	-	0.90	4.05	-	0.92	
		EQs	SMR-F_{min}	2.75	-		3.71	-		

Parking Structure A	6/0	EQs	SMR-F_{max}	2.16	-	0.83	2.48	-	0.87	
		EQs	SMR-F_{min}	1.79	-		2.16	-		
Hoffman Medical Center	9/1	EQs	SMR-F_{max}	1.64	-	0.68	1.65	-	0.75	
		EQs	SMR-F_{min}	1.11	-		1.24	-		
Whittier Lutheran Tower	10/-	1987 Whittier Narrows	SMR	0.69	7.1	0.59	1.63	1.7	0.84	
		1994 Northridge	SMR	0.76	6		1.22	8.1		
		2004 AVM	AVM	1.22	1.6		1.7	1.3		
Great Western Savings	13/-	1989 Loma Prieta	SMR	0.85	4	0.75	1.11	5.2	0.82	
		2004 AVM	AVM	1.13	1.8		1.35	1.4		
Pacific Park Plaza	30/-	1989 Loma Prieta	SMR	0.36	3.4	0.77	0.97	7.9	0.71	[33, 39, 40]
		2004 AVM	AVM	0.47	2.1		1.36	2.2		
San Fransico VA Hospital	6/-	1989 Loma Prieta	SMR	2.94	8.5	0.81	2.89	6.2	0.90	
		2004 AVM	AVM	3.61	2.5		3.21	3.7		
Loma Linda VA Hospital	4/-	1994 Northridge	SMR	3.58	7.4	0.99	4.08	7.9	1.05	
		2004 AVM	AVM	3.61	-		3.87	-		
Livermore VA Hospital	6/-	1989 Loma Prieta	SMR	2.7	0.6	0.59	4.5	0.7	-	
		2004 AVM	AVM	4.6	-		-	-		
Regional Passport Office	10/-	EQ	SMR	1.26	-	0.73	1.47	-	0.77	[42]
		AVM	AVM-Post-EQ	1.72	-		1.91	-		
Chilean Chamber of Construction Building	22/3	2010 Chile EQ	AVM-Pre-EQ	1.01	0.60	0.90	1.03	0.70	0.98	[35, 41]
		2010 Chile EQ	SMR	0.64	-		0.61	-		
		2010 Chile EQ	AVM-Post-EQ	0.84	0.60		0.86	0.60		
		24-01-1997 Chile EQ	SMR	0.986	2.7		1.002	1.7		
		20-04-1997 Chile EQ	SMR	0.996	1.5		0.996	1.5		
		19-06-1997 Chile EQ	SMR	1	1.7		1.02	1.4		
		14-10-1997 Chile EQ	SMR	0.967	1.4		0.977	1.5		

		12-01-1998 Chile EQ	SMR	0.972	1.4		1.005	1.6		
Robert A. Millikan Library	9/-	1967 FVM	FVM	1.45	-	0.86	1.9	-	0.88	[34]
		1970 Lytle Creek EQ	SMR	1.3	-		1.88	-		
		1971 San Fernando EQ	SMR	1	-		1.64	-		
		1974 FVM	FVM	1.21	-		1.77	-		
		1987 Whittier Narrows EQ	SMR	1	-		1.33	-		
		1988 FVM	FVM	1.18	-		1.7	-		
		1991 Sierra Madre EQ	SMR	0.92	-		1.39	-		
		1993 FVM	FVM	1.17	-		1.69	-		
		1994 Northridge EQ	SMR	0.94	-		1.33	-		
		1994 FVM	FVM	1.15	-		1.67	-		
		1995 FVM	FVM	1.15	-		1.68	-		
		2001 Beverly Hills EQ	SMR	1.16	-		1.68	-		
		2002 FVM	FVM	1.11	-		1.64	-		
		2002 FVM	FVM	1.14	-		1.67	-		
		2003 Big Bear EQ	SMR	1.07	-		1.61	-		
		2001-2003 continuous AVM	AVM	1.19	-		1.72	-		
		2003 San Simeon EQ	SMR	1.14	-		1.54	-		

EQ = Earthquake event, SMR: Strong motion record during the earthquake event, FVM = Forced Vibration Measurement, Pre-EQ = Measurement done prior to the earthquake event, Post-EQ = Measurement done after the earthquake event, SMR-F_{max} = Maximum natural frequency recorded during the earthquake event, SMR-F_{min} = Minimum natural frequency recorded during the earthquake event.

Looking at the collected data partly presented in Table 3-3, the following conclusions can be made:

I. <u>First mode of vibration</u>: 1- natural frequencies are decreased by [1-41] % and damping ratios are increased by a factor of [1.6-10.2] for the set of weak-to-strong ground motions, 2- the average decrease in natural frequencies is 24 %, and 3- damping ratios are increased by a factor of 4.0 on average.

II. Second mode of vibration: 1- a decrease of [0-36] % in the natural frequencies and an increase by a factor of [1.7-6.4] in damping ratios are observed, 2- natural frequencies are decreased by 19% and damping ratios are increased by a factor of 3.3 on average.

III. The mode shapes are not changed from ambient to strong vibration levels contingent upon the occurrence of no significant localized damage in the structure.

Considering the above margins, four different sets of modification factors have been considered to evaluate the impact of the variation in natural frequencies and damping ratios of building (caused by various intensity-level of ground motions), on the response of its NSCs. It should be noted that the modification factors are applied to the natural frequencies and damping ratios extracted from AVM. These four scenarios are as described next:

Case 1 - No modification factor: which means the original modal properties (i.e. natural frequencies and damping ratios) extracted from AVM are used without any alteration.

Case 2 - Decreasing natural frequencies by 10% and increasing modal damping ratios by a factor of 2.

Case 3 - Decreasing natural frequencies by 20% and increasing modal damping ratios by a factor of 3.

Case 4 - Decreasing natural frequencies by 30% and increasing modal damping ratios by a factor of 4.

Building#15 of the Montreal database (see Table 3-1) has been selected for the sake of presenting these four different cases and their effect on NSCs response parameters. The building has been subjected to the ensemble of 20 seismic records described in section 3.5.3. Then, FRS and inter-story drift curves have been generated for each scenario according to the proposed method and compared to each other. The building description and the results are explained in the following sections.

3.6 **Description of Building # 15 and its AVM results**

General structural information and the dynamic characteristics of building#15 extracted from AVM are summarized in Table 3-4. The AVM test was previously conducted on the building by Mirshafiei [21]. The coordinate system and North direction (N) adopted for the analysis are as shown below in the plan and elevation views. The floor plan changes at various levels of the building but the typical plan is as depicted. Black dots on the plan represent the location of the measurement points/sensor positions. Using two operational modal analysis techniques - namely, FDD and EFDD, the modal properties of the first three modes of vibration of the building have been extracted from AVM records. In the mode shape illustration, the blue color shapes show the building at rest and the green color represents the deformed modal shape of the building, corresponding to the extracted natural frequency.

Table 3-4 - Structural information and AVM results of Building # 15

Building # 15			
LLRS type	RCMRF	Construction year	1975
H_A / H_B (m)	18.6 / 2.4	Typical plan dimension (m)	
N_A / N_B	4 / 1	L = 46	W = 32
Typical plan view		**Elevation view**	

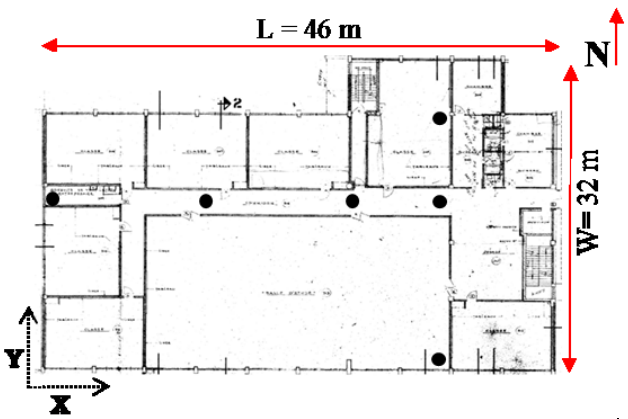

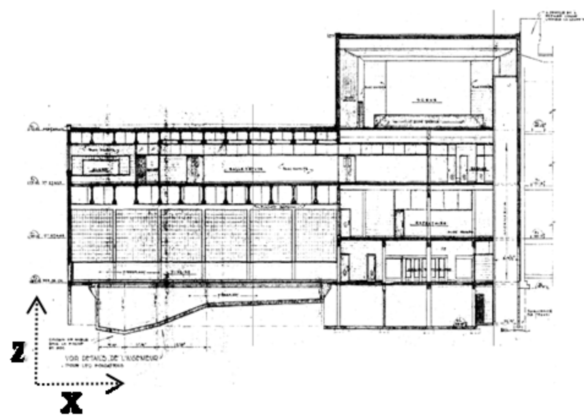

Modal properties extracted from AVM					
Mode 1 - Translation in X dir.		Mode 2 - Translation in Y dir.		Mode 3 - Torsion	
f = 3.38 Hz	ξ = 2.0 %	f = 4.52 Hz	ξ = 2.3 %	f = 5.47 Hz	ξ = 1.6 %

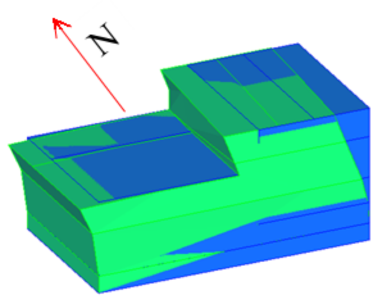

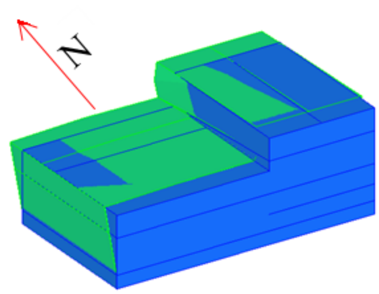

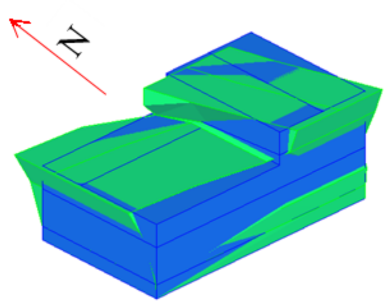

3.7 Results and discussion

The natural frequencies and modal damping ratios of Building #15 extracted from AVM have been adjusted according to the modification factors of cases 1 through 4 listed in Table 3-5. For each case, the building has been subjected to the ensemble of 20 seismic records (see section 3.5.3) in both orthogonal horizontal directions (i.e. X and Y), independently. FRS curves in terms of displacement, velocity, acceleration, pseudo-velocity, and pseudo-acceleration and inter-story drift curves have been generated at every floor of the building, in both the X and Y directions, for each seismic input and considering different NSC damping ratios as described in section 3.5.1. Due to space limitation, only the envelope FRS curves in terms of pseudo-accelerations (Figure 3.2) and inter-story drift curves (Figure 3.3) are presented for a 5% NSC damping ratio. On the FRS graphs, the minimum and maximum accelerations recommended by NBCC 2015 for seismic design of NSCs are also included for comparison. To compute the NBCC accelerations, C_p, R_p, I_w, and W_p factors are removed from Equation 3.1 (all values taken as 1) to be consistent with the results of proposed method. Consequently, the maximum and minimum values are calculated according to Equation 3.2. Lastly, it should be noted that the results are the averaged responses over the set of 20 records.

$$NBCC - Acceleration = 0.3F_aS_a(0.2)A_rA_x \qquad \textit{Equation 3.2}$$

Table 3-5 - Modified modal properties of Building #15

Case	Frequency modification factor	Damping modification factor	Mode	Natural frequency (Hz)	Damping ratio (%)
Case 1 (AVM)	1	1	1	3.4	2.0
			2	4.5	2.3
			3	5.5	1.6
Case 2	0.9	2	1	3.0	4.0
			2	4.1	4.6
			3	4.9	3.2
Case 3	0.8	3	1	2.7	6.0
			2	3.6	6.9
			3	4.4	4.8
Case 4	0.7	4	1	2.4	8.0
			2	3.2	9.2
			3	3.8	6.4

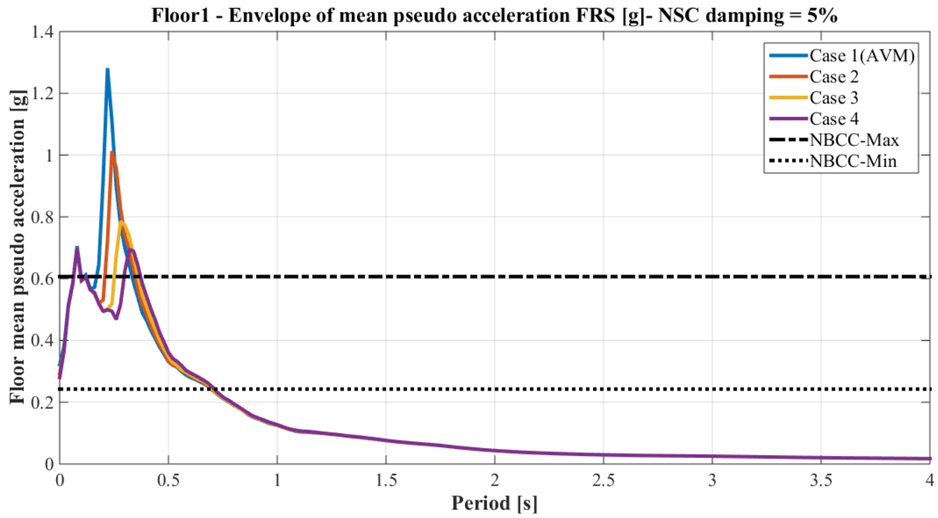
Floor1 - Envelope of mean pseudo acceleration FRS [g]- NSC damping = 5%
Floor mean pseudo acceleration [g]
Period [s]
0
0.2
0.4
0.6
0.8
1
1.2
1.4
0.5
1.5
2
2.5
3
3.5
4
Case 1(AVM)
Case 2
Case 3
Case 4
NBCC-Max
NBCC-Min

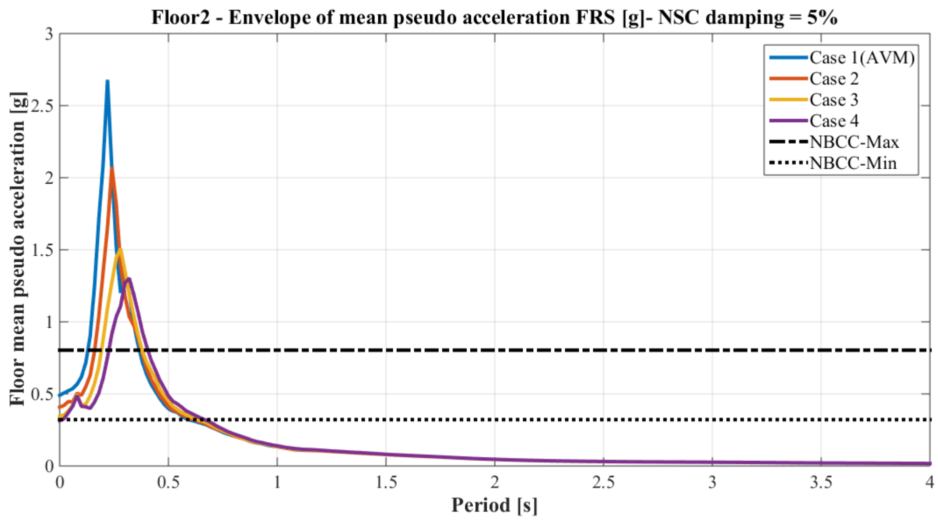
Floor2 - Envelope of mean pseudo acceleration FRS [g]- NSC damping = 5%
Floor mean pseudo acceleration [g]
Period [s]
0
0.5
1
1.5
2
2.5
3
3.5
4
Case 1(AVM)
Case 2
Case 3
Case 4
NBCC-Max
NBCC-Min

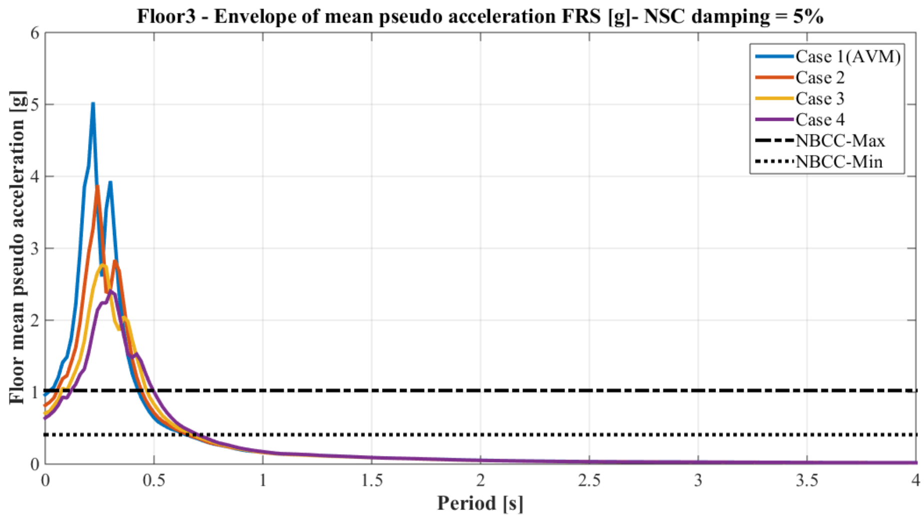
Floor3 - Envelope of mean pseudo acceleration FRS [g]- NSC damping = 5%
Floor mean pseudo acceleration [g]
Period [s]
0
1
2
3
4
5
6
0.5
1.5
2.5
3.5
Case 1(AVM)
Case 2
Case 3
Case 4
NBCC-Max
NBCC-Min

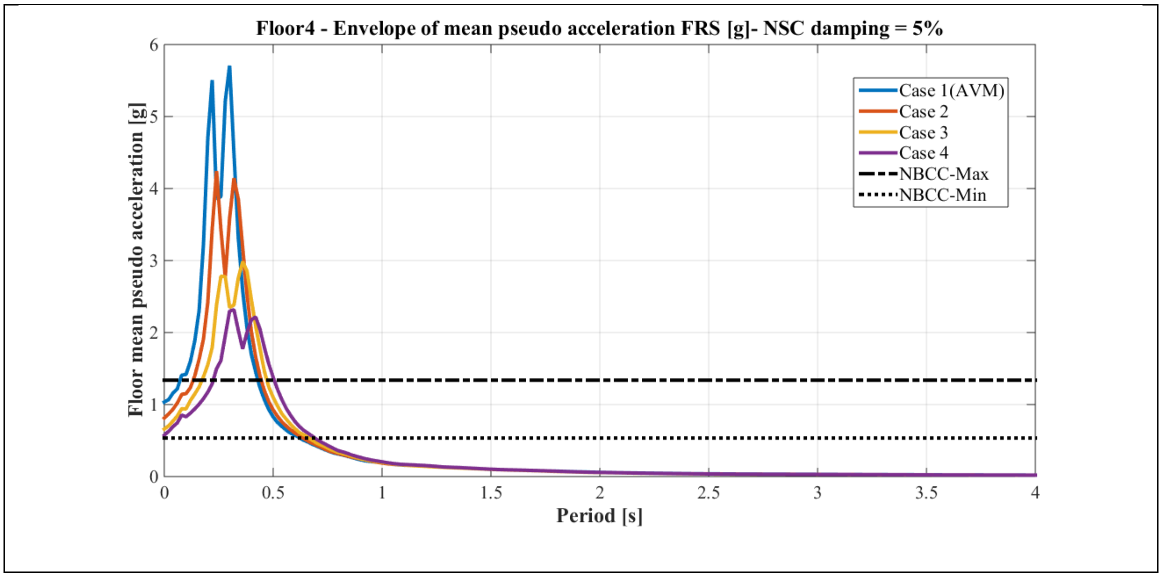

Figure 3.2 – Building#15: Envelope graph of pseudo acceleration FRS curves [g], NSC damping = 5 %.

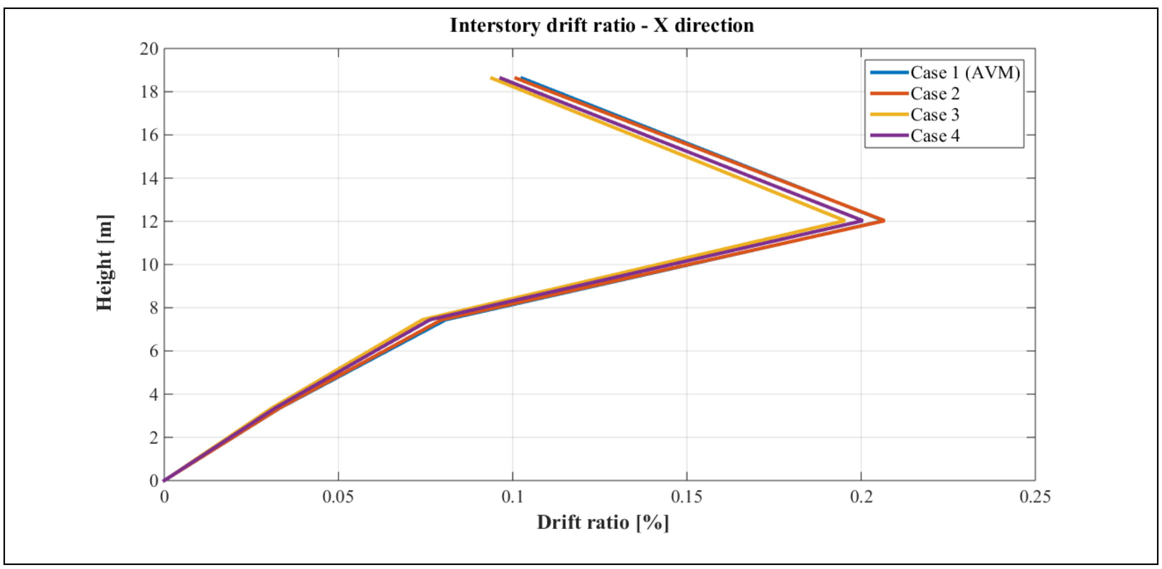

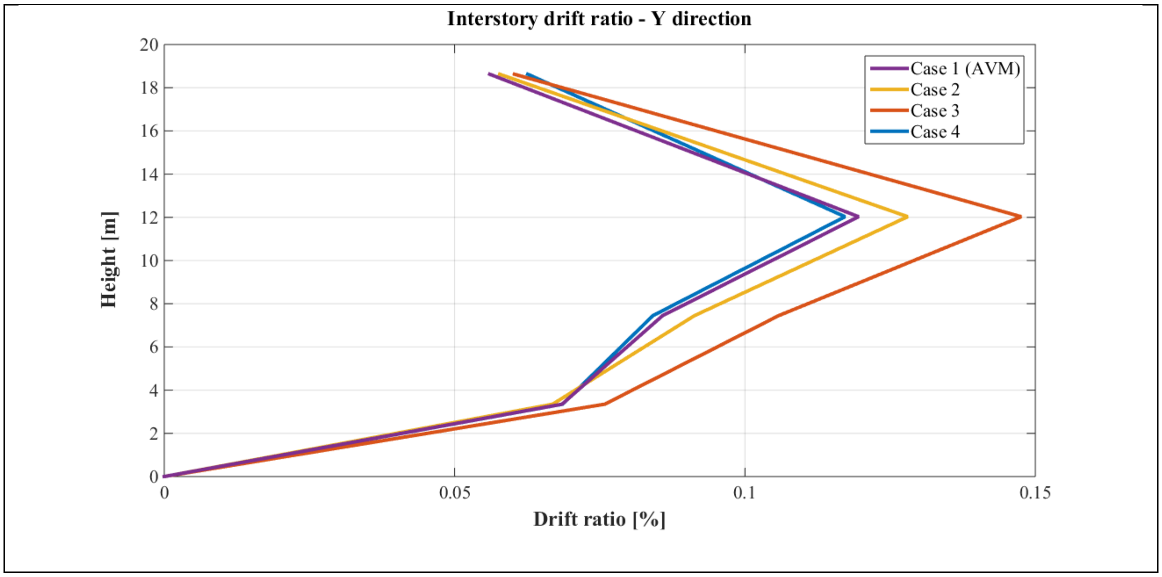

Figure 3.3 – Building#15: Averaged inter-story drift ratio curves in X and Y direction, NSC damping = 5%.

Observing Figure 3.2 and Figure 3.3 leads to the following conclusions:

- In general, the peaks in FRS envelope curves are attributed to the natural periods of the building (translational modes in X and Y directions and torsional mode) which are wandering toward larger periods moving from case 1 (AVM) to case 4 (30% decrease in natural frequencies). It is observed that there is a peak associated with the torsional mode of vibration while such effect is disregarded in international building design codes and standards including NBCC 2015: This is of high importance particularly in irregular structures where torsional effects are predominant. If a calculated peak is not associated with any modal frequency, it may be caused by the high frequency content of the seismic input.
- As expected, increasing the damping ratios decreases both the acceleration and displacement responses (due to increased energy dissipation) while increasing the natural periods tends to decrease the acceleration response and increase the displacement response due to the reduction in the global lateral stiffness of the

building. For the variation in frequency (or period), attention should be paid to the frequency content of the input ground accelerogram. If wandering of the building frequency causes a shift toward the region with larger frequency content of the input excitation, an increasing trend in the response might result.

- The effect of the modification of natural periods and damping ratios is more evident in the pseudo-acceleration response (Figure 3.2) than the drift response (Figure 3.3). It is due to the fact that increasing natural period and damping will have a similar trend to decrease the acceleration response while they have counteracting effects on the displacement response (which causes the drifts of cases 1 to 4 to be close).
- The Montreal building database mostly comprises post-disaster buildings (selected schools and community centers designated as emergency shelters) which should not undergo severe damages to remain operational throughout and after seismic events. In addition, these buildings are all located in a region with moderate seismicity according to NBCC UHS. Therefore, case 4 is not a good representation of the aforementioned conditions as it is associated with severe (possibly some permanent) structural damage occurring during strong ground motions. Excluding case 4 and considering the slight difference between cases 2 and 3 in terms of drift response, it is deemed reasonable to adopt the modification factors of case 2 and the rest of the database modal properties have been modified accordingly. It should be noted that the response parameter under study, which is either acceleration/force or displacement/drift, has a key role in selecting the appropriate set of modification factors. Here, as the main focus is on deriving

pseudo acceleration FRS, case 2 which results in most conservative outputs is adopted.

- Comparing the maximum acceleration value of NBCC 2015 with the experimental results indicates that Equation 3.2 underestimates the seismic force that is exerted to the NSCs whose natural frequency is in the vicinity of one of the natural frequencies of the primary system. This underestimation is even observable compared to case 4 that results in the lowest acceleration responses. Considering the minimum acceleration value recommended by NBCC, the underestimation is even more severe for the low period range of [0-0.7] s.

3.8 **Conclusions**

The study proposes an original approach to generate the experimental floor response spectra (FRS) and inter-story drift curves for non-structural components (NSCs) based on building modal properties extracted from ambient vibration measurements (AVM). The accuracy of the experimentally-derived FRS method has been validated through a case-study of a hospital building located in Montreal, Canada by comparing the detailed experimental and numerical results. Furthermore, an appropriate set of modification factors for natural frequency and damping ratios have been determined and validated through a case-study of a different building (#15 in Table 3-1) to extend the method to higher levels of ground shaking intensity. The proposed method is shown to be efficient and fast compared to time-consuming detailed numerical simulations as it does not require generating numerical models of the buildings (which is of course still necessary for buildings at the design stage).

Compared to the conventional FRS approach and current building code recommendations, the proposed method has several advantages and improvements including: 1- Dynamic interactions between the NSC and the building are taken into account as the method is based on AVM conducted during the normal operation of the building when NSCs are all in place. Hence, if there is any interaction between primary and secondary systems, its effect would be captured in AVM; 2- The method is capable of considering the effects of higher building modes and torsional behaviour of the primary system on NSC response; 3- The cross-correlation in floor motions is considered in the inter-story drift curves that are useful to assess the drift-sensitive components; and 4- FRS are generated using the real dynamic properties of building (frequencies and damping ratios) extracted from AVM and for various damping ratios considered for NSCs. The proposed method is a promising practical tool to evaluate the seismic behaviour and performance of NSCs in existing buildings undergoing low to moderate structural damage during design-level earthquakes.

3.9 References

1. The MathWorks Inc., *MATLAB*. 2014: Natick, MA.
2. Canadian Standard Association (CSA) *CAN/CSA-S832-06: Guidline for seismic risk reduction of operational and functional components (OFCs) of buildings*. 2006: Rexdale, ON, Canada.
3. Villaverde, R., *Fundamental concepts of earthquake engineering*. 2009, Boca Raton, FL: Taylor & Francis Group.
4. Taghavi, S., *Response Assessment of Nonstructural Building Elements*, in *Department of Civil and Environmental Engineering*. 2003, Stanford University: Stanford, California. p. 96.
5. Charleson, A., *Architectural design for earthquakes–a guide to the design of non-structural elements.* New Zealand Society for Earthquake Engineering (NZSEE), Wellington, 2007.
6. Chen, Y. and T. Soong, *Seismic response of secondary systems.* Engineering Structures, 1988. **10**(4): p. 218-228.
7. Singh, M., *Seismic design of secondary systems.* Probabilistic engineering mechanics, 1988. **3**(3): p. 151-158.

8. UBC, *Uniform building code*. 1935, International Conference of Building Officials (ICBO): Whittier, California.
9. National Earthquake Hazard Reduction Program (NEHRP), *Recommended provisions for seismic regulations for new buildings and other structures*. 2000, Building Seismic Safety Council: Washington, D.C.
10. American Society of Civil Engineers, *ASCE Standard 7-16: Minimum Design Loads for Buildings and Other Structures*. 2016, American Society of Civil Engineers: Reston, VA.
11. National Research Council of Canada (NRC), Institute for Research in Construction (IRC), *National Building Code of Canada (NBCC)*. 2015: Ottawa, ON, Canada.
12. National Building Code of Canada, *NRCC*. 1953, Associate Committee on the National Building Code: National Research Council of Canada, Ottawa, ON.
13. Adams, J. and G. Atkinson, *Development of seismic hazard maps for the proposed 2005 edition of the National Building Code of Canada.* Canadian Journal of Civil Engineering, 2003. **30**(2): p. 255-271.
14. Adams, J. and S. Halchuk, *Fourth generation seismic hazard maps of Canada: Values for over 650 Canadian localities intended for the 2005 National Building Code of Canada.* Geological Survey of Canada, 2003. **4459**: p. 1-155.
15. Sullivan, T.J., P.M. Calvi, and R. Nascimbene, *Towards improved floor spectra estimates for seismic design.* Earthquake and Structures, 2013. **4**(1): p. 109-132.
16. Oppenheim, A.V., R.W. Schafer, and J.R. Buck, *Discrete-time signal processing*. Vol. 1999. 1989: Prentice hall Englewood Cliffs, NJ.
17. Brincker, R., L. Zhang, and P. Andersen, *Modal identification of output-only systems using frequency domain decomposition.* Smart materials and structures, 2001. **10**(3): p. 441.
18. Gilles, D., *In situ dynamic characteristics of reinforced concrete shear wall buildings*, in *Department of Civil Engineering and Applied Mechanics*. 2011, McGill University: Montreal,QC. p. 295.
19. Asgarian, A., *Impact of seismic retrofit and presence of terra cotta masonry walls on the dynamic properties of a hospital building in Montreal, Canada*, in *Department of Civil Engineering and Applied Mechanics*. 2012, McGill Univeristy: Montreal, Canada. p. 156.
20. Structural Vibration Solution, *ARTeMIS Extractor, Software for Operational Modal Analysis*. 2010.
21. Mirshafiei, F., *A novel three-dimensional seismic assessment method (3DSAM) for buildings based on ambient vibration testing*, in *Department of Civil Engineering and Applied Mechanics*. 2015, McGill University: Montreal, Canada. p. 195.
22. Mirshafiei, F. and G. McClure, *Modified three-dimensional seismic assessment method for buildings based on ambient vibration tests: extrapolation to higher shaking levels and measuring the dynamic amplification portion of natural torsion.* Earthquake Engineering & Structural Dynamics, 2016.
23. Chopra, A.K. and F. Naeim, *Dynamics of Structures—Theory and Applications to Earthquake Engineering*. Earthquake Spectra. Vol. 23. 2007. 491.
24. Computers and Structures, I.C., *SAP 2000-advanced 14.0.0*. 2009: Berkeley. California.
25. A. Asgarian, F. Mirshafiei, and G. McClure, *Experimental floor response spectra for seismic evaluation of operational and functional components of building*, in *CSCE 2014, 4th International Structural Specialty Conference*. 2014: Halifax, NS, May 28 to 31. p. 10.

26. Atkinson, G.M., *Earthquake time histories compatible with the 2005 National building code of Canada uniform hazard spectrum.* Canadian Journal of Civil Engineering, 2009. **36**(6): p. 991-1000.
27. Atkinson, G.M. and D.M. Boore, *Earthquake ground-motion prediction equations for eastern North America.* Bulletin of the Seismological Society of America, 2006. **96**(6): p. 2181-2205.
28. Çelebi, M., *Comparison of damping in buildings under low-amplitude and strong motions.* Journal of wind engineering and industrial aerodynamics, 1996. **59**(2): p. 309-323.
29. Çelebi, M. *On the variation of fundamental frequency (period) of an undamaged building–a continuing discussion*. in *Proceedings of International conference on Experimental Vibration Analysis for Civil Engineering Structures (EVACES07)*. 2007. Porto, Portugal, October 24-27.
30. Çelebi, M., *Comparison of recorded dynamic characteristics of structures and ground during strong and weak shaking*, in *Increasing Seismic Safety by Combining Engineering Technologies and Seismological Data*. 2009, Springer. p. 99-115.
31. Todorovska, M., T. Hao, and M. Trifunac, *Building periods for use in earthquake resistant design codes earthquake response data compilation and analysis of time and amplitude variations*, in *Report CE 04-02*. 2004: Department of Civil Engineering, University of Southern California, Los Angeles, California,.
32. Todorovska, M., M. Trifunac, and T.-Y. Hao, *Variations of apparent building frequencies-lessons from full-scale earthquake observations*, in *1st European conference of earthquake engineering and seismology*. 2006: Geneva, Switzerland, September 3-8.
33. Dunand, F., P.-y. Bard, and J. Rodgers, *Comparison of the dynamic parameters extracted from weak, moderate and strong motion recorded in buildings*, in *1st European conference of earthquake engineering and seismology*. 2006: Geneva, Switzerland, September 3-8.
34. Clinton, J.F., et al., *The observed wander of the natural frequencies in a structure.* Bulletin of the Seismological Society of America, 2006. **96**(1): p. 237-257.
35. Carreño, R.P. and R.L. Boroschek, *Modal parameter variations due to earthquakes of different intensities*, in *Civil Engineering Topics, Volume 4*. 2011, Springer. p. 321-333.
36. Çelebi, M., L. Phan, and R. Marshall, *Dynamic characteristics of five tall buildings during strong and low-amplitude motions.* The structural design of tall buildings, 1993. **2**(1): p. 1-15.
37. Trifunac, M.D., T. Hao, and M. Todorovska, *Response of a 14-story reinforced concrete structure to nine earthquakes: 61 years of observation in the Hollywood storage building*, in *Report CE01-02*. 2001: Department of Civil Engineering, University of Southern California, Los Angeles, California,.
38. Hao, T., M. Trifunac, and M. Todorovska, *Instrumented buildings of University of Southern California—strong motion data, metadata and soil-structure system frequencies*, in *Report CE04-01*. 2004: Department of Civil Engineering, University of Southern California, Los Angeles, California,.
39. Dunand, F., *Pertinence du bruit de fond sismique pour la caractérisation dynamique et l'aide au diagnostic sismique des structures de génie civil*. 2005, Université Joseph-Fourier-Grenoble: Grenoble, France.

40. Dunand, F., et al., *Ambient vibration and earthquake strong-motion data sets for selected USGS extensively instrumented buildings*. 2004: In USGS Open-File Report 2004-1375.
41. Boroschek, R. and P. Lazcano. *Non-damage modal parameter variations on a 22 story reinforced concrete building*. in *International Modal Analysis Conference, IMAC XXVI*. 2008. Orlando, FL.
42. Singh, J., et al., *Identification of modal parameters of a multistoried RC building using ambient vibration and strong vibration records of Bhuj earthquake, 2001.* Journal of earthquake engineering, 2014. **18**(3): p. 444-457.

Chapter 4

In the previous chapter (Chapter 3) the developed methodology to generate FRS and inter-story drift curves using ambient vibration measurements has been discussed in detail. This chapter presents the detailed description of the validation of the proposed approach through a case-study of a St. Justine Hospital building, a paediatric hospital located in Montreal, Canada (Building#23 of the database). A detailed dynamic linear finite element model of the hospital buildings have been run using the same input excitations and floor response histories, FRS, and inter-story drift curves have been derived numerically. The comparison of the numerical results with the results of the proposed approach are presented here. It is noted that the proposed method is completely coded in the MATLAB program.

4 EXPERIMENTAL FLOOR RESPONSE SPECTRA FOR SEISMIC EVALUATION OF OPERATIONAL AND FUNCTIONAL COMPONENTS OF BUILDINGS

A. Asgarian, F. Mirshafiei, G. McClure

Department of Civil Engineering and Applied Mechanics, McGill University, Montréal, Canada

4.1 Abstract

In general, building components can be classified as: 1-Structural components/Primary system and 2- Non-structural components/Operational and Functional Components (OFCs) (terminology used in Canadian Standards Association CSA-S832). OFCs are also called secondary systems as they are not part of the main or intended load-resisting system of the building. However, their seismic performance plays a vital role in the overall performance of the building during and after an earthquake. This implies that the failure or malfunction of OFCs can cause the building to lose its functionality even though the structural components are still performing well. This matter is of significant importance particularly regarding post-disaster buildings.

The current available methods for seismic evaluation and analysis of OFCs can be generally categorized as: 1- Floor Response Spectra (FRS) approach and 2- Combined Primary-Secondary System (CPSS) approach. In summary, the former considers the primary and secondary systems as decoupled systems (i.e. no dynamic interaction between them) while the latter analyses them as a combined coupled system. This study is proposing an original approach to generate both the floor response spectra and inter-story drift curves based on experimental modal data obtained from Ambient Vibration Measurements (AVM). This

approach includes several improvements to both aforementioned approaches. It overcomes the fundamental shortcomings of the conventional FRS approach while taking advantage of its simplicity and practicality. Most importantly, it is capable of considering the dynamic interaction between the primary and secondary systems on the response of OFCs with no need to carry out combined system analysis. A detailed case study of a hospital wing building is provided to illustrate the proposed method.

Key words: Earthquake Engineering, Post-critical Building, Operation modal analysis, Non-structural Components

4.2 **Introduction**

Buildings are composed of two main types of components: structural components and non-structural components (NSCs). In Canadian Standards Association CSA-S832 [1], NSCs are termed Operational and Functional Components (OFCs). As OFCs are not meant to be a part of the main or intended load-resisting system of the structure, in structural dynamics literature, they are called “secondary systems” while the building structure is commonly referred to as “primary structure” or “supporting structure”.

The CSA S832-06(R11)[1] categorizes OFCs into three sub-groups based on their function including: Architectural components (external or internal), Building services components (mechanical, electrical, and telecommunication), and Building contents (common and specialized). Figure 4.1 schematically shows different types of OFCs [1]. OFCs can also be classified into three categories in accordance with the nature of their seismic response sensitivity: 1- Inter-storey-drift-sensitive components, 2- Floor-acceleration-sensitive components, and 3- both Inter-storey-drift- and floor-acceleration-sensitive components [2].

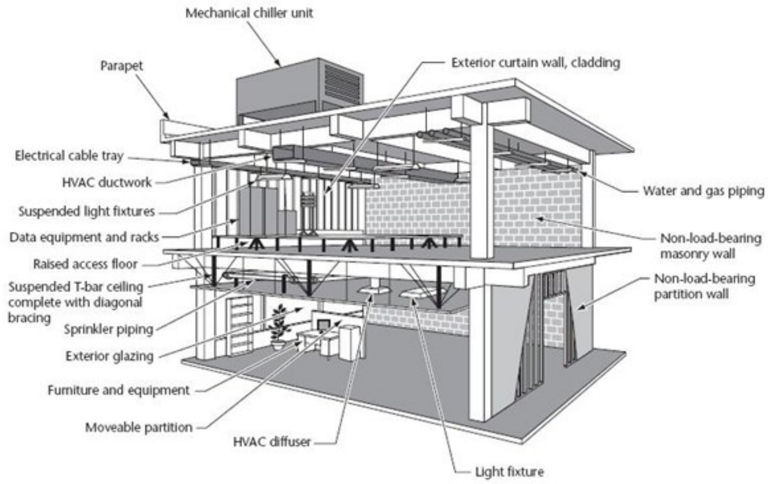

Figure 4.1 - Operational and functional components of buildings (CSA S832-6(R11): Pg 34)

Although OFCs are called secondary systems, they are far from being secondary in importance in terms of functionality and economical value. Their functionality and performance during and after an earthquake are of great significance specially in post-disaster buildings such as hospitals, emergency shelters, water treatment plants, etc., since failure or malfunction of OFCs can considerably impact building functionality even if the structural system has performed well during earthquake. OFCs failure can give rise to adverse consequences associated with life safety, building functionality, and property protection (i.e. economical aspects). As a matter of fact, the good seismic performance of OFCs is essential to achieve the life-safety performance objective that is mandatory for all buildings in Canada [3].

Experiences and observations from past earthquakes and current understanding of the seismic behaviour of building structures indicate that OFCs are exposed to large seismic forces and displacements during an earthquake and they deserve rational and careful seismic design and analysis procedures of their own since their performance plays a vital role in the overall performance of the building.

4.3 **Seismic analysis of OFCs**

4.3.1 Physical properties of OFCs and important factors in their seismic response

OFCs compose several characteristics (seven are listed below) which make them vulnerable to seismic excitation and should be taken into account in their seismic response analysis:

1- *OFC Location along the height of the building:* Components installed at high elevation (upper storeys) in medium- to high-rise buildings will be subjected to amplified seismic excitations compared to those on lower storeys.

2- *Dynamic interaction*: In certain “quasi-resonant” conditions, both the structure and OFCs can interact dynamically and mutually affect or modify each other’s seismic response.

3- *Tuning*: In general, the stiffness and weight of isolated components are both much lower than those of the supporting floor/wall structure. As a result, their natural frequencies might be close to one of the natural frequencies of local modes of the supporting structure, which causes resonant OFC motions.

4- *Low internal damping of OFCs*: Apart from architectural components, OFCs normally possess lower damping than that of the building. This difference in damping ratios of the primary and secondary systems causes the combined system to have non-classical damping and as a result natural frequencies and modes shapes are complex.

5-*Multiple-support excitations*: Architectural components and distributed OFCs are usually supported at multiple attachment points. Thus, they are subjected to differential motions at their supports and are affected by distortions.

6- *The dynamic response of the building structure*: As OFCs are attached to the building structure, they are directly subjected to the in-building seismic response (floor response) instead of the earthquake ground motion. Such in-building response is typically amplified and filtered according to the dynamic properties of the building seismic force resisting system (SFRS).

7- *Nonlinear response*: The response of OFCs and their anchorage systems can be affected by the materially nonlinear behaviour of both the primary structure and their own at high shaking levels.

4.3.2 OFC seismic analysis

During the past four decades, many attempts have been made to develop rational yet practical methods to analyse the seismic response of OFCs. However, scholars have not yet reached a consensus on a generally accepted method due to several difficulties attributed to aforementioned characteristics of OFCs which increase the complexity of the problem. In spite of all these difficulties, several methods for seismic design and analysis of OFCs have been developed, which can be classified into two general approaches: 1) Floor Response Spectrum (FRS) approach, and 2) Combined Primary-Secondary (P-S) system approach.

4.3.2.1 Floor response spectrum (FRS) approach

One of the first methods developed for analysis of OFCs is the Floor Response Spectrum (FRS) in which the primary and secondary systems are decoupled (i.e. no dynamic interaction between them is considered) and analysed individually. This method is also known by alternative names such as "systems-in-cascade"; or "in-structure response spectrum"[4]. In summary, the response acceleration time history of the primary system at the support locations of OFCs is first determined under the effect of a ground accelerogram compatible with the seismicity and geotechnical conditions of the building site. This floor acceleration time-history is then utilized as the base excitation for OFCs to generate a floor response spectrum [5].

In comparison with the combined primary-secondary (P-S) system model described in section 4.3.2.2, the FRS method is faster and involves less computational costs. This method has been proven to be reasonably accurate when considering those OFCs that are significantly lighter than the primary system, and that have natural frequencies well separated from those of the supporting structure, i.e. no resonance. Otherwise, it can lead to some gross error or over-conservative results which mainly come from disregarded dynamic interaction, non-classical damping effects, and cross-correlation for multi-supported OFCs [6, 7].

4.3.2.2 Combined Primary-Secondary System (CPSS) approach

The CPSS approach considers the primary and secondary systems together as a single unit coupled system. Therefore, it is able to fully account for dynamic interaction between OFCs and supporting structure.

Considering the primary and secondary systems as a whole, one can incorporate the following parameters into the analysis: dynamic interactions, different values of mass, stiffness, and damping ratio for the primary and secondary systems, and cross-correlation for multi-supported OFCs [8]. However, establishing a combined P-S system mandates working with complex mode shapes and frequencies, which renders any conventional method of analysis costly, imprecise and inefficient. Also, every time a change is made in the OFC parameters, the whole coupled structure needs to be reanalysed which is not practical, considering that the design of these two systems is conducted by different teams (structural/mechanical/architectural) and at different times.

4.3.3 Building code and standards requirements for seismic design of OFCs

4.3.3.1 General

Recent building codes address the seismic design of OFCs in new buildings more precisely than before the 1980s. Examples of the codes comprising seismic design requirements for OFCs in the United States are the Uniform Building Code (UBC) [9], the National Earthquake Hazard Reduction Program (NEHRP) provisions [10],and ASCE/SEI 7-10 [11]. In Canada, seismic design provisions for OFCs were first introduced in the 1953 edition of the NBCC [12]. Afterwards, and until 1995, every new NBCC edition included some improved requirements, typically following those of the various US codes. In 2006, a new Canadian standard CSAS832-06(R11) was introduced covering seismic risk considerations for OFCs in both new and existing buildings.[1]

4.3.3.2 Provisions of NBCC 2010 edition

The current edition of the National Building Code of Canada (NRC, 2015)[13]addresses the design of non-structural components against seismic effects by suggesting an empirical approach based on the Uniform Hazard Spectrum (UHS) approach used for the design of structures [14, 15].

The seismic force requirements are covered in Article 4.1.8.18. of NBCC 2015 Division B Part 4 with an empirical equation to calculate the lateral equivalent static force for which the components shall be designed.

Regarding the displacement demand, NBCC 2010 contains only requirements in terms of inter-story drift limits at any level based on the lateral deflections obtained from linear elastic analysis of the building. These limits are set as $0.01*h_s$ for post-disaster buildings (with earthquake importance factor $I_E = 1.5$), $0.02*h_s$, for schools ($I_E = 1.3$) and $0.025*h_s$, for all other buildings of normal importance category ($I_E = 1.0$). The lateral deflections obtained from linear elastic analysis are to be multiplied by R_dR_o/I_E to give more realistic values of anticipated deflections, where R_d is the force overstrength factor and R_o represents the energy dissipation capacity of the element or its connections. Further details about the history of improvement of design provisions for OFCs in Canada can be found in [16].

4.3.3.3 Canadian Standard CSA-S832

CSA-S832 [1] is the Canadian standard for "Seismic risk reduction of operational and functional components (OFCs) of buildings". This standard is used in conjunction with the NBCC Article 4.1.8.18. for the calculation of seismic demand parameters of OFCs of new buildings while it contains design provisions and guidelines for the seismic risk assessment and mitigation of OFCs in existing buildings. Depending on the OFC type, it recommends two approaches for seismic design of OFCs:

1- Prescriptive approach: which provides general concepts for design and performance of OFCs and includes the application of typical details, best practices, and seismic risk mitigation actions published in industry or manufacturer guidelines. The prescriptive approach is based on sound engineering standards and practices rather than analysis and calculations.

2- Analytical approach: which requires the design of OFCs and their connections to the building structure against the horizontal and vertical forces, drift ratios, and relative displacement induced by the design earthquake.

Common limitations of international codes for seismic design of OFCs are: 1- Most of them neglect the effect of OFC damping when estimating the acceleration demand, 2- They usually do not consider the effect of higher building modes in the OFC force calculations although this can become important in high-rise buildings [17], 3- The effect of the torsional motion of the primary system, particularly in irregular buildings, on the seismic response of its OFCs is not addressed; it can be considerable for those components located in periphery of the structure, 4- They assume a linear variation of the floor acceleration over the building height, 5- The seismic force on the OFC is calculated based on the spectral acceleration at short period (at 0.2 s). This choice is based on the fact that most components in buildings are stiff or rigid, and research from past earthquakes has shown that the OFC seismic forces best correlate with this acceleration ordinate [10]. However, a more accurate and economical approach is to consider the natural periods of OFCs, tuning, detuning, and resonance effects.

Despite the high level of current understanding of the seismic behaviour of OFCs, the building codes and standards still do not incorporate the developed techniques.

4.4 Experimental modal analysis: Ambient Vibration Measurements (AVM)

As part of this research, experimental modal analysis is done using the AVM records collected on several post-disaster buildings located in Montreal. In AVM, the velocities induced by ambient excitations in both two orthogonal horizontal directions and along the vertical are recorded at several locations in each building. Analysis of recorded data is carried out using two different operational modal analysis techniques- namely, Frequency Domain Decomposition-Peak Picking (FDD) and Enhanced Frequency Domain Decomposition-Peak Picking (EFDD), and the dynamic properties of the building including the lowest natural frequencies, corresponding mode shapes, and effective modal damping ratios, are extracted. These experimental dynamic properties are then used as input parameters to derive the response time-history and subsequently the FRS for selected floors of the buildings. Further explanations concerning AVM and experimental modal analysis of buildings can be found in [18].

4.5 **Proposed experimental FRS method**

Several empirical methods for seismic analysis of OFCs have been developed in the past and are used currently in the codes. However, a more rational approach to design OFCs against seismic excitations and to assess the seismic performance of OFCs in existing buildings involves the use of floor design spectra. The NBCC 2010 includes the most recent seismic hazard data for building design in the form of a Uniform Hazard Spectrum (UHS). However, floor design spectra for OFCs compatible with the NBCC 2010 UHS are currently not available. An original approach is proposed to generate the FRS based on experimental data obtained from ambient vibration measurements (AVM) on building floors.

The first phase of the project was to collect a database of the tested buildings properly covering different types of lateral load resisting systems (LLRS) (i.e. reinforced concrete buildings and steel structures), and various heights (i.e. low, medium, and high rise buildings) in which the AVM records have already been collected by the McGill team on the island of Montreal. This includes AVM tests carried out by Gilles (46 buildings, mostly high-rise ones) [19], Tischer (101 buildings, mostly low-rise) [20], and Mirshafiei (9 irregular buildings, ongoing research project) [21]. Relevant building information was collected including: construction year, LLRS type, soil type, building height, number of storeys, architectural and structural drawings, etc. Currently, the database is composed of 156 buildings in total from which 59 have sufficient available information for the procedure. As the main focus of the study is on the performance of OFCs in post-disaster or high importance buildings, the database mostly comprises schools, hospitals, and community/sports centres designated by *Centre de sécurité civile de Montréal*to serve as emergency shelters. Table 4-1 shows a classification of the 59 buildings of the database.

The recorded AVM data have been analysed to extract the building dominant dynamic properties (as explained previously) using the commercial software ARTeMIS Extractor ™ [22] As AVM testing is performed during the normal operation of the building with all the OFCs in place, the dynamic interaction between the secondary and primary structures, if present, is necessarily captured in the test and its effect on the modal properties of the building taken into account.

Table 4-1 - Classification of building database

Number of Storey / LLRS type	Low-rise buildings (1-3)	Medium-rise buildings (4-7)	High-rise buildings (≥ 8)	Total
Steel moment frame	3	0	0	3
Steel braced frame	1	2	3	6
Steel infill wall	2	0	0	2
Concrete moment frame	0	7	1	8
Concrete shear wall	3	11	7	21
Concrete infill wall	12	2	0	14
Precast concrete frame	3	0	0	3
Combined systems	1	0	1	2
TOTAL	25	22	12	59

The extracted modal properties and the estimated mass of the building floors are used as the input parameters for the response prediction approach (3D SAM method) developed by Mirshafiei and McClure [21]. The outcome is the response of the different floors of the building subjected to a ground motion record. The floor response is calculated in terms of both acceleration and displacement. The response time-histories are used as excitations for OFCs to develop the FRS corresponding to different floors of each building.

The FRS corresponding to selected floors of each building is derived for each base excitation record. In the next step, the FRSs are compared to each other to evaluate the effect of LLRS type, building height, location of the OFC along the building height, period ratio of secondary to primary systems, and soil site conditions. The proposed approach is promising in particular regarding the seismic evaluation of OFCs in post-disaster buildings that were constructed several decades ago. A clear advantage is that instead of generating the numerical model of the building (typically insufficient or inaccurate data available) to produce FRS, the FRS can be produced using the*in situ* dynamic properties of the building in its linear range of response. Another advantage of this method is that it utilizes the damping values and mode shapes extracted from AVM which represent the actual current condition and properties of the building. Spectra can be generated for different damping values of the OFCs to assess how it will affect the OFC response.

4.6 **Results and validation**

The validation of the proposed method is illustrated through the case study of Sainte-Justine Hospital in Montreal. The AVM tests were conducted on two selected blocks (#7 and #8) of the hospital. Modal analysis of AVM data was conducted using commercial software ARTeMIS Extractor ™ and dynamic properties of the buildings were extracted. Detailed linear elastic finite element (FE) models of the buildings had been generated in SAP 2000 v.14.0.0 [23] (Figure 4.2) and calibrated using experimental results, in a previous study [18].

Having extracted the dynamic properties of the building and given a synthetic ground accelerogram compatible with the NBCC 2010 UHS corresponding to Montreal, the floor response-history and FRS of selected floors (here top floor # 6 and middle floor # 2) are derived using the first 6 modes extracted from AVM.

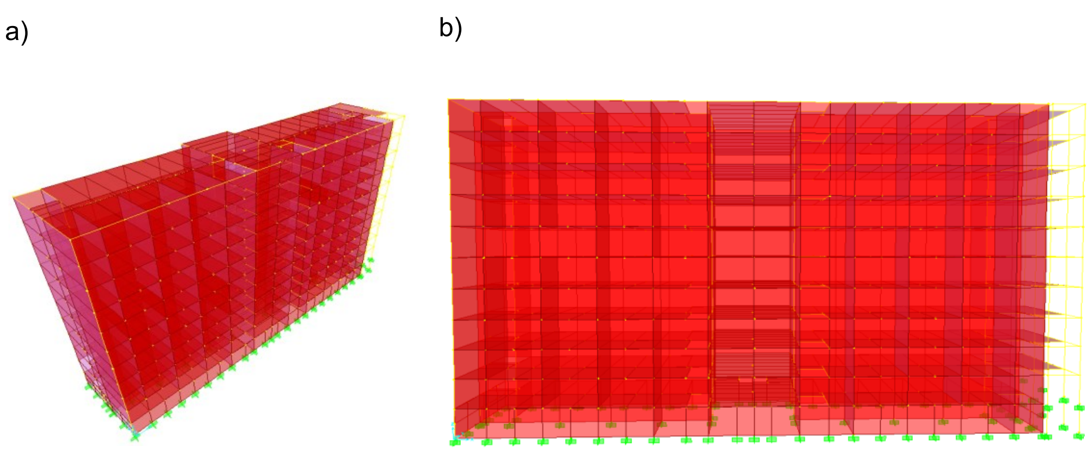

Figure 4.2 - Linear elastic FE model- Block#8: a & b) 3D views

The detailed FE models are subjected to the selected accelerograms as base excitation and the response histories for floors # 2 and 6 are generated by truncated modal superposition analysis considering the 6 lowest frequency modes of vibration. These floor response-histories are considered as base excitation for the OFCs to generate the FRS. Afterwards, the FRSs derived from both approaches (experimental and computational) are compared to each other for the sake of validation. Figure 4.3 and Figure 4.4 present the comparison between the floor response histories in terms of relative displacement and absolute acceleration of Center of Mass (CM) of 6th floor, respectively. Using these response histories, inter-story drift curves (Figure 4.5) displacement FRS (Figure 4.6), and acceleration FRS (Figure 4.7) for CM of 6th floor are derived (experimentally and numerically) and compared. The comparison shows a very good consistency and agreement between the experimental and numerical outcomes as it can be seen in Figure 4.6 and Figure 4.7 except the spike which can be seen at period of 0.16s in Figure 4.7. The inaccuracy is happening due to the numerical integration procedure used to derive the pseudo-acceleration (S_a) from the pseudo displacement (S_d) (S_a=ω^2.S_d). Therefore a little difference between numerical and experimental results in pseudo displacement at very short period\high frequency is artificially magnified in pseudo acceleration. However, this matter is not of concern since at the end, all the generated FRSs corresponding to different seismic records are averaged and a smooth averaged FRS curve is suggested for the sake of design. Consequently, it is concluded that the proposed method gives promising results and can be used for the rest of the data base with no further need to generate numerical models.

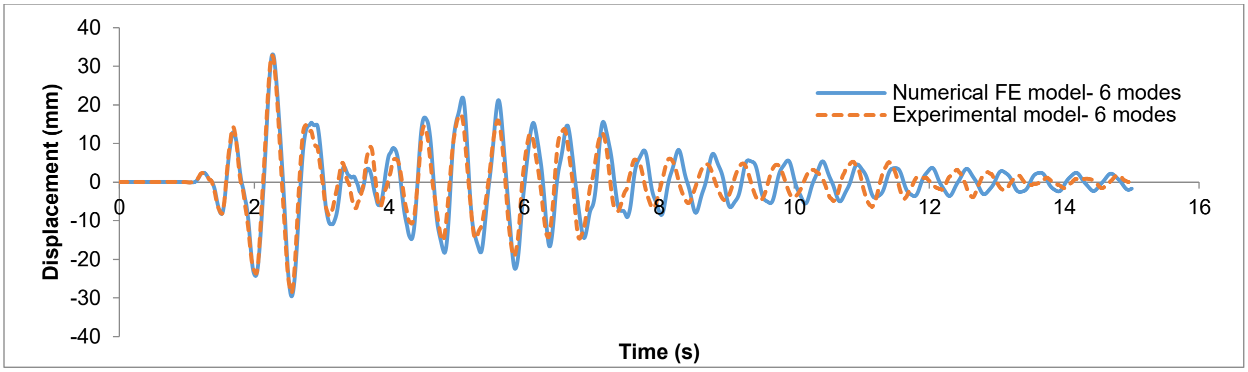

Figure 4.3 - Relative displacement of C.M of 6th floor in Y direction-Earthquake in Y direction

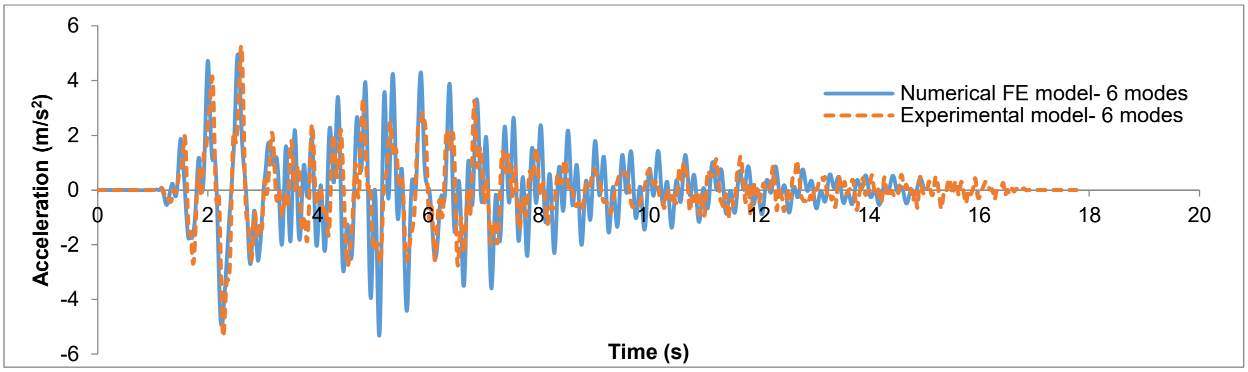

Figure 4.4 - Absolute acceleration of C.M of 6th floor in Y direction-Earthquake in Y direction

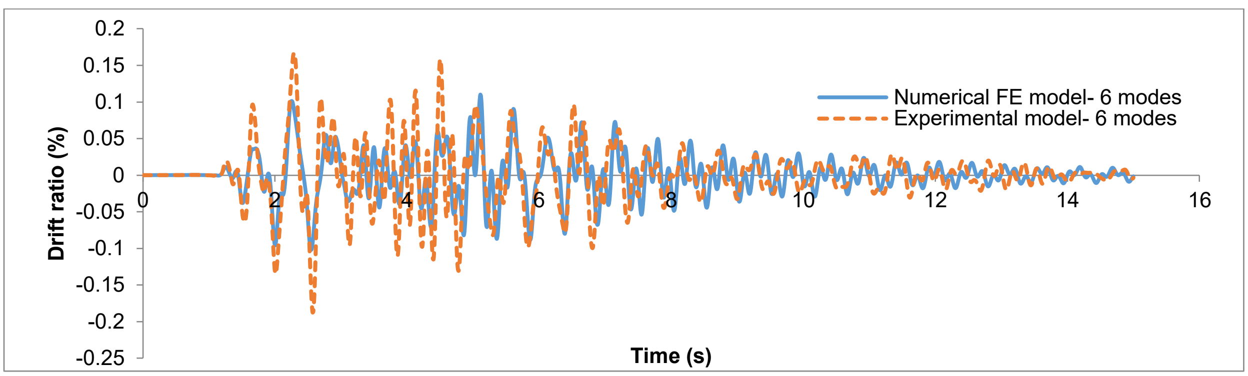

Figure 4.5 - Drift ratio of C.M of 6th floor in Y direction-Earthquake in Y direction

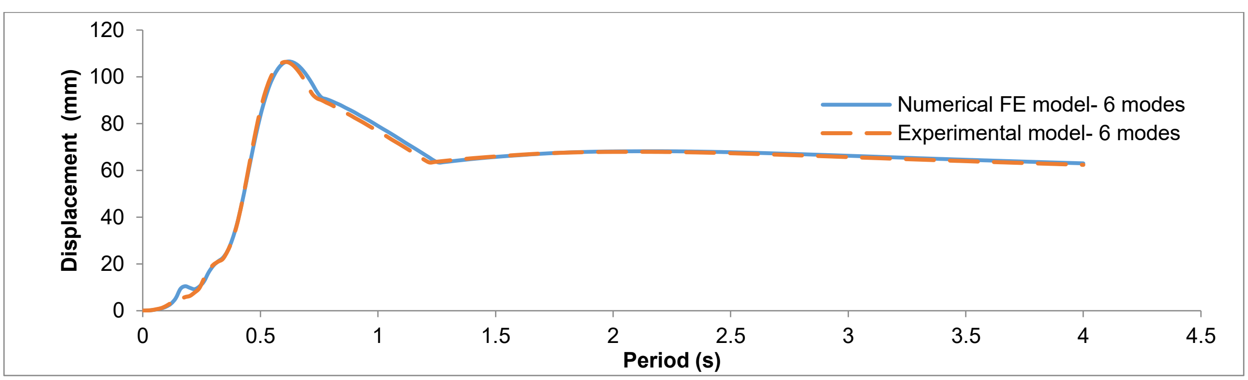

Figure 4.6 - FRS- Displacement of C.M of 6th floor in Y direction-Earthquake in Y direction- D=10%

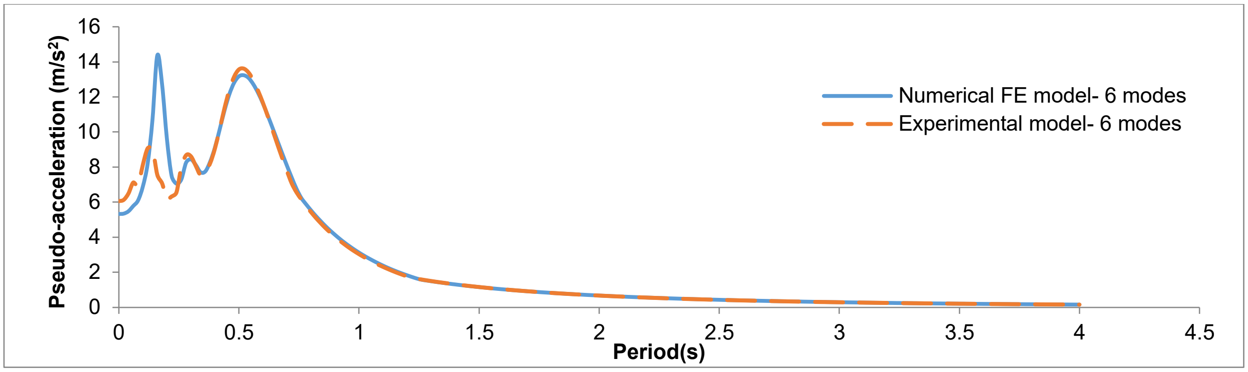

Figure 4.7 - FRS-Pseudo-acceleration of C.M of 6th floor in Y direction-Earthquake in Y direction- D=10%

4.7 Conclusions

An original method was proposed to derive the experimental FRS based on the AVM. It was shown that the proposed experimental method is producing accurate and reliable results compared to numerical finite element simulations. The method is very efficient and fast compared to time-consuming numerical simulations and it is a practical approach to assess OFCs in existing buildings which may have changed properties with time, changes which cannot be easily captured in numerical simulations. Since the method is based on AVM tests conducted during the normal operation of the buildings, it captures the effect of dynamic interaction between OFCs and primary system on seismic response of OFCs; this is an important improvement to the conventional FRS approach. Additionally, it can resolve the shortcomings of building codes and standards empirical simplified methods by considering the effect of higher building modes and torsional behaviour of the primary system on OFC response. The cross-correlation is taken care of by providing the inter-story drift curves and FRSs are generated using the real dynamic properties of building (frequencies and damping ratios) extracted from AVM and for different damping ratios assumed for OFCs. The proposed method is a promising tool to evaluate the seismic behaviour and performance of OFCs in existing buildings undergoing low to moderate structural damage.

4.8 **References**

1. Canadian Standard Association (CSA) *CAN/CSA-S832-06: Guidline for seismic risk reduction of operational and functional components (OFCs) of buildings*. 2006: Rexdale, ON, Canada.
2. Taghavi, S., *Response Assessment of Nonstructural Building Elements*, in *Department of Civil and Environmental Engineering*. 2003, Stanford University: Stanford, California. p. 96.
3. National Research Council of Canada (NRC), Institute for Research in Construction (IRC), *National Building Code of Canada (NBCC)*. 2010: Ottawa, ON, Canada.
4. Villaverde, R., *Earthquake resistant design of secondary structures: a report on the state of the art*, in *Proc., 11th World Conf. on Earthquake Engineering*. 1996, Elsevier Science Ltd.: Acapulco, Mexico. p. 13.
5. Igusa, T. and A. Der Kiureghian, *Dynamic response of multiply supported secondary systems.* Journal of Engineering Mechanics, 1985. **111**(1): p. 20-41.
6. Gupta, A.K. and J.M. Tembulkar, *Dynamic decoupling of secondary systems.* Nuclear engineering and design, 1984. **81**(3): p. 359-373.
7. Wang, Y., M. Subudhi, and P. Bezler, *Comparison Study of Time History and Response Spectrum: Responses for Multiply Supported Piping Systems*. 1983: Brookhaven National Laboratory.
8. Asfura, A. and A.D. Kiureghian, *Floor response spectrum method for seismic analysis of multiply supported secondary systems.* Earthquake engineering & structural dynamics, 1986. **14**(2): p. 245-265.
9. UBC, *Uniform building code*. 1935, International Conference of Building Officials (ICBO): Whittier, California.
10. National Earthquake Hazard Reduction Program (NEHRP), *Recommended provisions for seismic regulations for new buildings and other structures*. 2000, Building Seismic Safety Council: Washington, D.C.
11. American Society of Civil Engineers, *ASCE Standard 7-16: Minimum Design Loads for Buildings and Other Structures*. 2016, American Society of Civil Engineers: Reston, VA.
12. National Building Code of Canada, *NRCC*. 1953, Associate Committee on the National Building Code: National Research Council of Canada, Ottawa, ON.
13. National Research Council Canada (NRC), I.f.R.i.C.I., *National Building Code of Canada (NBCC)*. 2010.
14. Adams, J. and G. Atkinson, *Development of seismic hazard maps for the proposed 2005 edition of the National Building Code of Canada.* Canadian Journal of Civil Engineering, 2003. **30**(2): p. 255-271.
15. Adams, J. and S. Halchuk, *Fourth generation seismic hazard maps of Canada: Values for over 650 Canadian localities intended for the 2005 National Building Code of Canada.* Geological Survey of Canada, 2003. **4459**: p. 1-155.

16. Assi, R., *Seismic analysis of telecommunication towers mounted on building rooftops*, in *Department of Civil Engineering and Applied Mechanics*. 2006, McGill University: Montreal. p. 348.
17. Sullivan, T.J., P.M. Calvi, and R. Nascimbene, *Towards improved floor spectra estimates for seismic design.* Earthquake and Structures, 2013. **4**(1): p. 109-132.
18. Asgarian, A., *Impact of seismic retrofit and presence of terra cotta masonry walls on the dynamic properties of a hospital building in Montreal, Canada*, in *Department of Civil Engineering and Applied Mechanics*. 2012, McGill Univeristy: Montreal, Canada. p. 156.
19. Gilles, D., *In situ dynamic characteristics of reinforced concrete shear wall buildings*, in *Department of Civil Engineering and Applied Mechanics*. 2011, McGill University: Montreal,QC. p. 295.
20. Tischer, H., *Rapid seismic vulnerability assessment of school building in Québec* in *Department of Civil Engineering and Applied Mechanics*. 2012, McGill Univerisity: Montreal. p. 258.
21. F. Mirshafiei and G. McClure, *Experimental modal analysis of emergency shelters in Montréal, Canada*, in *15 World Conference on Earthquake Engineering*. 2012: Lisboa, Portugal.
22. Structural Vibration Solution, *ARTeMIS Extractor, Software for Operational Modal Analysis*. 2010.
23. Computers and Structures, I.C., *SAP 2000-advanced 14.0.0*. 2009: Berkeley. California.

Chapter 5

The developed method to generate experimental FRS and inter-story drift curves was described in **Chapter 3** and its validation through a case-study was discussed in **Chapter 4**. In this chapter (**Chapter 5)**, the proposed method is employed over the entire database of the buildings. The generated Pseudo Acceleration Floor Response Spectrum (PA-FRS) for the buildings are utilized to evaluate the effect of key parameters (i.e. Tuning, elevation of NSCs, damping of NSCs) on the acceleration response of NSCs. Moreover, the results were used to develop an original approach to produce Floor Design Spectra (FDS) for the roof level and 5% NSC damping directly from 5% damped Uniform Hazard Spectra (UHS). The proposed method is formulated for RC low and medium rise buildings and a set of equations is recommended for each building type. The FDS curves derived for the building database are presented and compared with the provisions of three well-known international building codes: NBCC 2015 [1], ASCE SEI-7-16 [2], and Eurocode 8 [3].

5 Direct generation of Floor Design Spectra (FDS) from Uniform Hazard Spectra (UHS) - Part I: Formulation of the method.

A. Asgarian[(1)], G. McClure[(2)]

[(1)] Ph.D. candidate, Department of Civil Engineering and Applied Mechanics, McGill University, Canada, amin.asgarian@mail.mcgill.ca

[(2)] Professor, Department of Civil Engineering and Applied Mechanics, McGill University, Canada, ghyslaine.mcclure@mcgill.ca

5.1 Abstract

Proper seismic design and assessment of Non-Structural Components (NSCs) is contingent upon having an accurate estimation of floor seismic demands (i.e. acceleration, displacement, and inter-story drift demands). Currently, most of the international codes incorporate empirical equations to calculate equivalent static seismic forces for which NSCs and their anchorage system must be designed to resist. These equations, in general, are functions of the component's mass and the peak seismic acceleration to which NSCs are subjected to during strong earthquakes. However, recent studies have shown that these recommendations suffer from several shortcomings such as neglecting the higher mode effect, tuning effects between the component and the supporting structure, and NSCs internal damping, to name a few, which cause underestimation of the component seismic acceleration demand.

This work is aimed to circumvent the aforementioned shortcomings of code provisions as well as improving them by proposing a simplified, practical, and yet accurate approach to generate acceleration Floor Design Spectra (FDS) in buildings directly from their corresponding Uniform Hazard Spectra (UHS) (i.e. design spectra for structural components). It makes use of a database of 27 Reinforced Concrete (RC) buildings (12 low-rise, 10 medium-rise, and 5 high-rise building all located in Montréal, Canada) in which AVM tests have been conducted. Most of these buildings are designated as post-disaster facilities or emergency shelters by the City of Montréal. In the study, the buildings are subjected to a set of 20 compatible seismic records and Floor Response Spectra (FRS) in terms of pseudo acceleration are derived using the proposed approach for every floor of the building in two orthogonal horizontal directions considering 4 different NSCs damping ratios (i.e. 2, 5, 10, and 20% of critical viscous damping). The main factors affecting NSCs response are statistically evaluated; these factors are the location of NSCs in building, the NSCs damping ratios, the tuning of NSCs natural period with one of the natural periods of the supporting structure, and the effect of the higher modes of the supporting structure. The entire spectral region of the FRS is divided into three distinct regions namely short-period, fundamental period, and long period regions. The derived roof floor response spectra for NSCs with 5% damping are compared with the 5% damping UHS values, and a procedure is proposed to generate roof FDS for NSCs with 5% damping directly from the 5% damped UHS in each spectral region. The generated FDS provide a powerful, practical, and accurate tool for seismic design and assessment of acceleration-sensitive NSCs particularly in existing post-critical buildings which have to remain functional during or immediately after an earthquake and therefore cannot tolerate any damage to critical NSCs.

Keywords: Operational and Functional Components (OFCs); Operational Modal Analysis (OMA); Earthquake Engineering; Seismic Assessment and Design.

5.2 **Introduction**

Non-structural Components (NSCs) of buildings are those elements housed or mounted in buildings that are not meant to carry any types of load or in other words, they are not a part of the load-bearing structural system. Nevertheless, NSCs may be subjected to large-seismically induced forces/displacements during earthquakes [4]. Extensive reports of NSCs damage and failures have been made based on post-earthquake reconnaissance inspections following destructive earthquakes such as the 1964 Alaska earthquake [5], the 1971 San Fernando earthquake [6, 7], the 1987 Whittier earthquake [8, 9], the 1989 Loma Prieta earthquake [9], the 1994 Northridge earthquake [9-12], the 1995 Kobe earthquake [11], the 1999 Chi-Chi and Kocaeli (Taiwan) earthquakes [11], the 2001 El Salvador earthquake[13], the 2001 Nisqually Earthquake [9], the 2006 Hawaii earthquake [14, 15], the 2010 Chile earthquake [16, 17], the 2010 and 2011 New Zealand earthquakes [17], the 2010 Haiti earthquake [18], and the 2012 Emilia earthquake [19] to name a few in chronological order. According to the nature of the seismic response sensitivity and failure mechanism of NSCs, they can be categorized as either drift-sensitive or acceleration-sensitive components [20]. Damage to drift-sensitive components is caused by seismically induced displacements and inter-story drift. An instance of studies addressing the seismic assessment of this type of NSCs through developing relative displacement floor spectra is the work by Calvi [21]. Acceleration-sensitive components, which are the main focus of this study, undergo damage because of the inertia forces induced by the floor acceleration which is, in general, larger than that of the ground level. Several studies have focused on enhancing the understanding of acceleration demand on NSCs by estimating Peak Floor Acceleration

(PFA) or Peak Component Acceleration (PCA) and also by developing practical approaches for seismic design of this type of components [22-25].

Poor seismic performance of NSCs is an important cause of life-safety hazards, economic losses, and loss of building functionality, which may be critical for post-disaster buildings. As observed in many past earthquakes, economic and functionality losses can exceed the ones caused by structural damage considering that: 1- damage to NSCs typically occurs at seismic intensities lower than those required to trigger structural damage, and 2- NSCs account for a major portion of total direct building cost (as much as 82%, 87% and 92% of the total investment in office, hotel and hospital buildings in the United States according to Taghavi [20]). Consequently, the cost associated with NSCs failure can be more than the replacement cost of the building especially when the loss of inventory and downtime cost are taken into account [26, 27]. Hence, maintaining the harmonization between seismic performance of NSCs and their supporting structural system is key to guarantee the satisfactory performance of the entire building.

Comparing to structural components, there is much less information and guidelines available for seismic analysis and design of NSCs. Although most of the recent building codes and standards have dedicated a section to seismic design of NSCs [1-3], these provisions are mostly empirical and based on engineering judgement and intuition rather than experimental and analytical results, which partly explains the improper performance of NSCs in relatively recent earthquakes. Most of the modern building codes address the seismic design of acceleration-sensitive components through the recommended equivalent static seismic force demand approach. The empirical equations suggested in different codes follow the same concept and suffer from common drawbacks which are further discussed in section 5.3.

This paper presents the study of 27 existing reinforced concrete (RC) buildings, all located in Montréal, Canada and designated as post-disaster structures. The database covers different height levels including 12 low-rises, 10 medium-rises, and 5 high-rises. The lower-frequency modal characteristics of all buildings have been extracted from Ambient Vibration Measurements (AVM) conducted during normal operation of the buildings with all NSCs in place. Therefore, the dynamic interactions between the NSCs and their supporting system are captured, if there are any. The extracted dynamic properties of the buildings have been modified and used as part of the proposed procedure. Using the proposed method, floor response spectra and inter-story drift curves have been produced with no need of detailed numerical modeling of the building structure. The validation of the method has been done through the detailed linear numerical modeling of Building #23 of the database (see Table 5-2) and by comparing the numerical results with the outputs of the proposed approach: validation details are presented in [28-30]. The method was then employed for the entire database and Pseudo Acceleration Floor Response Spectra (PA-FRS) have been derived for every floor of each building considering 4 different critical viscous damping ratios for NSCs (2, 5, 10, and 20%). The effects of different parameters on NSCs response have been evaluated and presented. The experimentally derived results have been statistically analysed and a formulation is recommended to generate Floor Design Spectra (FDS) for the top floor/roof of the buildings considering 5% viscous damping for NSCs directly from 5% damped Uniform Hazard Spectra (UHS). The FDS is generated specifically for each building based on its fundamental period and design spectral acceleration, considering the effects of higher modes and torsional behaviour of the supporting system. The proposed method improves conventional approaches and code recommendations in several aspects and is fast, practical, and accurate. The derived FDS can be used for seismic assessment of acceleration-sensitive NSCs in existing buildings. The application of the method can also be extended to seismic design of acceleration-sensitive NSCs in new structures. The next milestone is to extend the recommended formulation to generate FDS for any given viscous damping ratio and elevation of NSCs in the building.

5.3 Building code requirements for acceleration-sensitive non-structural components

Seismic design of acceleration-sensitive NSCs is addressed in most of the current building codes and standards through empirical equations recommended to calculate the equivalent static seismic force that the component and its anchor system must resist. Table 5-1 summarizes the seismic force requirements for NSCs in Canada (National Building Code of Canada- NBCC 2015 [1]), United States (ASCE SEI-7-16 [2]), and Europe (Eurocode 8, EN. 1988. 1. 2004. [3]). As shown in Table 5-1, the equations all follow the same concept which is the multiplication of the design Peak Ground Acceleration (PGA) by some modification factors to compute the seismic acceleration/force demand on the NSC. In general, these modification factors comprise: 1- Component importance factor, which accounts for the seismic risk associated with the failure of the NSC; 2- Component dynamic amplification factor, which represents the dynamic amplification of the component relative to the position of its attachment (i.e. tuning/detuning effects with the supporting structure); 3- Component response reduction factor, which expresses the energy dissipation capacity of the NSC and its attachments; and 4- Component elevation modification factor, which accounts for the variation of Peak Floor Acceleration (PFA) along the building height. However, these provisions still suffer from important shortcomings as they disregard the effect of NSCs damping ratios, higher building modes, and torsional behaviour of the supporting structure on the response of NSCs [31]. It should be noted that these building codes also contain seismic design requirements for drift-sensitive components in the form of either inter-story drift limits or displacement design spectra, which are not addressed in this study.

5.4 **Methodology of the proposed approach**

In this research, a total of 27 existing RC buildings (12 low-rises, 10 medium-rise, and 5 high-rises, which had been already tested by AVM) have been studied in detail (see Table 5-2 for description of the building database). After extracting the building dynamic properties from AVM records and estimating the building floor mass and in-plane rotary inertia according to the information in structural and architectural drawings, an equivalent linear model of each building was generated using the 3D-SAM approach [32]. As the AVM results yield the dynamic properties of buildings under low-amplitude excitations and knowing that these properties will vary with the intensity of excitation [33, 34], a set of modification factors have been proposed by the authors to extend the applicability of the method to higher-amplitude excitations. These modification factors were derived after a careful review of studies on permanently instrumented RC buildings [28]. Using the 3D-SAM procedure and subjecting the buildings to a set of 20 synthetic ground accelerograms compatible with the UHS of NBCC 2015 for Montréal, the floor response histories of the buildings in two orthogonal horizontal directions have been generated. The derived acceleration floor response histories were then

Table 5-1 - Building code seismic force requirements for acceleration-sensitive NSCs

Code	Recommendations	Seismic force demand	Design PGA	Building importance factor	Component importance factor	Component dynamic amplification factor	Component response reduction factor	Component elevation modification factor	Component weight
NBCC 2015 (Division B-Part 4)	$\boldsymbol{V_P = 0.3F_aS_a(0.2)I_ES_PW_P}$ $0.7 \leq S_P = \frac{C_PA_rA_x}{R_P} \leq 4.0$ $A_x = 1 + 2\frac{h_x}{h_n}$	V_P	$0.3F_aS_a(0.2)I_E$	I_E	C_P	A_r	R_P	A_x	W_P
ASCE-SEI-07-16 (Chapter 13)	$\boldsymbol{F_P = \frac{0.4a_PS_{DS}}{\left(R_P/I_P\right)} \times \left(1 + 2\frac{Z}{H}\right) \times W_P}$ $1.6S_{DS}I_PW_P \leq F_P \leq 0.3S_{DS}I_PW_P$	F_P	$0.4S_{DS}$	-	I_P	a_P	R_P	$\left(1 + 2\frac{Z}{H}\right)$	W_P
Eurocode 8 (Part 4.3.5)	$\boldsymbol{F_a = (S_aW_a\gamma_a)/q_a}$ $S_a = \alpha.S.\left[\frac{3\left(1+\frac{Z}{H}\right)}{1+\left(1-\frac{T_a}{T_1}\right)^2} - 0.5\right] \geq \alpha S$	F_a	$\alpha.S$	-	γ_a	$1 + \left(1 - \frac{T_a}{T_1}\right)^2$	q_a	$3\left(1 + \frac{Z}{H}\right)$	W_a

considered as the base excitation for NSCs and FRS curves have been generated for components with critical viscous damping ratios of 2, 5, 10, and 20 % and fundamental periods of [0-4] seconds with interval of 0.02 s. Automatic generation of the FRS has been implemented in MATLAB [35] adopting direct integration with Newmark's linear acceleration method [36] to solve the equation of motion of NSCs. Approximately 132,000 FRS curves have been generated for the selected RC buildings. The description of the building database, the record selection process and the characteristics of the ground motions, discussion on the proposed modification factors, a description of the FRS generator MATLAB code, and the validation of the proposed method through detailed numerical analysis of Building #23 of the database have been presented by the authors in [28-30]. The experimentally derived PA-FRS have been used for statistical analysis to, first, study the effect of the main parameters affecting NSCs' response (presented in section 5.5) and, second, to develop a procedure to generate FDS for building roofs (given ξ_{NSC} = 5%) directly from the 5% damped UHS of NBCC 2015 (presented in section 5.6) corresponding to the building location. Two separate sets of equations are proposed for low-rise and medium-rise buildings to generate FDS in three distinct spectral regions; namely short-period, fundamental-period, and long-period regions. Although the proposed methodology remains valid for high-rise buildings, no recommendations have been made for this category since the number of high-rises in the database was not deemed sufficient for such recommendations. This can be done as a future study by adding more AVM-tested high-rises to the database. It should also be noted that this study is mainly focused on post-disaster buildings that are mostly low/medium-rise buildings so the exclusion of high-rise buildings at this step does not impair the scope of the project. The last milestone is to extend the application of the proposed method to generate FDS for selection of any damping ratio and elevation of NSCs, which is covered in another publication by the authors [37].

Table 5-2 – Building characteristics and AVM results

Building Category	**Build #**	**LLRS type**	**Construction year**	**H_A/H_B (m)**	**N_A/N_B**	**Mode 1**		**Mode 2**		**Mode 3**		**NBCC period (s)**
						Translational mode		**Translational mode**		**Torsional mode**		
						AVM Period (s)	**AVM ξ (%)**	**AVM Period (s)**	**AVM ξ (%)**	**AVM Period (s)**	**AVM ξ (%)**	

Low-rise buildings	1	RCSW	1969	6.5/1.5	1/1	0.15	1.15	0.13	1.81	0.12	0.16	0.20
	2	RCSW	1969	6.5/1.5	1/1	0.27	4.10	0.24	1.90	NA	NA	0.20
	3	RCMF	1957	8.6/6.4	2/1	0.15	2.90	0.12	1.40	0.10	2.40	0.38
	4	RCMF	1957	7.7/3.3	2/1	0.18	1.50	0.18	1.30	0.10	2.00	0.35
	5	RCMF	1963	7.5/2.7	2/1	0.20	1.18	0.16	1.55	0.11	0.42	0.34
	6	RCMF	1963	7.5/2.7	2/1	0.18	2.53	0.13	1.17	NA	NA	0.34
	7	RCMF	1963	7.5/2.7	2/1	0.18	3.17	0.14	2.14	0.11	0.75	0.34
	8	RCMF	1993	8.4/3.3	2/1	0.19	2.00	0.18	1.80	0.13	2.10	0.37
	9	RCMF	1961	8.4/4.7	2/1	0.23	1.70	0.21	1.70	0.16	3.30	0.37
	10	RCMF	1964	17.1/NA	2/1	0.38	3.60	0.38	3.90	0.15	1.40	0.63
	11	RCMF	1975	10.8/2.7	3/1	0.15	2.00	0.13	2.30	0.11	1.60	0.45
	12	RCMF	1964	13.0/4.1	3/1	0.38	4.10	0.38	4.00	0.23	2.90	0.51
Medium-rise buildings	13	RCMF	1967	13.0/2.2	4/1	0.22	1.44	0.19	1.08	0.11	0.67	0.51
	14	RCMF	1964	12.0/3.1	4/1	0.18	2.72	0.15	2.70	0.12	0.09	0.48
	15	RCMF	1975	18.6/2.4	4/1	0.30	2.00	0.22	2.30	0.18	1.60	0.67
	16	RCMF	1975	15.9/5.1	4/2	0.30	2.00	0.22	2.90	0.18	2.60	0.60
	17	RCMF	1969	18.1/0.0	5/0	0.29	0.81	0.29	0.39	0.16	0.20	0.66
	18	RCSW	1998	19.6/3.6	5/1	0.40	2.32	0.36	1.66	0.28	2.76	0.47
	19	RCMF	1961	20.2/3.1	7/1	0.36	1.74	0.32	1.34	0.30	1.09	0.71
	20	RCMF	1961	20.2/3.1	7/1	0.37	1.42	0.31	0.75	0.29	1.01	0.71
	21	RCMF	1962	20.2/3.1	7/1	0.37	1.63	0.31	1.41	0.28	1.07	0.71
	22	RCSW	1971	28.0/6.7	7/2	0.59	3.61	0.46	4.35	0.36	1.72	0.61
High-rise buildings	23	RCMF	1957	36.0/3.5	10/1	0.53	1.72	0.40	1.22	0.37	1.09	1.10
	24	RCMF	1965	45.6/7.4	13/2	1.30	3.70	1.03	3.3	0.96	3.70	1.32
	25	RCSW	1969	55.4/8.4	13/2	0.70	1.79	0.68	1.70	0.41	2.04	1.01
	26	RCSW	1978	51.2/6.3	16/2	0.96	1.89	0.87	1.78	0.42	1.30	0.96
	27	RCMF	1965	58.7/7.9	18/NA	1.25	2.54	1.03	2.87	0.94	2.15	1.59

RCSW = Reinforced Concrete Shear Wall system, RCMF = Reinforced Concrete Moment-resisting Frame system, HA = Height above ground level (m), HB = Height below ground level (m), NA = Number of floors above ground level, NB = Number of floors below ground level, ξ = Modal viscous damping ratio (percentage of critical value).

5.5 **Key parameters affecting the acceleration response of NSCs**

Prior to generating FDS, we have studied the main factors of NSC acceleration response and their impact in a quantitative manner to enhance the understanding of component's seismic behaviour. These are: 1) tuning of the NSC fundamental period with those of the supporting structure, 2) location of NSC in the building, and 3) NSC internal damping.

There are three distinct types of accelerations referred to in the following section. They are defined here for clarity: 1- Peak Ground Acceleration (PGA), that is the maximum horizontal ground acceleration expected to occur during an earthquake at a selected location; 2-Peak Floor Acceleration (PFA), that is the maximum horizontal acceleration response of a selected floor during an earthquake which also represents the spectral acceleration of an infinitely stiff NSC (T_{NSC} = 0.0 s); and 3- Peak Component Acceleration (PCA), that is the maximum acceleration demand of all NSCs (i.e. both rigid and flexible components) located at the selected floor.

5.5.1 Tuning of fundamental period of NSCs with building modal periods

Tuning of the fundamental periods of NSCs with those of their supporting structure (including first and higher modes) significantly increases the acceleration response of NSCs, as shown in Figure 5.1 where the vertical axis is the roof PA-FRS normalized by PFA and the horizontal axis is the NSCs period (T_{NSC}) normalized by fundamental period of the buildings ($T_{1\text{-}B}$). Results for low-rise, medium-rise, and high-rise buildings are plotted in Figure 5.1.a, b, and c, respectively. In each figure, gray lines represent the normalized PA-FRS of the individual buildings in the category accompanied with their median (red line) and median+σ (84th percentile, blue line).

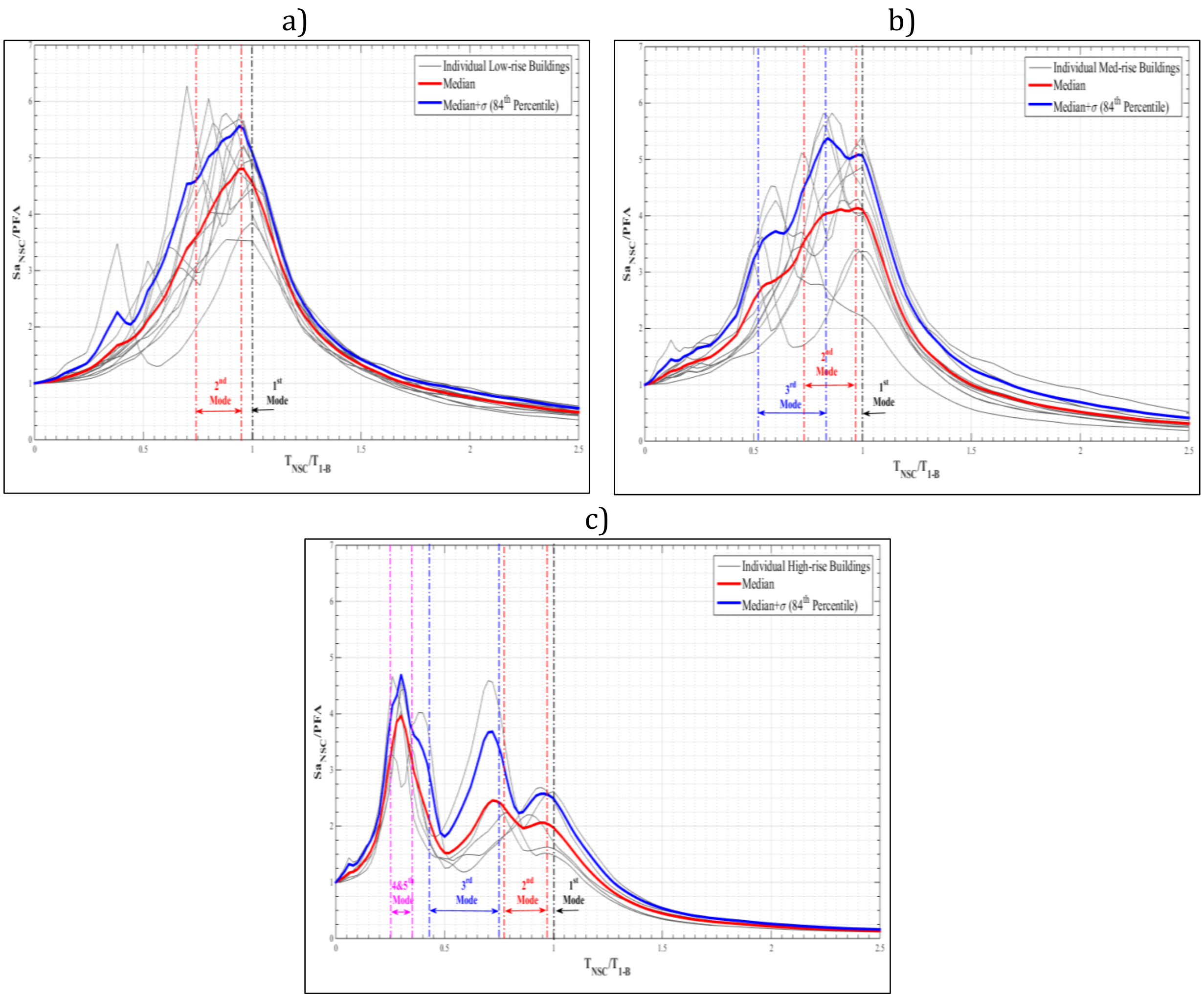

Figure 5.1 – Roof PA-FRS normalized by Peak Floor Acceleration (PFA) vs (TNSC / T1-B), ξNSC = 5%: a) Low-rise buildings; b) Medium-rise buildings; c) High-rise buildings.

Each gray line is the median+σ of the PA-FRS of one building over the entire set of selected ground motions. The ratios of modal periods of each building to its fundamental period (T_{i-B}/T_{1-B}) are calculated and the range of these ratios for all the buildings in each category are illustrated in Figure 5.1 using the vertical dotted lines. For instance, in Figure 5.1.a the range of (T_2/T_1) for all the low-rise buildings is defined by the two red dotted lines. As expected, NSCs with period close to one of the building modal periods experience higher acceleration demand than those with no tuning effect. In low and medium rise buildings, the PCA (i.e. highest component acceleration demand) is experienced by the components tuned with the

1st and 2nd modes of the buildings. Note that in this study a 3D model of each building is considered and the ground motions are applied independently in two orthogonal horizontal directions. The first two modes of the buildings are the fundamental sway modes in two perpendicular directions of the structure plan. In medium-rises, a lower peak is also observed in the vicinity of the 3rd modal period of the building which is, in most cases, a torsional mode. In high-rises, however, the highest acceleration demand of NSCs is happening in the vicinity of 4th and 5th modal periods of the building (i.e. second sway modes of the buildings) and <u>not</u> at the 1st or 2nd mode. This highlights the significance of the higher mode effects on NSC responses in tall buildings, which is disregarded by building codes. An important improvement of this study compared to previous work (e.g. [22, 24, 25, 38] which have used 2D models of buildings) is to consider real buildings in three dimensions, which enables the consideration of torsional modes as well as combined torsional-translational ones that are very common in irregular buildings.

5.5.2 Elevation of NSCs in the building

The acceleration response of NSCs is considerably changed along the height of the building. For instance, Figure 5.2 shows the results of Building #20 in terms of acceleration response of NSC at every floor, in Figure 5.2.a, and the normalized responses with respect to the roof value, in Figure 5.2.b. As it can be seen, the component acceleration response, in general, increases with increased floor elevation. Filtering of the component responses by the dynamic properties of the building is usually amplified with elevation. Noting that the PA-FRS at ground level is directly derived from ground motions (i.e. no filtering by the building properties) explains the difference between the PA-FRS of the ground floor with the floors above, in Figure 5.2. The variation of PFA/PGA along the building height is depicted for low, med, and high-rises in Figure 5.3.a, b, and c, respectively and is compared with the recommendations of NBCC 2015 [1], ASCE-SEI-07 [2], and Eurocode 8 [3]. Each colored circle represents the output of one building over the entire set of ground motions, dashed lines are the mean value (red color) and the mean±σ values (blue color) of all the same-category buildings, and the solid lines represent the code recommendations. NBCC and ASCE (black solid line) recommend the same linear variation of PFA/PGA (based on the assumption of the 1st mode building response) from 1.0 at ground level to 3.0 at roof level while the Eurocode 8 (gray solid line) recommends 2.5 for the roof level. The results show that although the linear variation assumption might be acceptable for low-rise buildings, it is not quite accurate for the medium and high-rises where the higher mode effect is significant. Considering the median+σ (84th percentile) value of the responses, the codes are underestimating the PFA/PGA ratios at every floor and roof of the low-rises as well as in the top half of the mid-rises, while overestimating the ratio in the top-half of the high-rises. The amplification of the maximum component acceleration (PCA) at each level with respect to the corresponding PFA is shown for low and mid-rise buildings in Figure 5.4.a and b, respectively and compared with the corresponding codes values obtained from NBCC 2015, ASCE, and Eurocode 8. The legend is the same as in Figure 5.3. Looking at the mean+σ results for the low and medium-rise buildings, the PCA/PFA ratio increases exponentially from ground level to half-height of the buildings ($0<Z/H<0.5$) and remains almost constant at an approximate value of 6.0 for the upper half ($0.5<Z/H<1.0$). The NBCC 2015 and ASCE-SEI-07 assume a constant ratio of PCA/PFA=2.5 along the height while Eurocode 8 assumes a linear decrease from 2.5 at ground level to 2.2 at roof. The results show that all three building codes are considerably underestimating the amplification of component acceleration with respect to the PFA. It should be mentioned that the high-rises do not show the same trend as the low/medium-rises. In conclusion, the precise evaluation of the effect of NSCs location in the building on their acceleration response spectrum requires a method capable of considering the higher modes effect.

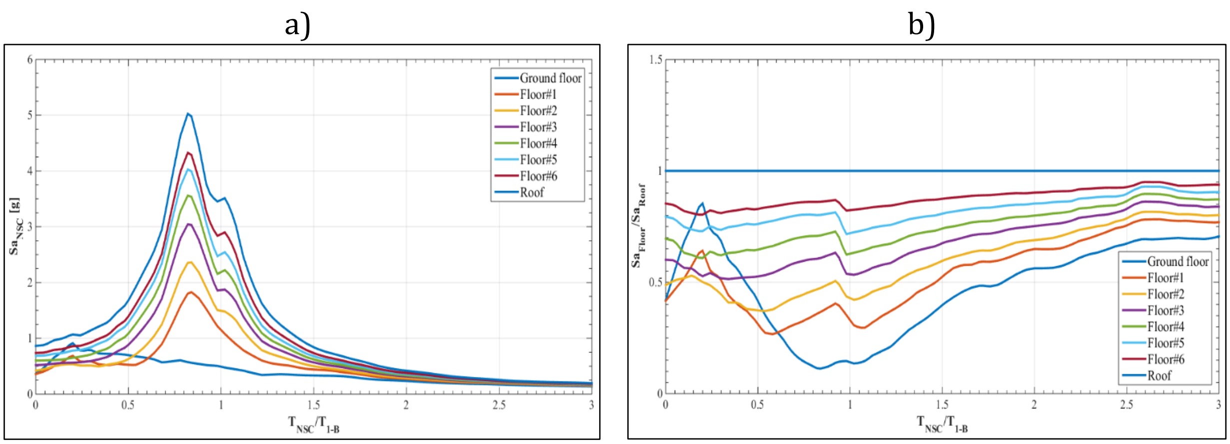

Figure 5.2 – Building #20, ξ_{NSC} = 5%: a) PA-FRS of all levels; b) PA-FRS of all levels normalized by roof values.

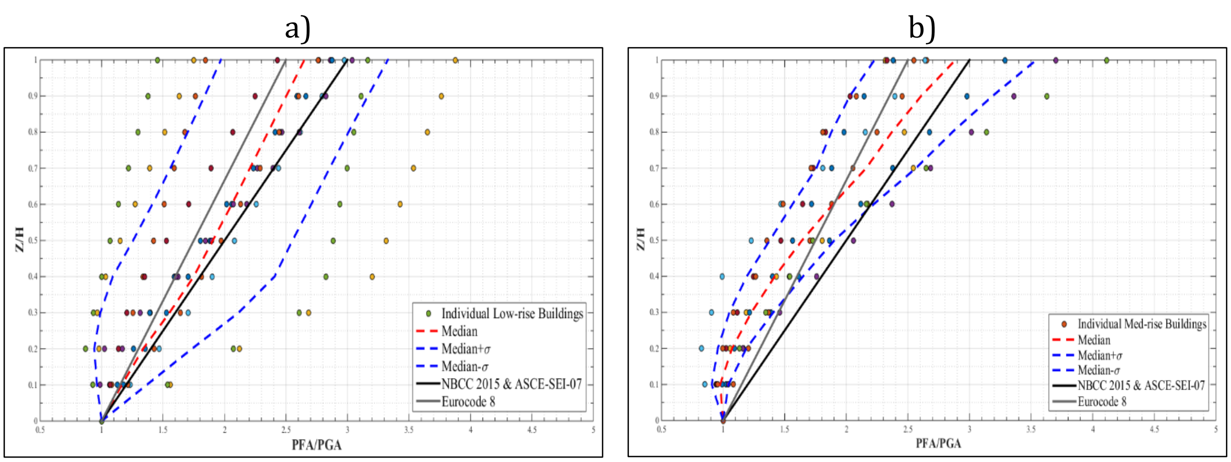

c)

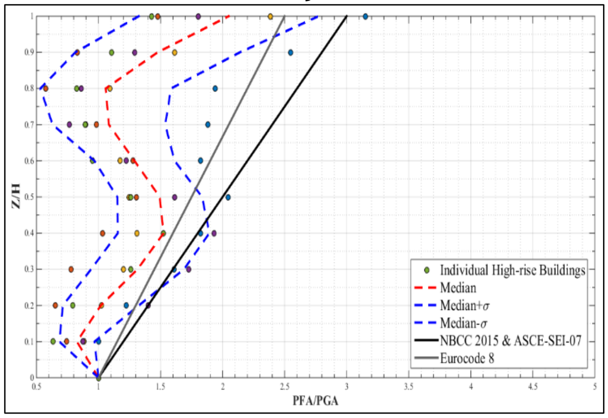

Figure 5.3 – Peak Floor Acceleration (PFA) normalized by Peak Ground Acceleration (PGA) vs relative height (Z/H), ξ_{NSC} = 5%: a) Low-rise buildings; b) Medium-rise buildings; c) High-rise buildings.

a) b)

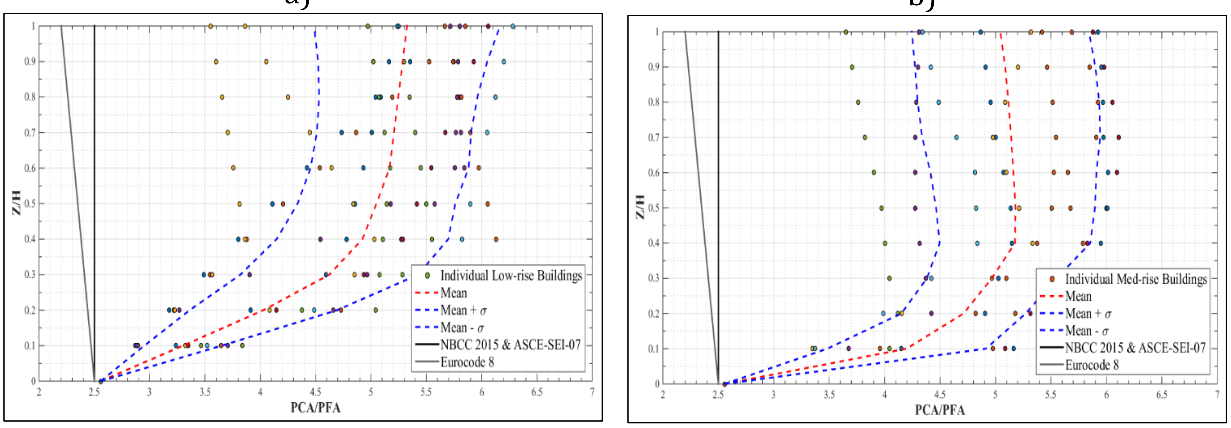

Figure 5.4 – Peak Component Acceleration (PCA) normalized by Peak Floor Acceleration (PFA) vs relative height (Z/H), ξ_{NSC} = 5%: a) Low-rise buildings; b) Medium-rise buildings.

5.5.3 NSC damping ratios

The internal damping of NSCs is another key factor of the component response that considerably affects both the shape and magnitude of the PA-FRS; decreasing the component damping ratio will result in PA-FRS with sharper and higher amplitude peaks. In this study, the damping ratios considered for NSCs are of 2, 5, 10, and 20 % viscous damping. This range is deemed appropriate to cover all different types of NSCs. For example, the FRS results of Building #4 (3-story low-rise) and Building #20 (7-story medium-rise) are illustrated in Figure 5.5 and Figure 5.6, respectively. Figures "a" represent the PA-FRS at roof level of each building given four different damping ratios where each solid line is the envelope of the X and Y direction responses as the analysis was done in both directions separately. Additionally, the final output for each direction is, in turn, the median+σ (84th percentile) of the responses over the entire set of input ground motions. As expected, the higher the ξ_{NSC} is, the lower and smoother the peaks will be. In figures "b", the PA-FRS for all four ξ_{NSC} values are normalized with respect to the PA-FRS with ξ_{NSC}=5% at every floor and presented as a function of $T_{NSC}/T_{1\text{-}B}$. The maximum variations (i.e. highest ratios) correspond to the natural periods of the buildings (1st or higher modes), due to the tuning effect. The results of all floors are close and consistent with each other, meaning that the relative effect of NSC damping is independent of the location of the component along the building height. Looking at figures "b", some discrepancies can be observed between the bottom floor or lowest two floors and the rest of the floors, only within the short-period region of the spectra. This is because the response of the bottom floors is dominated by the characteristics of the ground motion while the response at upper floors is dominated by the building characteristics. Furthermore, increasing ξ_{NSC} from 2% to 20% in both buildings will approximately decrease the PCA from 160% to 40% with respect to the PCA of ξ_{NSC}=5%. None of the aforementioned building codes takes this effect into account when computing the seismic acceleration demand on NSCs which makes their estimation inaccurate. Here, the FDS will be derived for NSC with 5% damping to be consistent with the 5% damped UHS. However, the methodology is extended to cover different NSC damping ratios as presented in [37].

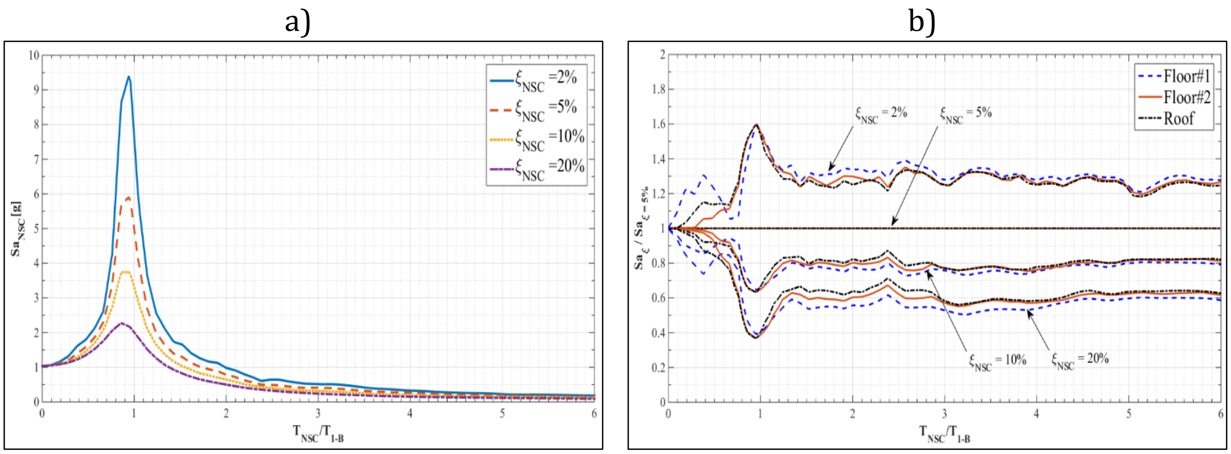

Figure 5.5 – Low-rise Building #4, 3-story: a) Roof PA-FRS given ξ_{NSC} = 2, 5, 10, 20 % vs (T_{NSC} / T_{1-B}); b) Normalized PA-FRS at every floor, for all ξ_{NSC} with respect to the values for ξ_{NSC} =5%.

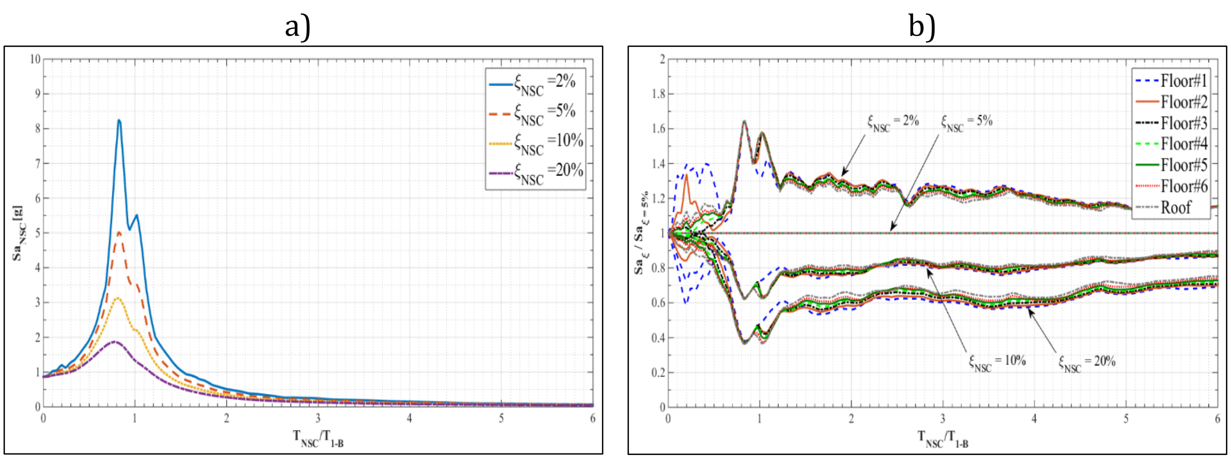

Figure 5.6 - Mid-rise Building #18, 7-story: a) Roof PA-FRS given ξ_{NSC} = 2, 5, 10, 20 % vs (T_{NSC} / T_{1-B}); b) Normalized PA-FRS at every floor, for all ξ_{NSC} with respect to the values for ξ_{NSC} =5%.

5.6 Generation of roof FDS directly from UHS for ξ_{NSC} =5%

As discussed previously, a reliable approach for seismic assessment and analysis of acceleration-sensitive NSCs must be capable of accommodating the shortcomings of the modern building code provisions and improving their accuracy while maintaining their simplicity and practicality. Similar to the seismic design of structural components according to the design response spectrum method (e.g. based on the Uniform Hazard Spectrum (UHS) recommended by NBCC 2015 [1]), the seismic assessment of NSCs can be done through floor design spectra, but such spectra are not currently available in design codes and standards. Therefore, this study is filling this important gap by introducing an original methodology to generate FDS directly from UHS based on experimental data obtained from AVM. Firstly, the FDS for the building roof given 5% viscous damping for NSCs is generated which is consistent with the 5% damped UHS and, secondly, the method is extended to any floor level ($0 \leq Z/H \leq 1$) and ξ_{NSC} of interest ($1\% \leq \xi_{NSC} \leq 20\%$). The first step is presented in more detail here while the reader is referred to Asgarian and McClure [37] for the second step.

To summarize, each building of the database has been subjected to a set of 20 ground motions (compatible with the UHS of NBCC 2015 for Montreal) in X and Y directions and analysed in both directions independently. Using the proposed approach, the PA-FRS is generated for every floor considering four different values of ξ_{NSC}, once in the X direction with the seismic records applied along X and then in the Y direction with records applied along Y. As all buildings are considered in three dimensions in this study, applying the seismic records in the X direction, for instance, will yield PA-FRS results in both the X and Y directions at each floor. However, in general, the PA-FRS obtained in the same direction as the record is dominant and, hence, selected for further processing. The median+σ (84th percentile) PA-FRS corresponding to seismic inputs in the both X and Y directions are computed and their envelope is used as the basis for the analysis. To facilitate comparisons of the results among the different buildings, two types of normalization have been used. Considering the envelope PA-FRS of one building which represents Sa_{-NSC} vs T_{NSC}, first T_{NSC} is normalized by the fundamental natural period of the building (T_{1-B}) and second, the Sa_{-NSC} is normalized by the building design spectral acceleration recommended by NBCC 2015 (i.e. UHS value at T_{1-B}). The component damping value ξ_{NSC}=5% is selected as the reference so as to normalize the PA-FRS by the 5% damped UHS value (UHS ($T_{1\text{-}B}$)) prescribed for the building location. Knowing that different building heights categories (low, medium, and high- rise buildings) show different trends in their PA-FRS (as discussed in section 5.5), each building-height category is studied separately using the same methodology. The entire spectral region is divided into three distinct ranges namely short-period ($0<T_{NSC}/T_{1\text{-}B}\leq 0.7$), fundamental-period ($0.7\leq T_{NSC}/T_{1\text{-}B}\leq 1.0$), and long-period regions ($1.0\leq T_{NSC}/T_{1\text{-}B}$), and the relation between the FDS and UHS is sought in each part. Figure 5.7 schematically shows how the spectral acceleration is idealized in each spectral region. While the same idealization is adopted for low and medium-rise buildings, different set of factors are derived for each building-category based on the results. It is understood that although the recommendations are derived for RC buildings, the proposed methodology can be employed to different structural materials and building types, as long as sufficient AVM data are available to validate the model. The next sections describe the specific formulations for the FDS applicable to NSCs in low and medium-rise RC buildings.

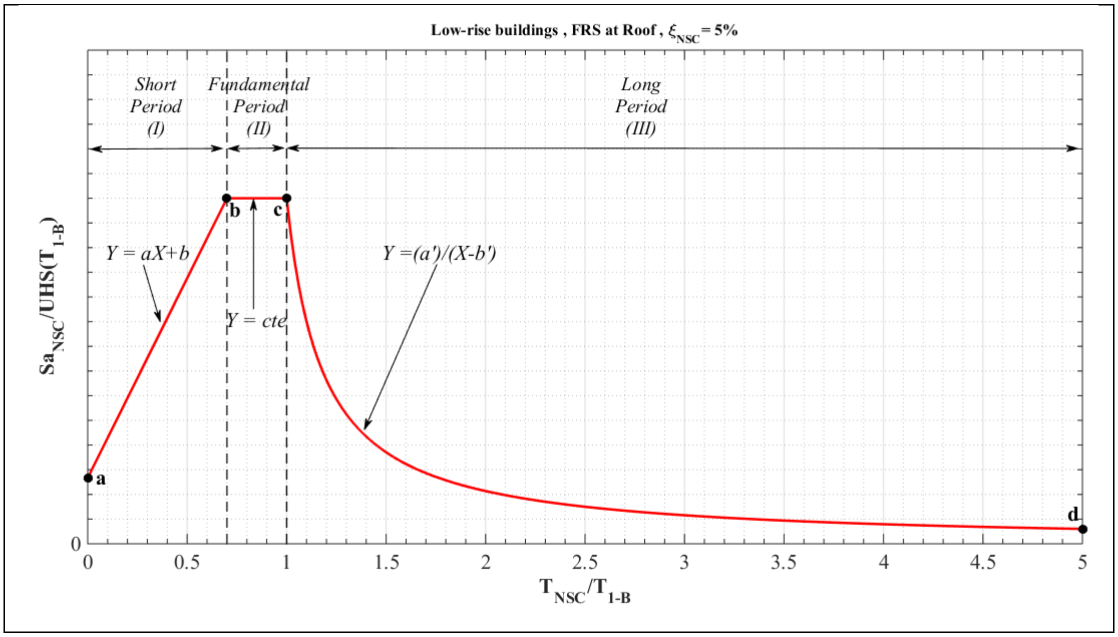

Figure 5.7 – Schematic of the proposed FDS and idealization of spectral acceleration for NSCs

5.6.1 Low-rise RC buildings

Figure 5.8 shows the proposed FDS for the roof level of low-rise buildings considering 5% viscous damping for NSCs. Gray lines represent the generated envelope PA-FRS at the roof level of the individual low-rise buildings of the database and the red and blue dashed lines show the median and median+σ (84^{th} percentile) curves, respectively. The solid black line is the proposed normalized FDS which is produced according to Equation 5.1:

$$Low-rise: \frac{S_{a_{NSC}}}{UHS(T_{1-B})} = \begin{cases} 12.14\left(\frac{T_{NSC}}{T_{1-B}}\right) + 2.0: & 0.0 \le \frac{T_{NSC}}{T_{1-B}} \le 0.7 \\ 10.5: & 0.7 \le \frac{T_{NSC}}{T_{1-B}} \le 1.0 \\ \frac{1.89}{\frac{T_{NSC}}{T_{1-B}} - 0.82}: & 1.0 \le \frac{T_{NSC}}{T_{1-B}} \le 5.0 \end{cases} \qquad \textit{Equation 5.1}$$

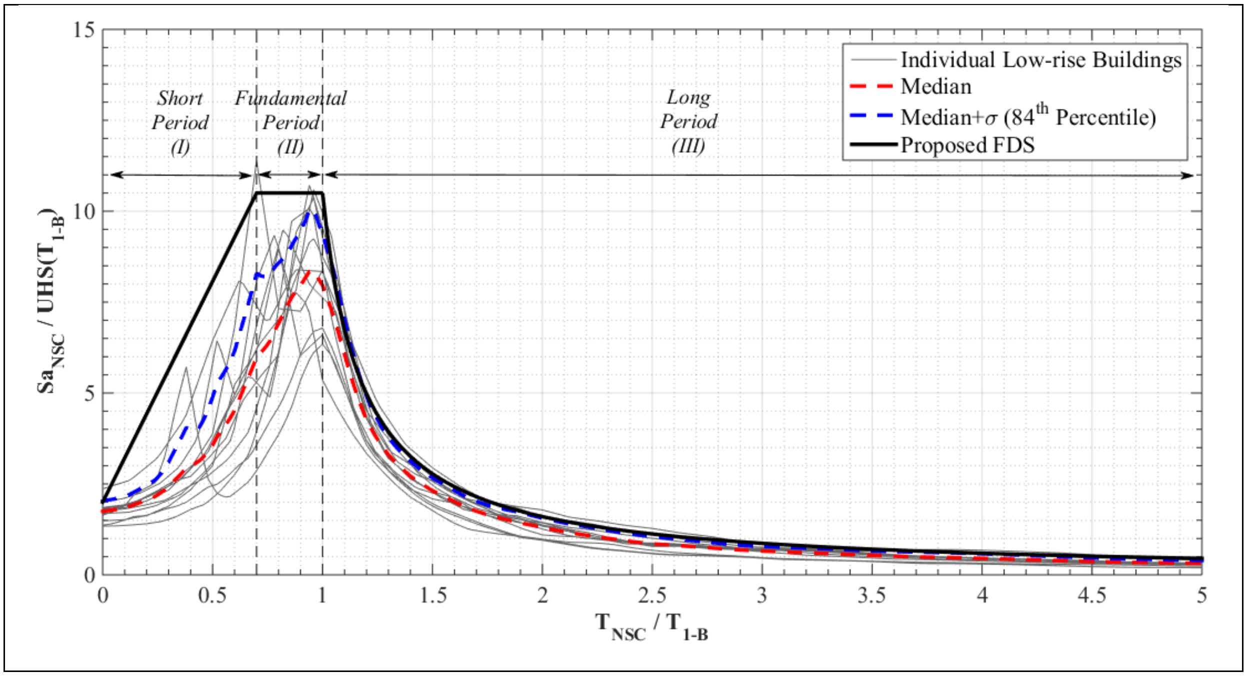

Figure 5.8 – Proposed FDS for roof level of low-rise buildings given ξ_{NSC}=5%.

For 5.0 ≤ T_{NSC}/T_{1-B}, a conservative and simple approach is proposed where the $Sa_{NSC}/UHS(T_{1-B})$ is decreased linearly from its value at T_{NSC}/T_{1-B} = 5.0 to half of that at T_{NSC}/T_{1-B} =10.0. Using these normalized spectra, it is easy to generate exclusive FDS for a specific building in terms of Sa_{NSC} vs T_{NSC}: the normalized values are to be multiplied back by the T_{1-B} and $UHS(T_{1-B})$. The generated FDS is dependent on the dynamic properties of the building, meaning that an exclusive FDS can be derived for each building. Figure 5.9 shows the proposed FDS for the roof of all low-rises in the database compared to their experimentally derived roof PA-FRS and the design recommendations of NBCC 2015 & ASCE-SEI-07 (dashed blue line) and Eurocode 8 (dashed red line). Note that in calculating the code recommendations, the design ground acceleration recommended by NBCC 2015 (i.e. $0.3\times F_a\times S_a(0.2)$) is used for all three codes to keep the results consistent and the building and component importance factors (I_E and I_p) are eliminated from the calculations. Also, the component response reduction factors which account for energy dissipation of NSCs are removed (in this spectral approach all NSCs are considered as linear SDOF systems). This way the code acceleration demands on NSCs are comparable with the proposed FDS as well as the experimentally derived PA-FRS. The results in Figure 5.9 show consistency between the proposed FDS and PA-FRS, which indicate the reliability and accuracy of the proposed approach. It is seen that the current building codes underestimate the acceleration demand on NSCs located at roof level of the low-rise buildings specially in the fundamental building period region (tuning range) where the highest acceleration demand is happening.

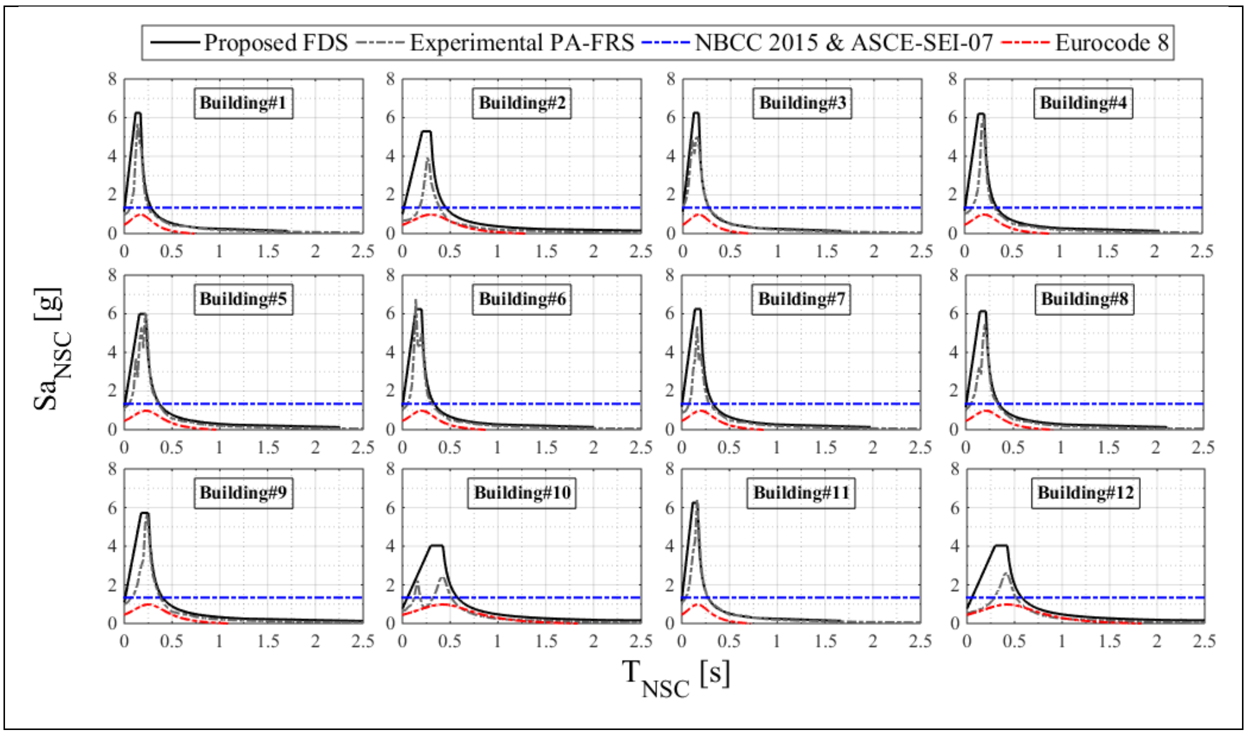

Figure 5.9 –Proposed FDS compared with experimentally derived PA-FRS and code recommendations for the low-rise buildings, Roof level, ξ_{NSC}=5%.

5.6.2 Medium-rise RC buildings

This section presents the results and recommendations for medium-rise buildings, similar to section 5.6.1. Figure 5.10 shows the proposed FDS at roof level for medium-rise buildings considering 5% viscous damping for NSCs. The legend is the same as in Figure 5.8. The proposed normalized FDS is produced according to Equation 5.2. For $5.0 \leq T_{NSC}/T_{1\text{-}B}$ the same approach can be used as for low-rises. Given the $T_{1\text{-}B}$ and UHS($T_{1\text{-}B}$) for the medium-rises, their corresponding FDS are computed and compared with their experimentally derived PA-FRS in Figure 5.11. Again, the proposed FDS shows consistency with the actual PA-FRS. The current building codes underestimate the acceleration demand on NSCs mounted on the roof of the medium-rises as well.

$$Medium - rise : \frac{S_{a_{NSC}}}{UHS(T_{1-B})} = \begin{cases} 12.88\left(\frac{T_{NSC}}{T_{1-B}}\right) + 3.0 : & 0.0 \leq \frac{T_{NSC}}{T_{1-B}} \leq 0.7 \\ 12.0 \ : & 0.7 \leq \frac{T_{NSC}}{T_{1-B}} \leq 1.0 \\ \frac{1.68}{\frac{T_{NSC}}{T_{1-B}} - 0.86} \ : & 1.0 \leq \frac{T_{NSC}}{T_{1-B}} \leq 5.0 \end{cases} \qquad \textit{Equation 5.2}$$

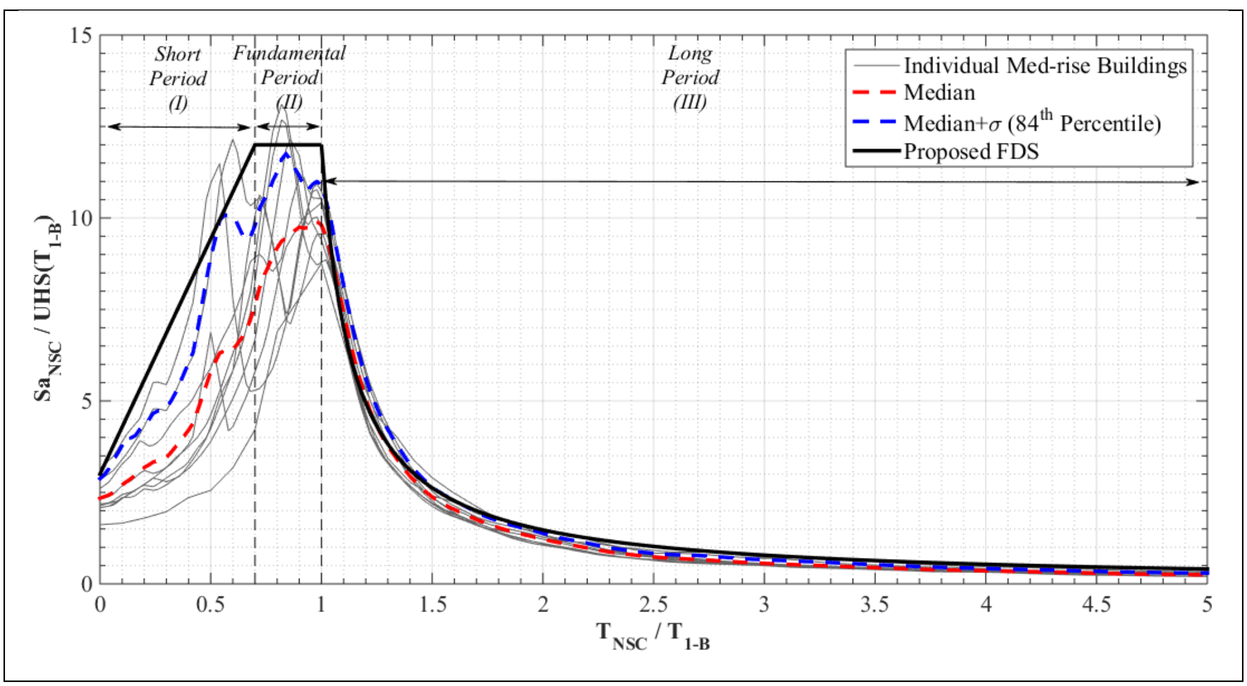

Figure 5.10 – Proposed FDS for roof level of medium-rise buildings given ξ_{NSC}=5%.

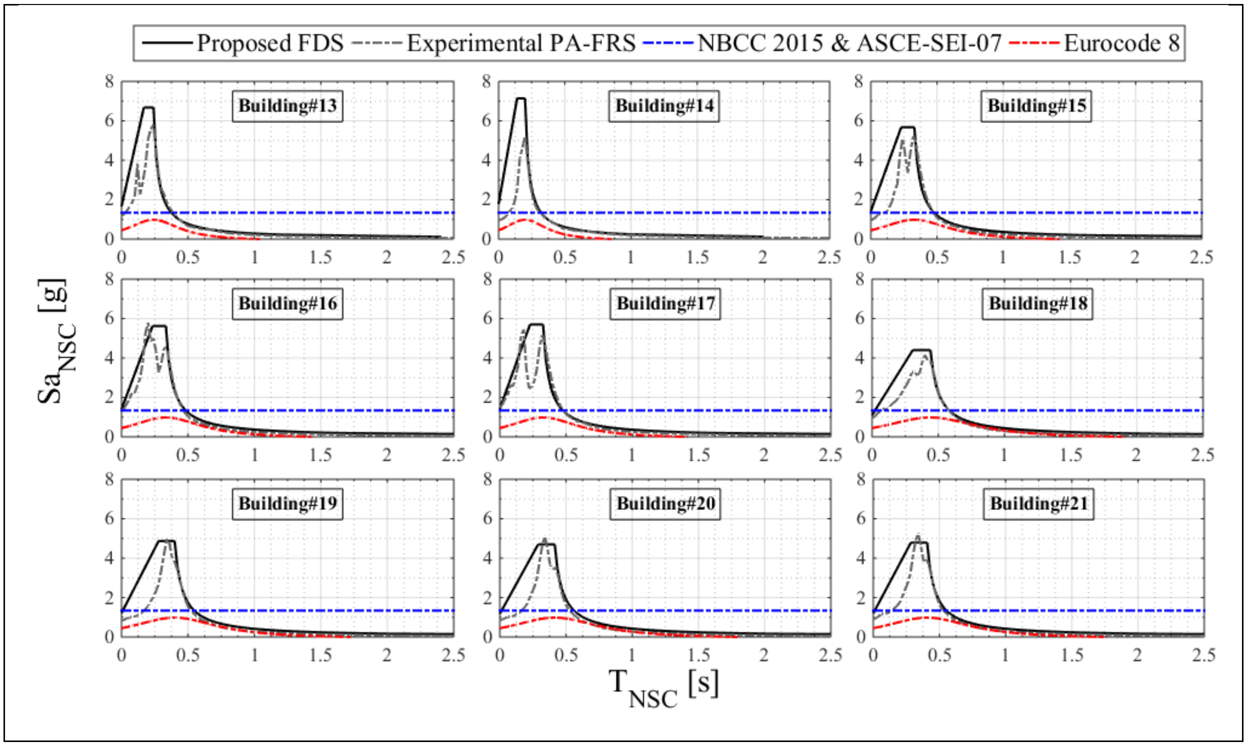

Figure 5.11 –Proposed FDS compared with experimentally derived PA-FRS for the medium-rise buildings, Roof level, ξ_{NSC}=5%.

5.6.3 High-rise RC buildings

Figure 5.12 depicts the experimentally-derived roof PA-FRS for the five high-rise buildings (gray lines) accompanied with their median (red dashed line) and median+σ (84th percentile) (blue dashed line) curves. The proposed methodology can be also employed to derive the FDS for this category upon having a sufficient number of cases in the building data base. Particular attention should be paid to the fact that for high-rises, the dominant response peaks are not happening in the fundamental-period region ($0.7 \le T_{NSC}/T_{1\text{-}B} \le 1.0$) (tuning range) due to the relative importance of the building higher modes of vibration.

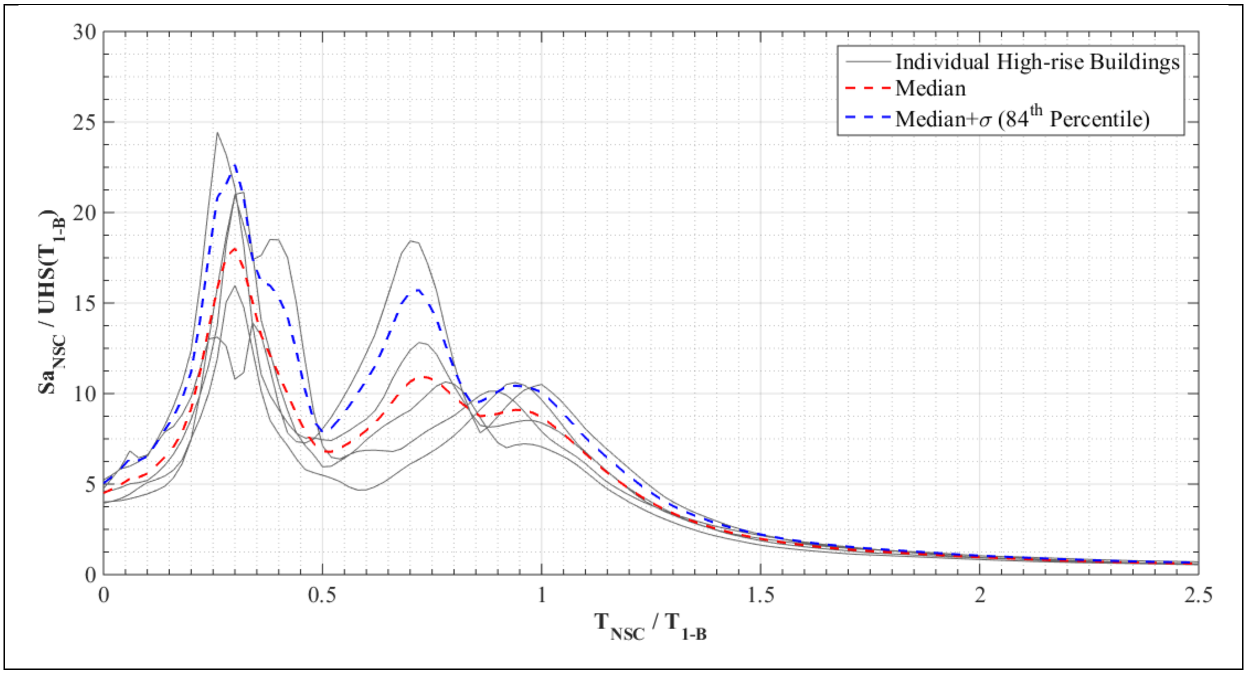

Figure 5.12 – Proposed FDS for roof level of high-rise buildings given ξ_{NSC}=5%.

5.7 Conclusion

In this study, a total of 27 existing reinforced concrete buildings, all designated as post-disaster buildings and located in Montreal, Canada, have been analysed. The building database comprises 12 low-rise, 10 medium-rise, and 5 high-rise buildings. The buildings are subjected to an ensemble of ground motions compatible to the Uniform Hazard Spectrum prescribed in the 2015 National Building Code of Canada. An original method is proposed to generate experimental PA-FRS and inter-story drift curves for non-structural building components (NSCs) based on the building modal properties extracted from AVM records ([28, 30]). The PA-FRS values have been generated for every floor of the buildings considering four different damping ratios for NSCs (i.e. 2, 5, 10, and 20 % viscous damping). As real three-dimensional buildings are considered and their dynamic properties are extracted from AVM test records, the effect of higher modes and torsional behaviour of the supporting buildings as well as the dynamic interactions between the existing NSCs and the building structure are considered, while they are not in the conventional FRS methods. Using the generated PA-FRS, the effects of key parameters such as the NSC-building tuning effect, the location of NSCs along building height, and the internal damping of NSCs, on the acceleration response of the components have been evaluated statistically and compared to the recommendations of three modern building codes (NBCC 2015, ASCE-SEI-07, and Eurocode 8). The results indicate that the NSC response can be directly correlated to the fundamental building mode response assumed in the empirical method adopted by all three codes in low and medium-rise buildings. This assumption is no longer valid for the high-rises where the effect of higher modes is significant (Figure 5.3). In addition, it was shown that the building codes underestimate the amplification of component acceleration with respect to the acceleration of the supporting floor (i.e. PCA/PFA ratio, Figure 5.4). It was shown that the NSCs damping has considerable effect on the component acceleration response which is also disregarded by the current building code provisions (Figure 5.5 and Figure 5.6). The experimentally-derived PA-FRS have been studied statistically and a methodology proposed to generate the roof FDS for components with 5% damping directly from 5% damped building UHS. The methodology has been deployed to the low and medium-rise building results independently and two sets of equations are recommended to produce the roof FDS directly from the code-specified UHS and covering three distinct spectral regions (i.e. short, fundamental/tuning, and long-period regions). The proposed approach uses the dynamic properties of the building (i.e. $T_{1\text{-}B}$ and UHS($T_{1\text{-}B}$)) as input variables, meaning that for each building an exclusive FDS is produced which accounts for its specific modal characteristics extracted from AVM test records.

The final recommendations of this work are applicable to low and medium-rise RC buildings. However, the proposed methodology is of general applicability and can be extended to cover high-rise RC buildings as well as steel structures or any other building category as long as sufficient AVM data are available. The next milestone is to extend the approach to cover different NSC damping ratios and locations of NSCs along the building height: this is presented in detail in reference [37]. FDS have been generated for all the low and medium-rises of the RC building database and compared with their experimentally derived PA-FRS for roof level and 5% damping of NSCs. The comparison showed that the generated FDS are consistent with PA-FRS and the method is reliable. In conclusion, the approach is shown to be practical, accurate, and fast to produce FDS for seismic design or assessment of acceleration-sensitive NSCs particularly in existing post-critical buildings. It is emphasized that the proposed method does not require any finite element modeling of the building as all building modal characteristics are derived from AVM records.

5.8 References

1. National Research Council of Canada (NRC), Institute for Research in Construction (IRC), *National Building Code of Canada (NBCC)*. 2015: Ottawa, ON, Canada.
2. American Society of Civil Engineers, *ASCE Standard 7-16: Minimum Design Loads for Buildings and Other Structures*. 2016, American Society of Civil Engineers: Reston, VA.
3. Comite Europeen de Normalization, *Eurocode 8–Design of Structures for earthquake resistance–Part 1: General rules, seismic actions and rules for buildings*, in *EN-1998-1*. 2004: Brussels, Belgium.
4. Villaverde, R., *Earthquake resistant design of secondary structures: a report on the state of the art*, in *Proc., 11th World Conf. on Earthquake Engineering*. 1996, Elsevier Science Ltd.: Acapulco, Mexico. p. 13.
5. Ayres, J.M., T.-Y. Sun, and F.R. Brown, *Nonstructural damage to buildings.* The Great Alaska Earthquake of 1964: Engineering, Division of Earth Sciences, National Research Council, National Academy of Sciences, 1973: p. 346-456.
6. Ayres, J.M. and T.-Y. Sun, *Nonstructural damage.* The San Fernando, California Earthquake of February 9, 1971., US Department of Commerce, National Ocean and Atmospheric Administration, 1973. **1(B)**: p. 736-742.

7. Gates, W. and G. McGavin. *Lessons learned from the 1994 Northridge earthquake on the vulnerability of nonstructural systems*. in *Proceedings of the Seminar on Seismic Design, Retrofit, and Performance of Nonstructural Components, ATC*. 1998.
8. Schiff, A., *The Whittier Narrows, California Earthquake of October 1, 1987—Response of Elevators.* Earthquake Spectra, 1988. **4**(2): p. 367-375.
9. Filiatrault, A., C. Christopoulos, and C. Stearns, *Guidelines, specifications, and seismic performance characterization of nonstructural building components and equipment*. 2002: Pacific Earthquake Engineering Research Center.
10. McKevitt, W., P. Timler, and K. Lo, *Nonstructural damage from the Northridge earthquake.* Canadian Journal of Civil Engineering, 1995. **22**(2): p. 428-437.
11. Myrtle, R.C., et al., *Classification and prioritization of essential systems in hospitals under extreme events.* Earthquake Spectra, 2005. **21**(3): p. 779-802.
12. Patrucco, H.A. and G.L. McGavin, *Survey of Nonstructural Damage to Healthcare Facilities by the January 1994 Northridge Earthquake*. 1995: HMC Group.
13. Boroschek, R. and R. Retamales, *Damage observed in El Salvador's public hospital system during the January 13, 2001 earthquake.* WHO/PAHO Collaborating Center for Disaster Mitigation in Health Facilities, University of Chile, Santiago, Chile, 2001.
14. Chock, G., et al., *Compilation of Observations of the October 15, 2006 Kiholo Bay (Mw 6. 7) and Mahukona (Mw 6.0) Earthquakes, Hawai 'i.* Earthquake Engineering Research Institute, 2006. **31**.
15. Gupta, A. and B. McDonald. *Performance of building structures during the October 15, 2006 Hawaii earthquake*. in *Proceedings of the The 14thWorld Conference on Earthquake Engineering*. 2008.
16. Miranda, E., et al., *Performance of nonstructural components during the 27 February 2010 Chile earthquake.* Earthquake Spectra, 2012. **28**(S1): p. S453-S471.
17. Fujisaki, E., et al., *Seismic vulnerability of power supply: lessons learned from recent earthquakes and future horizons of research*, in *Proceedings of 9th international conference on structural dynamics (EURODYN 2014)*. 2014, European Association for Structural Dynamics: Porto, Portugal. p. 345-350.
18. Eberhard, M.O., et al., *Mw 7.0 Haiti Earthquake of January 12, 2010: USGS/EERI Advance Reconnaissance Team Report*, in *US Geological Survey Open-File Report 2010-1048*. 2013, BiblioGov. p. 64.
19. Magliulo, G., et al., *The Emilia earthquake: seismic performance of precast reinforced concrete buildings.* Earthquake Spectra, 2014. **30**(2): p. 891-912.
20. Taghavi, S., *Response Assessment of Nonstructural Building Elements*, in *Department of Civil and Environmental Engineering*. 2003, Stanford University: Stanford, California. p. 96.
21. Calvi, P.M., *Relative displacement floor spectra for seismic design of non structural elements.* Journal of Earthquake Engineering, 2014. **18**(7): p. 1037-1059.
22. Medina, R.A., R. Sankaranarayanan, and K.M. Kingston, *Floor response spectra for light components mounted on regular moment-resisting frame structures.* Engineering Structures, 2006. **28**(14): p. 1927-1940.
23. Wieser, J., et al., *Floor accelerations in yielding special moment resisting frame structures.* Earthquake Spectra, 2013. **29**(3): p. 987-1002.

24. C. Petrone, et al., *Evaluation of the seismic demand on acceleration sensitive nonstructural components in RC frame structures*, in *Second European conference on earthquake engineering and seismology*. August,25-29,2014: Instanbul, Turkey.
25. Shooshtari, M.S., M. Naumoski, N. Foo, S., *Floor response spectra for seismic design of operational and functional components of concrete buildings in Canada.* Canadian Journal of Civil Engineering, 2010. **37**(12): p. 1590-1599.
26. Scholl, R., *Nonstructural issues of seismic design and construction.* EERI 84-04. 1984., Oakland, CA: Earthquake Engineering Research Institute.
27. Taghavi, S. and E. Miranda. *Probabilistic study of peak floor acceleration demands in nonlinear structures*. in *Proceedings of the 15th World Conference on Earthquake Engineering,*. 2012. Lisbon, Portugal.
28. A. Asgarian and G. McClure, *Generation of experimental floor response spectra for seismic assessment of Non-Structural Components (NSCs) based on ambient vibration measurements.* Manuscript submitted for publication, 2017: p. 22.
29. A. Asgarian, F. Mirshafiei, and G. McClure, *Experimental floor response spectra for seismic evaluation of operational and functional components of building*, in *CSCE 2014, 4th International Structural Specialty Conference*. 2014: Halifax, NS, May 28 to 31. p. 10.
30. A. Asgarian and G. McClure, *New methodology for seismic assessment of non-structural building components based on ambient vibration measurements*, in *16th World Conference on Earthquake*. 2017: Santiago, Chile. p. 12.
31. Sullivan, T.J., P.M. Calvi, and R. Nascimbene, *Towards improved floor spectra estimates for seismic design.* Earthquake and Structures, 2013. **4**(1): p. 109-132.
32. Mirshafiei, F., M. Mirshafiei, and G. McClure, *A new three-dimensional seismic assessment method (3D-SAM) for buildings based on experimental modal analysis.* Computers & Structures, 2017. **180**: p. 125-137.
33. Carreño, R.P. and R.L. Boroschek, *Modal parameter variations due to earthquakes of different intensities*, in *Civil Engineering Topics, Volume 4*. 2011, Springer. p. 321-333.
34. Çelebi, M., *Comparison of recorded dynamic characteristics of structures and ground during strong and weak shaking*, in *Increasing Seismic Safety by Combining Engineering Technologies and Seismological Data*. 2009, Springer. p. 99-115.
35. The MathWorks Inc., *MATLAB*. 2014: Natick, MA.
36. Chopra, A.K. and F. Naeim, *Dynamics of Structures—Theory and Applications to Earthquake Engineering*. Earthquake Spectra. Vol. 23. 2007. 491.
37. Asgarian, A. and G. McClure, *Direct generation of Floor Design Spectra (FDS) from Uniform Hazard Spectra (UHS) - Pat II: Extension and Application of the method.* Manuscript submitted for publication, 2017: p. 20.
38. Sankaranarayanan, R. and R.A. Medina, *Acceleration response modification factors for nonstructural components attached to inelastic moment-resisting frame structures.* Earthquake engineering & structural dynamics, 2007. **36**(14): p. 2189-2210.

Chapter 6

In the previous chapter (**Chapter 5**), an original method was presented to generate FDS directly from UHS provided that NSCs are located on roof level and have 5% internal viscous damping. This chapter (**Chapter 6**) describes the extension of the proposed method to generate FDS for any selected floor level and NSC damping ratio. For the sake of extension, the effect of NSCs damping ratio and their location along the height of the building were quantified using statistical analysis which are discussed in this chapter. The extended proposed approach is first formulated for low and medium rise RC buildings and then employed over the entire building database using the written MATLAB routine. The derived FDS for one low-rise (Building#4) and one medium-rise (Building#18) building are illustrated to present the application of the extended proposed approach and its outputs.

6 Direct generation of Floor Design Spectra (FDS) from Uniform Hazard Spectra (UHS) - Part II: Extension and Application of the method.

A. Asgarian[(1)], G. McClure[(2)]

[(1)] Ph.D. candidate, Department of Civil Engineering and Applied Mechanics, McGill University, Canada, amin.asgarian@mail.mcgill.ca

[(2)] Professor, Department of Civil Engineering and Applied Mechanics, McGill University, Canada, ghyslaine.mcclure@mcgill.ca

6.1 Abstract

Increasing the demand for high performance structures calls for design and analysis methods to accurately estimate the seismic demand on both structural and Non-Structural Components (NSCs). Seismic design and analysis of structural elements have been extensively studied and improved by numerous researchers and practitioners and these improvements are well-reflected in the building codes. Current codes also address the seismic design of acceleration-sensitive NSCs through empirical equations that calculate the equivalent static seismic force demand. However, these equations have been shown by recent studies to be unreliable in most cases as they do not properly account for some key factors when deriving the acceleration response of NSCs as well as the supporting structure. Thereby, there is a need for a reliable method which is capable of overcoming the drawbacks of the code provisions while being simple, fast, and practical. In an attempt to fill this gap, an original approach has been previously proposed by the authors to generate the experimentally derived floor response spectra. Employing the method over the database of 27 existing RC buildings (12 low-rise, 10 medium-rise, and 5 high-rises all located in

Montreal, Canada), Pseudo Acceleration Floor Response Spectra (PA-FRS) were derived for every floor of the buildings considering four different NSC damping ratios (2, 5, 10, and 20% of critical viscous damping). The generated PA-FRS were statistically analysed and two sets of equations were proposed to produce Floor Design Spectra (FDS) for low and medium-rise RC buildings directly from 5% damped design response spectrum (Uniform Hazard Spectrum (UHS) of NBCC 2015 for Montreal to be specific). The FDS is produced in three distinct spectral regions (i.e. short, fundamental, and large period regions) for NSCs with 5% viscous damping located at roof level. This paper examines the effects of NSCs damping ratio and their location in the building on the PA-FRS through statistical analysis. Consequently, a height factor and a damping modification factor are introduced to extend the methodology to generate FDS for any floor level and NSCs damping ratio of interest. These two factors have been employed over the entire database from which one low-rise (Building#4) and one medium-rise (Building#18) are selected for illustration. Using the proposed method, an exclusive FDS is produced for each building taking its dynamic characteristics (i.e. its natural period and its design spectra acceleration) into account. The generated FDS can serve as a fast and powerful means for seismic assessment and design of NSCs particularly in existing post-critical structures. The application of the method can be extended to steel structures in future work.

Keywords: Spectrum-to-spectrum method; Operational and Functional Components (OFCs); Secondary systems; Earthquake Engineering; Seismic Assessment and Design.

6.2 **Introduction**

In response to the current increasing demand for high performance structures, careful attention must be paid to seismic design and assessment of Non-Structural Components (NSCs) in buildings. As experienced in past earthquakes, many buildings have failed meeting their performance objectives solely due to failure/malfunction of their NSCs while the structural elements and systems have performed satisfactorily as per design. Damage to NSCs is often ensued by some undesired aftereffects which are mainly associated with: a) life-safety hazards (i.e. fatalities/injuries caused by falling/overturning NSCs and etc. [1-3]), b) property loss due to direct/indirect damage costs (e.g. major part of approximate economic loss of 25 billion dollar in 2010 Maule, Chile earthquake [4] and 2 billion dollar in 2001 Nisqually (Seattle) earthquake [5]), and c)- loss of building functionality (e.g. impairment or complete shut-down of 130 hospitals in 2010 Maule, Chile earthquake [4] and of 32 commercial data processing centers in 1989 Loma Prieta earthquake [6]). A comprehensive description of these consequences accompanied with several examples can be found in FEMA E-74, "Reducing the Risk of Nonstructural Earthquake Damage – A Partial Guide" [7].

These observations clearly demonstrate the essential need for a reliable approach to properly quantify the two main Engineering Demand Parameters (EDP) needed for seismic design/analysis of NSCs. Depending on the type of NSCs, two EDPs are required: 1- story drift/displacement demand needed for drift-sensitive components, and 2- component acceleration demand needed for acceleration-sensitive components. After the introduction of the displacement-based design approach, firstly in 1993 in New Zealand [8], many studies

(Priestley et al.[9], Sullivan [10], Calvi [11] and Welch et al. [12], to name a few) have focused on quantifying story drift demand and as a result a range of reliable approaches have been developed to estimate this demand parameter. However, there still appears to be a need for a simplified method which can properly quantifies acceleration demand on NSCs (i.e. acceleration-sensitive components). In this regard, most of the current building codes contain empirical equations to estimate NSC acceleration demand but they remain incapable of considering several key factors such as the effects of building higher frequency modes and torsional modes, the effects of tuning/detuning of the primary and secondary systems, and the effect of NSCs internal damping. These shortcomings cause the code estimation of the acceleration demand on NSCs to be often inaccurate and unreliable as shown in several studies such as [13-16]. In an attempt to introduce alternative approaches capable of resolving these issues, there have been many efforts (see [14, 17-20], among others) to develop Floor Response Spectra (FRS), which provide the acceleration demand on NSCs as a function of their fundamental period so each component can be assessed exclusively.

A step forward to these improvements is to develop Floor Design Spectra (FDS) that can be used for seismic assessment of NSCs in a similar way as Design Response Spectra (DRS) are for structural elements. The authors have previously introduced the methodology to generate Pseudo Acceleration Floor Response Spectrum (PA-FRS) using data extracted from Ambient Vibration Measurement (AVM) records [21]. The methodology has been applied to a database of 27 existing Reinforced Concrete (RC) frame buildings, all located in Montreal Canada and designated as post-disaster buildings. PA-FRS have been derived for every floor of the buildings considering four different NSC critical damping ratios. The generated PA-FRS have been statistically analysed and a set of equations was proposed to generate FDS for low and medium-rise RC frame buildings directly from the corresponding 5% damped Uniform Hazard Spectra (UHS) [22]. At this stage, the proposed method was limited to generate the FDS only atop the building (i.e. for roof level or Z/H=1.0) and for NSCs with 5% viscous damping ratio (ξ_{NSC}=5%). This paper examines the effect of NSCs location in the building (Z/H) and internal damping ratios (ξ_{NSC}) on the FDS using statistical analysis and it extends the application of the method to cover any selection of floor level (0.0≤Z/H≤1.0) and NSCs' damping ratios (1%≤ξ_{NSC}≤30%). Two additional terms are introduced and added to the previously derived equations for roof level to account for the NSCs' floor location (Z/H) and damping (ξ_{NSC}). In the following sections, the extended methodology is described in details and its application through two complete case-studies, Building#4 (low-rise) and #18(medium-rise) of the database, is presented.

6.3 **Code provisions for acceleration-sensitive NSCs**

Acceleration-sensitive NSCs are those components which are designed against seismically induced acceleration/force while building drift is not a controlling factor for them. Current building codes address these components by establishing a set of design requirements in the form of empirical equations to calculate the equivalent static seismic force that the components and their connections must resist. Table 6-1 briefly summarizes the recommendation of three well-known building codes: 1- Canadian e (NBCC 2015 [23]), 2- American (ASCE/SEI-07-16 [24]), and European (Eurocode 8, EN. 1988. 1. 2004. [25]). Detailed descriptions of the parameters and their recommended values can be found in [23-25]. All these code equations are conceptually similar in the sense that they compute the seismic force demand as a multiplication of component weight by the component peak acceleration. They also have similar shortcomings as they do not consider the effects of higher frequency and torsional modes of the primary system and the effects of NSC damping. Except for Eurocode 8, the other two also disregard the tuning effect (i.e. matching the natural period of NSCs with one of the fundamental periods of supporting system which causes resonance). This is why in many cases, the code estimation of acceleration demand on NSCs is of limited accuracy and reliability.

Table 6-1 - Code provisions for acceleration-sensitive NSCs

NBCC 2015 (Division B-Part 4)	$\boldsymbol{V_P = 0.3F_aS_a(0.2)I_ES_PW_P}$; $0.7 \leq S_P = \frac{C_PA_rA_x}{R_P} \leq 4.0$, $A_x = 1 + 2\frac{h_x}{h_n}$
ASCE/SEI-07-10 (Chapter 13)	$\boldsymbol{F_P = \frac{0.4a_PS_{DS}}{\left(R_P/I_P\right)} \times \left(1 + 2\frac{Z}{H}\right) \times W_P}$; $1.6S_{DS}I_PW_P \leq F_P \leq 0.3S_{DS}I_PW_P$
Eurocode 8 (Part 4.3.5)	$\boldsymbol{F_a = \left(S_aW_a\gamma_a\right)/q_a}$; $S_a = \alpha.S.\left[\frac{3\left(1+\frac{Z}{H}\right)}{1+\left(1-\frac{T_a}{T_1}\right)^2} - 0.5\right] \geq \alpha S$

6.4 Methodology to extend the proposed approach

Figure 6.1 schematically explains the steps of the research methodology. The study was initiated by collecting a database of AVM records and structural details for 27 existing Reinforced Concrete (RC) frame buildings comprising 12 low-rises, 10 medium-rises, and 5 high-rises, all located in Montreal, Canada and designated as post-disaster structures. The main dynamic properties of the buildings were extracted from AVM records using frequency domain techniques and were subsequently modified to be compatible with higher amplitude excitations such as experienced during earthquakes. A complete discussion of the modification factors is presented by the authors in [21]. The floor mass and rotary inertia were estimated according to the structural and architectural drawings. The estimated floor mass and rotary inertia together with the modified dynamic properties for seismic response constitute the input parameters to generate the equivalent 3D model of the buildings according to 3D-SAM approach [26]. An ensemble of 20 seismic records compatible with the NBCC 2015 UHS for Montreal [23] were obtained based on the works by Atkinson et al. [27-29] and used as input excitations. The building models were subjected to the earthquake records in orthogonal horizontal directions (i.e. X and Y) independently and analysed using the 3D-SAM method. The floor response histories of every floor of the buildings were derived in terms of relative displacement and absolute acceleration. A program has been implemented in MATLAB [30] which takes the floor response histories as input and runs the NSCs analysis and derives the inter-story drift curves and the PA-FRS for any selection of floor level, NSCs damping ratio, and NSCs period range of interest. Direct integration with Newmark's linear acceleration method is adopted to solve the equation of motion of NSCs. A detailed description of the MATLAB code and its validation can be found in [21, 31]. The MATLAB code has been run for every floor of all the buildings considering four NSC damping ratios (2, 5, 10, and 20% critical viscous damping) and approximately 132,000 PA-FRS have been generated. Recall that the main research goal was to develop an approach for generation of FDS directly from UHS. This was achieved through extensive statistical analysis of the generated PA-FRS. At the first step, a set of equations were recommended by the authors in [21], which generates FDS directly from UHS for each building exclusively using its natural frequency (T_{1-B}) and its design spectral acceleration (UHS(T_{1-B})), while the method was limited to produce FDS for roof level and 5% NSC damping. This paper extends the proposed methodology to generate FDS for NSCs located at any floor level and having any viscous damping ratio. The effect of NSCs' location\elevation in the building (i.e. Z/H) is quantified through statistical analysis of the generated PA-FRA for different floor levels of the various buildings. Similarly, the effect of NSCs damping ratios is measured by studying the results corresponding to various NSCs damping ratios in detailed analyses. Finally a set of complete equations is recommended to develop FDS directly from UHS for any selection of floor level ($0.0 \leq Z/H \leq 1.0$) and NSCs' damping ratio ($1\% \leq \xi_{NSC} \leq 30\%$). The proposed approach is fast and reliable to generate FDS with no need for neither structural nor non-structural numerical analysis while accounting for the effects of the dynamic properties of both systems. The proposed method improves the code recommendations and conventional approaches in several ways which will be further discussed in the paper. A detailed description of the methodology has been previously presented by the authors in [21, 22, 31].

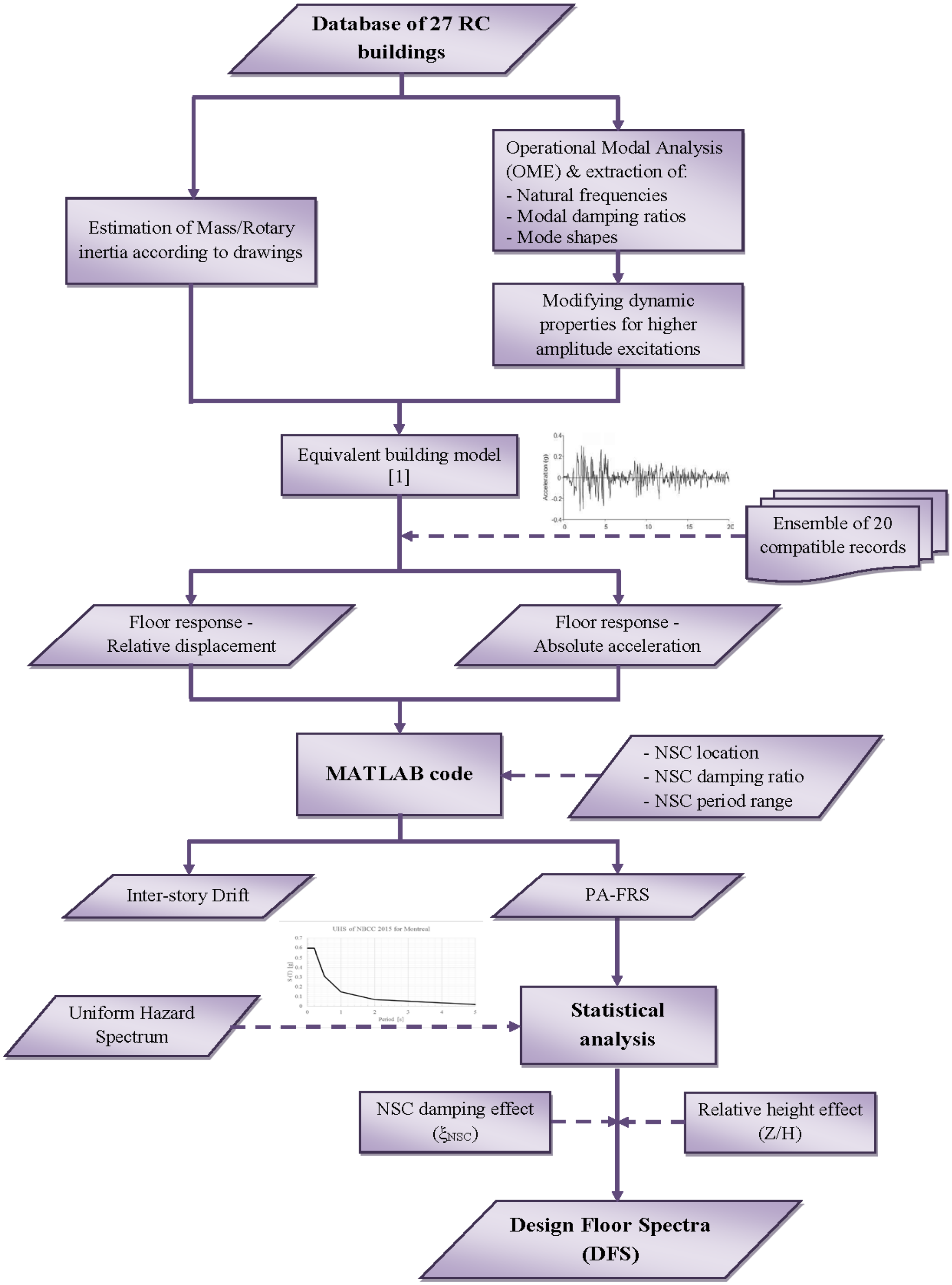

Figure 6.1 – Flow-chart of the research methodology

6.5 **Effect of NSCs' elevation on FDS**

The seismic acceleration demand on NSCs varies depending on the location\elevation of the component in the building. Moving up from ground level to roof level, the NSC acceleration response will, in general, increase and be filtered by the dynamic characteristics of the building rather than the frequency content of the ground motion. The generation of FDS for roof level of RC buildings was described in a companion paper [22] and this second part extends the application of the proposed method to any selected floor level. To do so, the effect of NSCs' location along the height of the building on the FDS, referred to as the relative height effect (denoted Z/H hereafter), is addressed through statistical analysis of the generated PA-FRS for different floor levels. Recalling the proposed approach [22], the entire spectral region is divided into three distinct segments, namely short-period (0<TNSC/T1-B≤0.7), building fundamental-period (0.7≤ TNSC/T1-B ≤1.0), and long-period region (1.0≤ TNSC/T1-B); the relation between the FDS and UHS was sought in each region given Z/H=1.0 (i.e. NSCs located at the roof level only) and ξNSC=5% (NSCs viscous damping ratio equal to 5%). Similarly, the relative height effect is studied here in each spectral regions separately. This was done to be consistent with the previous methodology, and to account for the possibility that the effect of the relative height on FDS might be different in each spectral region. To quantify this effect, the generated PA-FRS for different floor levels of each building were put in the same graph and the horizontal axis (i.e. T¬NCS) was normalized by the natural period of the corresponding building (T-1-B), which causes most of the peaks to be located in the fundamental-period region (0.7≤ TNSC/T1-B ≤1.0). For instance, Figure 6.2.a depicts the PA-FRS of all five floors (including roof and excluding ground floor) of Building#18 given 5% NSC viscous damping. As the FDS generation has been already

formulated for the roof level and ξ_{NSC}=5%, the roof response was taken as the basis of the analysis and the PA-FRS of all floor levels in each building ($Sa_{NSC\text{-}Fl}$) are normalized with respect to the roof level spectral acceleration values ($Sa_{NSC\text{-}Roof}$) given ξNSC=5% for all floors. Figure 6.2b illustrates this normalized PA-FRS obtained for Building#18. The NSCs damping ratio is kept constant as 5% at this stage to illustrate only the effect of relative NSC location along building height. Note that the PA-FRS of the ground floor is excluded from the analysis as it is influenced only by the dynamic characteristics of the seismic excitation. Next, the median+σ of $Sa_{NSC\text{-}Fl}$/ $Sa_{NSC\text{-}Roof}$ ratio over each selected spectral regions (i.e. short, fundamental, and long period regions) is calculated at each floor level and the scatter of these ratios vs their corresponding relative height (Z/H) is plotted and a curve is fitted to the data points in each of the three spectral regions. The effects of relative height in low and medium rise buildings are observed to be different, so each building category is addressed separately but using the same methodology, as discussed next.

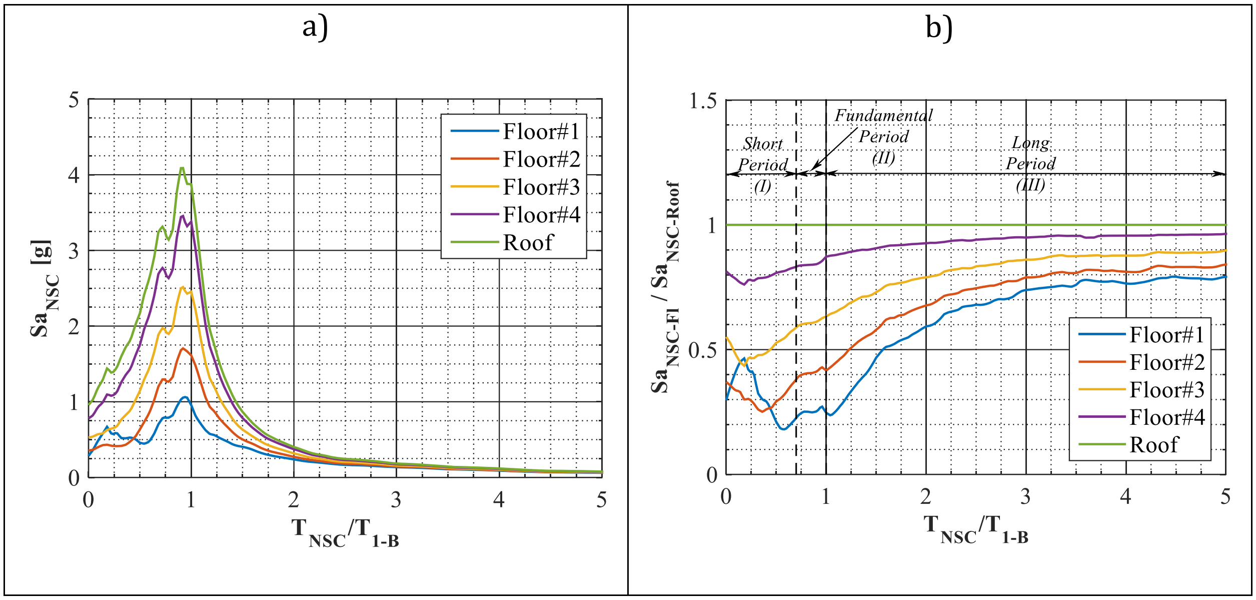

Figure 6.2– Building#18, ξ_{NSC}=5%: a) PA-FRS for all floors of the building; b) Normalized PA-FRS of all floors with respect to the roof.

6.5.1 Low-rise building

The scatter of the ($Sa_{NSC\text{-}Fl}$ / $Sa_{NSC\text{-}Roof}$) ratio vs relative height (Z/H) for the short and fundamental period regions ($0.0< T_{NSC}/T_{1\text{-}B} \leq 1.0$) and the long period region ($1.0\leq T_{NSC}/T_{1\text{-}B} \leq 5.0$) is illustrated in Figure 6.3.a and Figure 6.3.b, respectively. A linear trend of the PA-FRS is assumed and a linear function is fitted to the data points. As the effect of relative height over the short and fundamental period regions was found very similar, the data points for these two spectral regions are combined and one set of recommendations is made for both regions. However, the long period range presents a different behaviour and was studied separately. The equation of the fitted line accompanied with its coefficient of correlation (R^2 value) can be seen on the graphs. Using these equations, the previously produced FDS for roof level given ξ_{NSC}=5% can be now modified for the lower floor levels. The effect of NSC damping is addressed in the next section and incorporated as well. The final FDS recommendations for RC low-rises are illustrated for Building#4 in section 0. These new recommendations bring important improvements to current analytical FRS methods: 1- the study is done directly on the PA-FRS not on the floor acceleration so it accounts for both the structural and non-structural dynamic interaction effects more precisely; 2- the relative height effect is different for each building height category (i.e. low, medium, and high) and each spectral region (i.e. short- medium, and long period) ; and 3- the effect of higher frequency and torsional modes of the primary system on the acceleration response of the NSCs is accounted for implicitly.

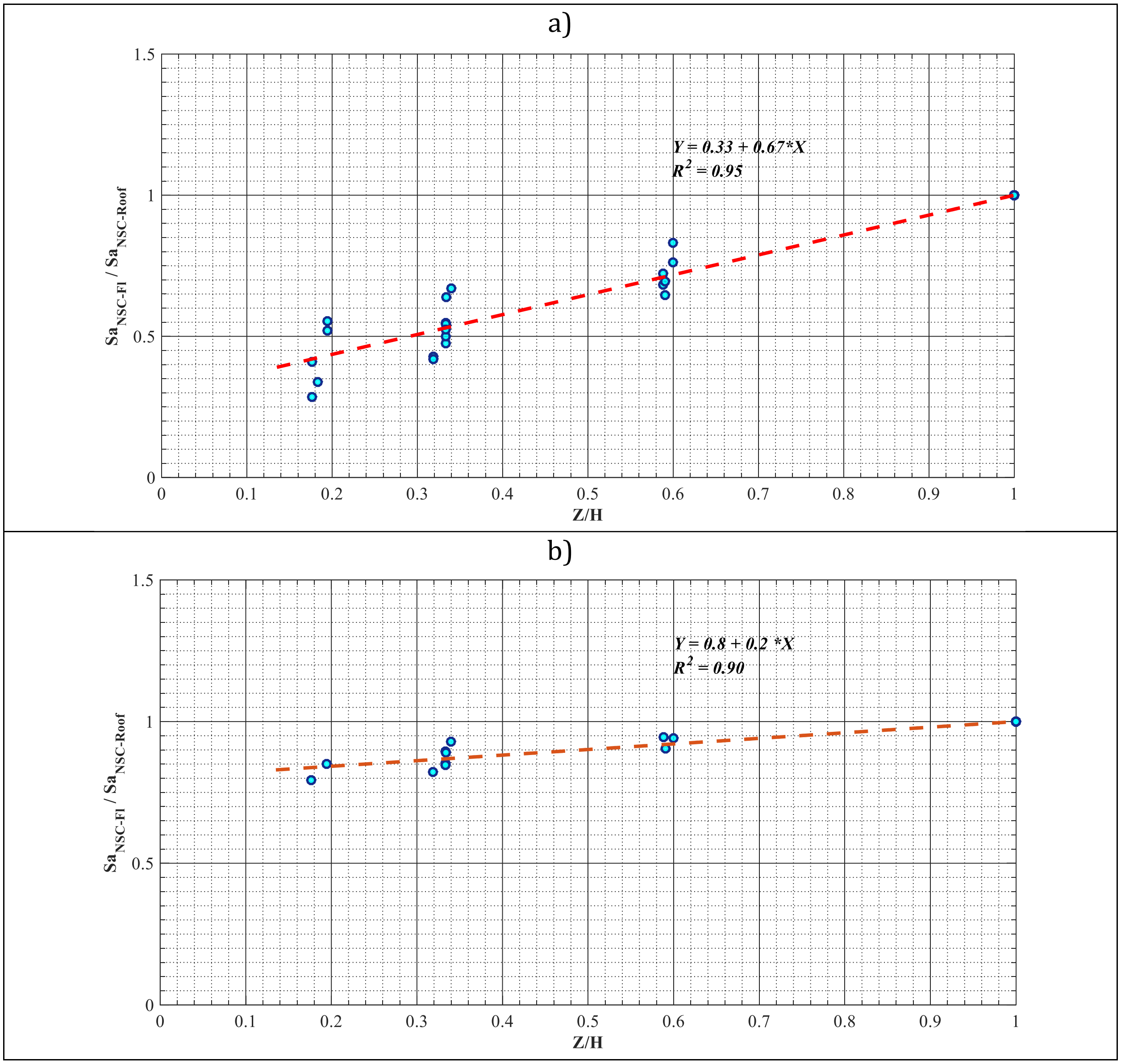

*Figure 6.3 – Scatter of ($Sa_{NSC\text{-}Fl}$ / $Sa_{NSC\text{-}Roof}$) ratio vs relative height (Z/H) for **low-rises** given ξ_{NSC}=5%: a) median+σ of the ratios over short & fundamental period regions; b) median+σ of the ratios over long period region.*

6.5.2 Medium-rise building

The same analysis as above is performed for the medium-rise buildings of the data base. The data points of the short and fundamental period regions are combined again due to their similar trends but long period region is again addressed separately. In medium rise buildings, the points are distributed more evenly along the horizontal axis compared to the clustered pattern observed in the low rises: This is essentially caused by the larger number of floor levels in medium rises. The results of the short & fundamental period and long period regions are illustrated in Figure 6.4.a and Figure 6.4.b, respectively. As can be seen, the recommendations for medium and low rises are different while the building codes do not make that distinction. Illustration of the final recommendations for RC medium-rise buildings is shown for Building#18 in section 6.7.2.

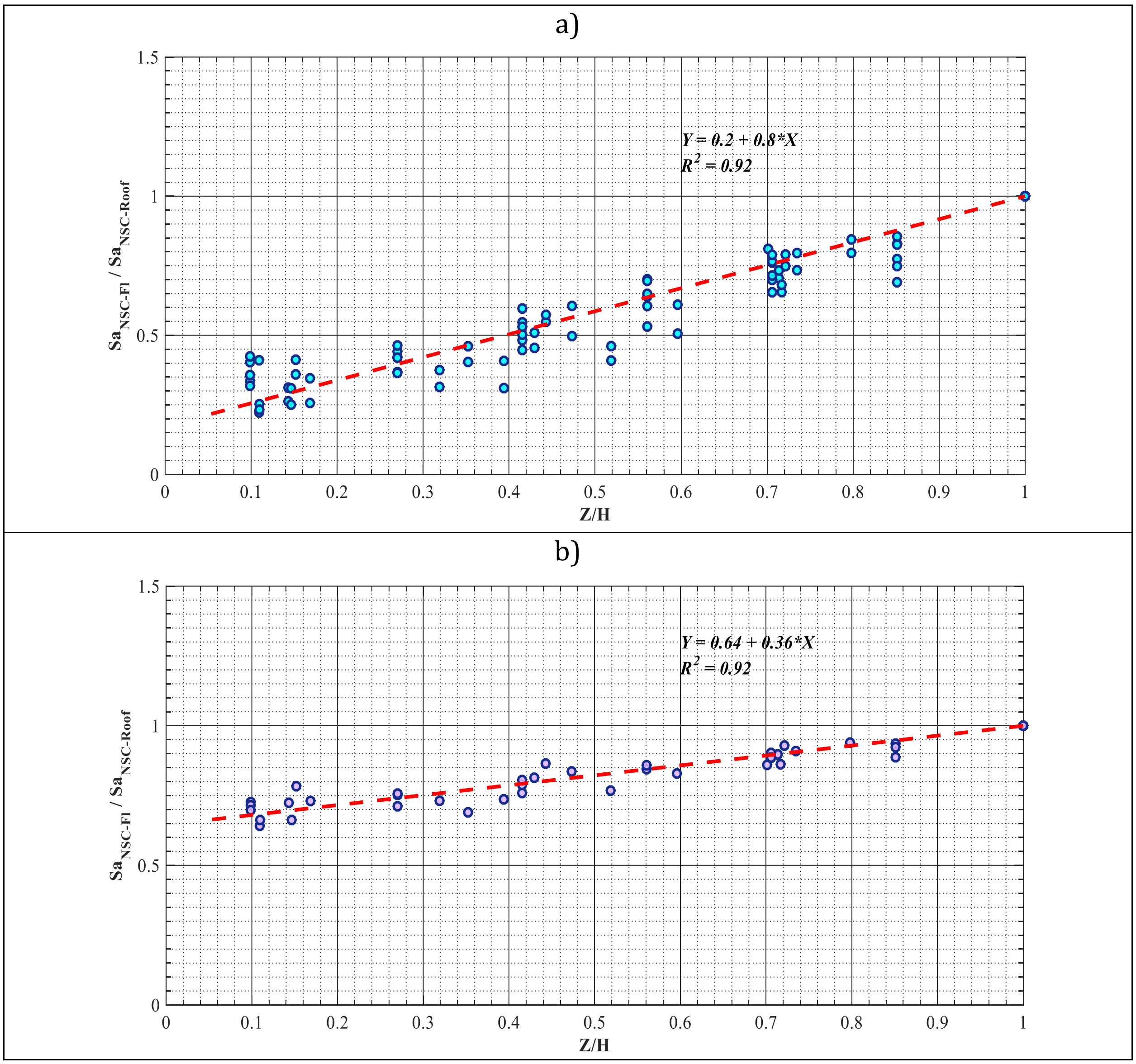

Figure 6.4 - Scatter of (Sa_{NSC-Fl} / $Sa_{NSC-Roof}$) ratio vs relative height (Z/H) for ***medium-rise buildings*** *given ξ_{NSC}=5%: a) median+σ of the ratios over short & fundamental period regions; b) median+σ of the ratios over long period region.*

6.6 **Effect of NSCs' internal damping on FDS**

The effect of NSCs' damping on FDS is quantified using the same statistical methodology adopted for the study of relative height effect. To measure this effect, the generated PA-FRS for different NSCs damping ratios (2, 5, 10 and 20 % of viscous critical) at each floor level were plotted on the same graph and the horizontal axis (i.e. T_{NCS}) was normalized by the natural period of the corresponding building ($T\text{-}_{1\text{-}B}$), which brings most of the peak responses in the fundamental-period region ($0.7 \leq T_{NSC}/T_{1\text{-}B} \leq 1.0$). Figure 6.5.a depicts the PA-FRS for the roof of Building#18 considering four different NSCs damping ratios. The PA-FRS for ξ_{NSC}=5% at each floor level is taken as the reference for the analysis and the PA-FRS values for all four ξ_{NSC} at each floor are normalized with respect to the PA-FRS values for ξ_{NSC}=5% of the corresponding floor and presented as a function of $T_{NSC}/T_{1\text{-}B}$. Figure 6.5.b illustrates the normalized PA-FRS for different NSCs damping ratios at the roof of Building#18 ($Sa_{\xi} / Sa_{\xi=5\%}$ vs $T_{NSC}/T_{1\text{-}B}$). This process is repeated for every floor of each building. It is observed that the results of all floors are close and consistent with each other in each building, meaning that the relative effect of NSC damping is independent of the NSC location along building height. Finally, all the results are plotted in one graph (see Figure 6.5.c for Building#18 results) and the median+σ of $Sa_{\xi}/ Sa_{\xi=5\%}$ ratio over each selected spectral region (i.e. short, fundamental, and long period regions) is calculated; the scatter of these ratios vs their corresponding NSCs damping ratio (ξ_{NSC}) is plotted and a curve is fitted to the data points. The fitted curves for each spectral region represent how the acceleration demand on NSCs varies as a function of NSCs damping ratio. The effect of NSCs damping in low and medium rise buildings is observed to be close and, hence, their data points are combined and studied together. The results are presented in details in the following section.

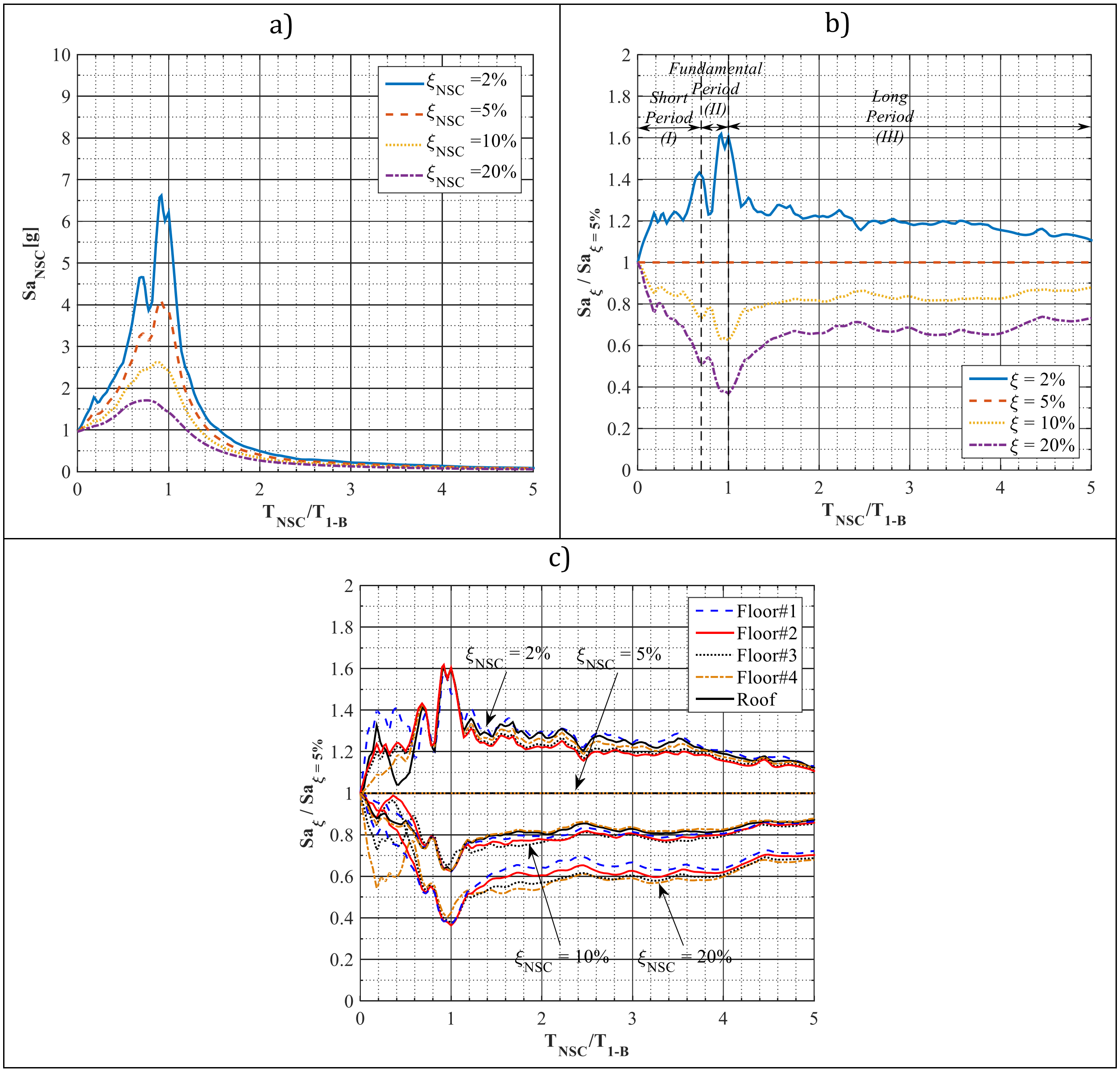

Figure 6.5 - Building #18: a) Roof PA-FRS given ξ_{NSC} = 2, 5, 10, 20 % vs (T_{NSC} / T_{1-B}); b) Normalized PA-FRS at roof, for all ξ_{NSC} with respect to the values for ξ_{NSC} =5%; c) Normalized PA-FRS at all floors, for all ξ_{NSC} with respect to the values for ξ_{NSC} =5% at corresponding floor.

6.6.1 Low and Medium-rise buildings

The scatters of the (Sa_{ξ} / $Sa_{\xi=5\%}$) ratio vs NSCs damping ratio (ξ_{NSC}) for the short (0.0< T_{NSC}/T_{1-B} ≤0.7), fundamental (0.7< T_{NSC}/T_{1-B} ≤1.0), and long period regions (1.0< T_{NSC}/T_{1-B}

≤5.0 are illustrated in Figure 6.6.a, b, and c, respectively. Different exponential and rational functions have been tested for data fitting. The comparison of the fitted curves showed that the rational function in the form of Y=(a.X+b)/(X+c) best represents the data. As the effects of NSC damping over different spectral regions were found to be different, separate analyses have been done in each segment. However, due to the closeness of the low and medium rise building results, their data points are combined and one set of recommendations is made for both building categories. The equation of the fitted curve accompanied with its R^2 value can be seen on the graphs. Using these equations, the previously produced FDS for ξ_{NSC}=5% is modified for the other ξ_{NSC} values. The application of the final recommendations for RC low and medium rise buildings is illustrated for Building#4 (low-rise) and #18 (medium-rise) in section 0. The consideration the effect of NSC damping ratios in generating FDS is a key improvement of this study compared to the code recommendations and conventional approaches that do not account for this important factor. In addition, the proposed methodology differentiates between various building categories (low, medium, and high-rise) as well as different spectral regions.

a)

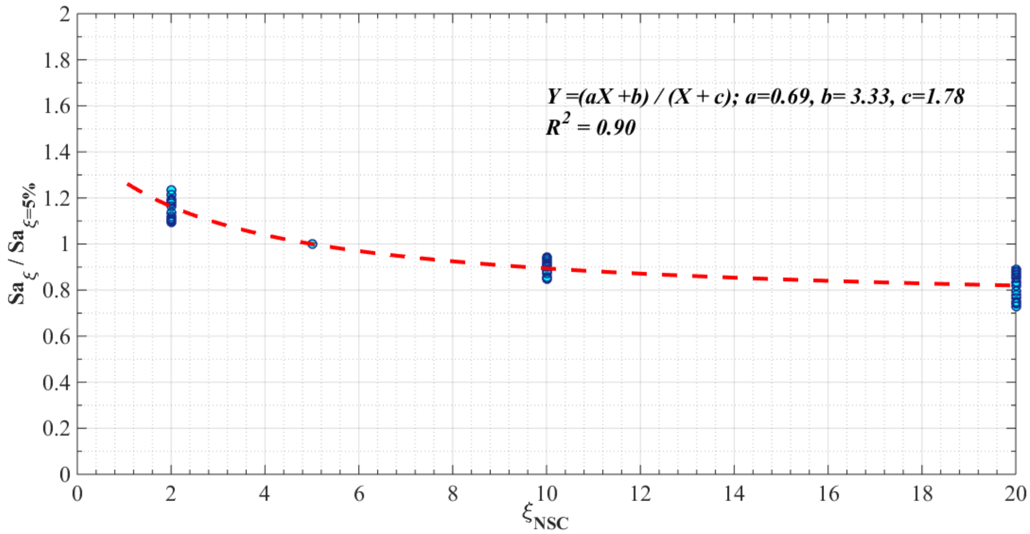
Y =(aX +b) / (X + c); a=0.69, b= 3.33, c=1.78
R^2 = 0.90
Sa_ξ / Sa_ξ=5%
ξ_NSC
0 2 4 6 8 10 12 14 16 18 20
0 0.2 0.4 0.6 0.8 1 1.2 1.4 1.6 1.8 2

b)

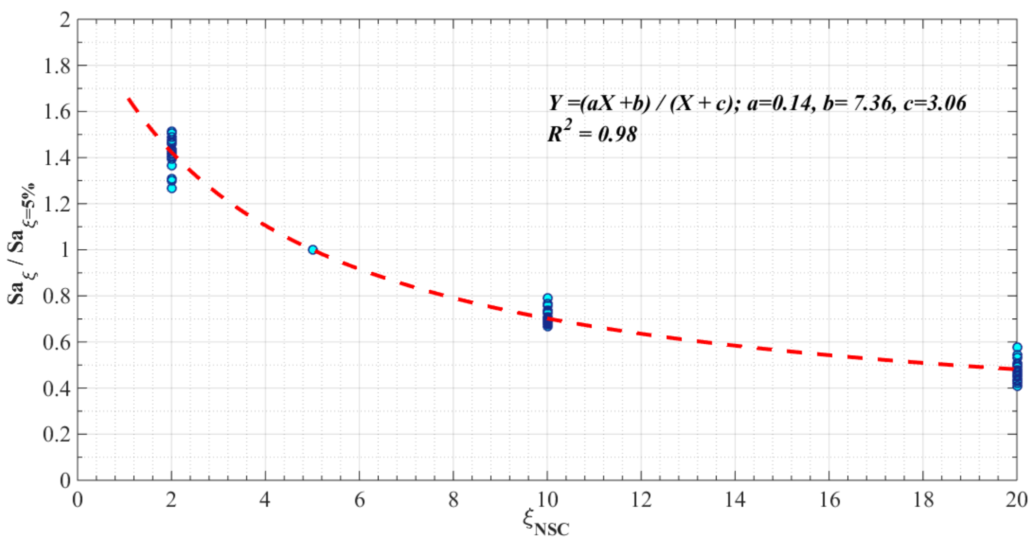
Y =(aX +b) / (X + c); a=0.14, b= 7.36, c=3.06
R^2 = 0.98
Sa_ξ / Sa_ξ=5%
ξ_NSC
0 2 4 6 8 10 12 14 16 18 20
0 0.2 0.4 0.6 0.8 1 1.2 1.4 1.6 1.8 2

c)

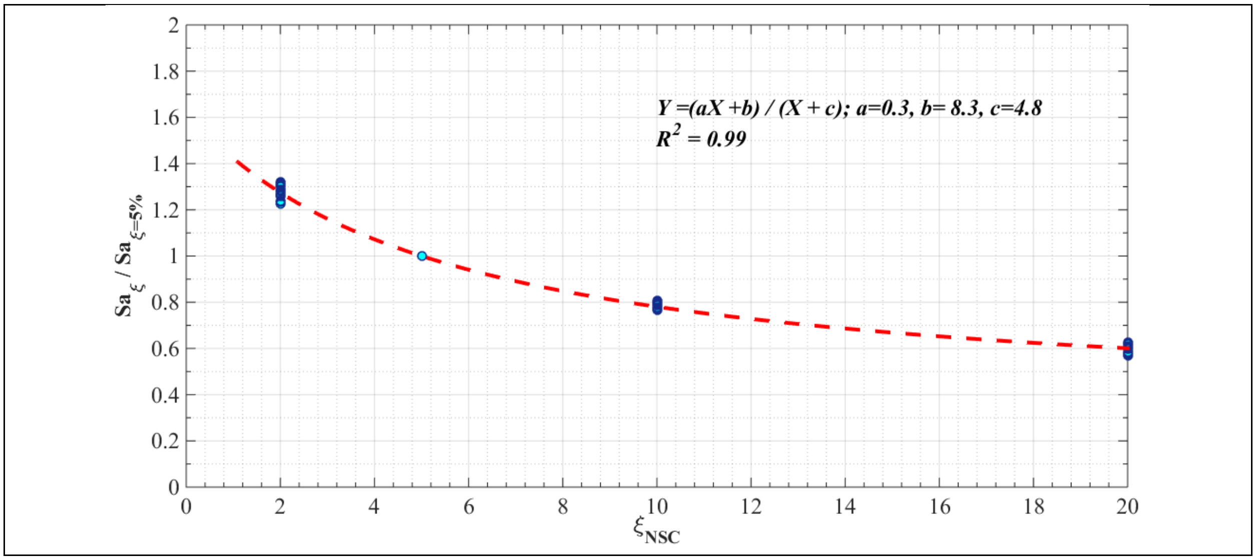

*Figure 6.6 - Scatter of (Sa_{ξ} / $Sa_{\xi=5\%}$) ratio vs NSC damping ratio (ξ_{NSC}) for **<u>low and medium-rise</u>** buildings given: a) median+σ of the ratios over short period regions; b) median+σ of the ratios over fundamental period region; c) median+σ of the ratios over long period region.*

6.7 FDS generation directly from UHS given any selected floor level and ξ_{NSC}

This section presents a set of equations recommended to develop FDS directly from UHS for any selection of floor level ($0.0 \leq Z/H \leq 1.0$) and NSCs' damping ratio ($1\% \leq \xi_{NSC} \leq 30\%$) in both low and medium rise buildings. In the companion paper [22], the FDS generation for roof level and 5% NSC damping was presented. Figure 6.7 – Schematic of the proposed FDS and idealization of spectral acceleration for NSCs schematically shows how the spectral acceleration is idealized in each spectral region for both low and medium rises. In this study, the methodology is extended to account for the effects of relative height (Z/H) and NSC damping ratios of NSCs through use of two sets of modification factors described in sections 6.5 and 6.6. The final recommendations for low and medium rise buildings are described in sections 6.7.1 and 6.7.2, respectively.

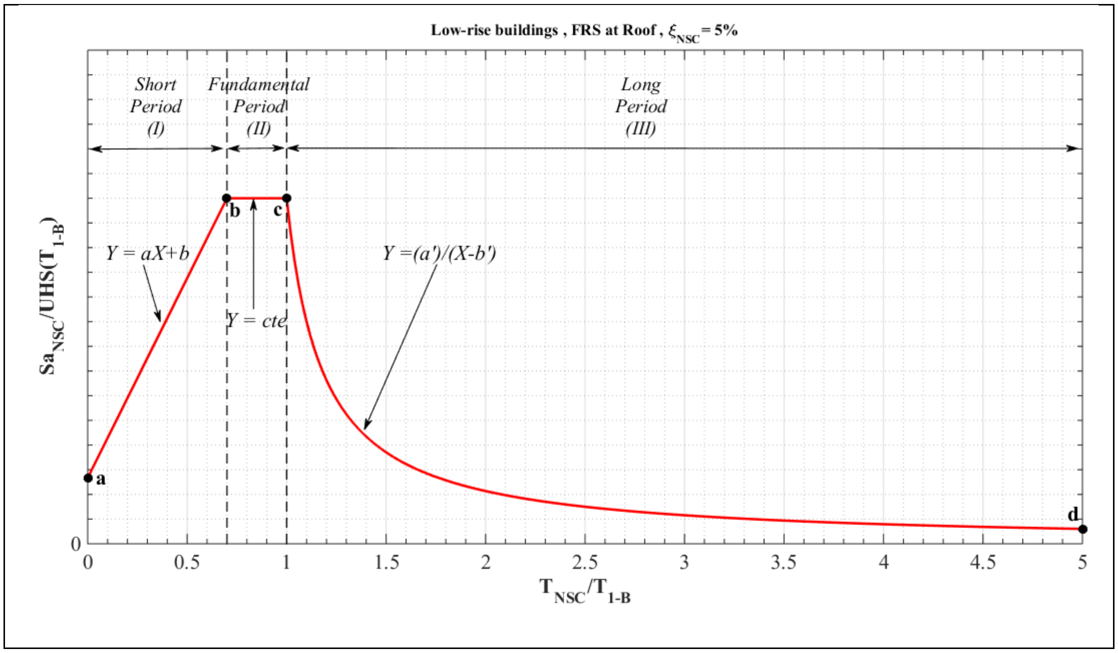

Figure 6.7 – Schematic of the proposed FDS and idealization of spectral acceleration for NSCs

6.7.1 Low-rise buildings

As illustrated in Figure 6.7 – Schematic of the proposed FDS and idealization of spectral acceleration for NSCs, the recommended FDS has a linear variation in the short-period region (point "a" to point "b"), a constant value in fundamental-period region (points "b" to "c"), and decays according to a rational function in the long-period region (points "c" to "d"). The following equations describe how the FDS values are calculated in each spectral region for RC low-rise buildings. It should be mentioned that in all the recommended equations, the first bracket is to calculate the FDS values at roof level given 5% NSC damping, the second bracket is the modification factor which accounts for relative height effect ($0.0 \leq Z/H \leq 1.0$), and the third bracket is the modification factor that accounts for NSCs' damping effect ($1\% \leq \xi_{NSC} \leq 30\%$).

In the short-period region, the FDS values are increased linearly from point “a” at $T_{NSC}/T_{1\text{-}B}$ = 0.0 to point “b” at $T_{NSC}/T_{1\text{-}B}$ = 0.7. Values of point “a” and “b” can be calculated according to Equation 6.1:

$$\frac{Sa_{NSC}}{UHS(T_{1-B})} = \begin{cases} [2.0] \times \left[0.33 + 0.67\left(\frac{Z}{H}\right)\right] \times \left[\frac{0.69 \times \xi_{NSC} + 3.33}{\xi_{NSC} + 1.78}\right] & @ \quad \text{"a"}, \quad \frac{T_{NSC}}{T_{1-B}} = 0.0 \\ [10.5] \times \left[0.33 + 0.67\left(\frac{Z}{H}\right)\right] \times \left[\frac{0.14 \times \xi_{NSC} + 7.36}{\xi_{NSC} + 3.06}\right] & @ \quad \text{"b"}, \quad \frac{T_{NSC}}{T_{1-B}} = 0.7 \end{cases} \qquad \textit{Equation 6.1}$$

In the fundamental-period region, the FDS has a constant value determined at point “b” using Equation 6.1, between points “b” at $T_{NSC}/T_{1\text{-}B}$ = 0.7 and “c” at $T_{NSC}/T_{1\text{-}B}$ = 1.0. In the long-period region, the value of FDS is calculated according to Equation 6.2:

$$\frac{Sa_{NSC}}{UHS(T_{1-B})} = min \begin{Bmatrix} [10.5] \times \left[0.33 + 0.67\left(\frac{Z}{H}\right)\right] \times \left[\frac{0.14 \times \xi_{NSC} + 7.36}{\xi_{NSC} + 3.06}\right] \\ \left[\frac{1.89}{\left(\frac{T_{NSC}}{T_{1-B}}\right) - 0.82}\right] \times \left[0.8 + 0.2\left(\frac{Z}{H}\right)\right] \times \left[\frac{0.3 \times \xi_{NSC} + 8.3}{\xi_{NSC} + 4.8}\right] \end{Bmatrix} \quad : \quad 1.0 \le \frac{T_{NSC}}{T_{1-B}} \le 5.0 \qquad \textit{Equation 6.2}$$

The FDS is taken as the minimum of the two proposed equations because the rational function corresponding to the long-period region (lower part of Equation 6.2) does, in some cases, overestimate the FDS values in the vicinity of $T_{NSC}/T_{1\text{-}B}$ = 1.0. If FDS is required to be extended for a longer range, 5.0 ≤ $T_{NSC}/T_{1\text{-}B}$ ≤10.0, a conservative and simple approach is proposed where the $Sa_{NSC}/UHS(T_{1\text{-}B})$ is decreased linearly from its value at $T_{NSC}/T_{1\text{-}B}$ = 5.0 to half of that at $T_{NSC}/T_{1\text{-}B}$ =10.0.

6.7.2 Medium-rise buildings

For RC medium-rise buildings, FDS is generated using the same methodology as described for low-rise buildings (See section 6.7.1) but using a different set of equations are described below.

In the short-period region, the FDS values are increased linearly from point "a" at $T_{NSC}/T_{1\text{-}B}$ = 0.0 to point "b" at $T_{NSC}/T_{1\text{-}B}$ = 0.7. Values of point "a" and "b" can be calculated according to Equation 6.3:

$$\frac{Sa_{NSC}}{UHS(T_{1-B})} = \begin{cases} [3.0] \times \left[0.2 + 0.8\left(\frac{Z}{H}\right)\right] \times \left[\frac{0.69 \times \xi_{NSC} + 3.33}{\xi_{NSC} + 1.78}\right] & @ \quad \text{"a"}, \quad \frac{T_{NSC}}{T_{1-B}} = 0.0 \\ [12.0] \times \left[0.2 + 0.8\left(\frac{Z}{H}\right)\right] \times \left[\frac{0.14 \times \xi_{NSC} + 7.36}{\xi_{NSC} + 3.06}\right] & @ \quad \text{"b"}, \quad \frac{T_{NSC}}{T_{1-B}} = 0.7 \end{cases} \qquad \textit{Equation 6.3}$$

In the fundamental-period region, the FDS has the constant value determined at point "b" using Equation 6.3, between points "b" at $T_{NSC}/T_{1\text{-}B}$ = 0.7 and "c" at $T_{NSC}/T_{1\text{-}B}$ = 1.0. In the long-period region, the value of FDS is calculated according to Equation 6.4:

$$\frac{Sa_{NSC}}{UHS(T_{1-B})} = min \left\{ \begin{matrix} [12.0] \times \left[0.2 + 0.8\left(\frac{Z}{H}\right)\right] \times \left[\frac{0.14 \times \xi_{NSC} + 7.36}{\xi_{NSC} + 3.06}\right] \\ \left[\frac{1.68}{\left(\frac{T_{NSC}}{T_{1-B}}\right) - 0.86}\right] \times \left[0.64 + 0.36\left(\frac{Z}{H}\right)\right] \times \left[\frac{0.3 \times \xi_{NSC} + 8.3}{\xi_{NSC} + 4.8}\right] \end{matrix} \right\} \quad : \quad 1.0 \leq \frac{T_{NSC}}{T_{1-B}} \leq 5.0 \qquad \textit{Equation 6.4}$$

As explained previously for lower-rise buildings, the FDS is taken as the minimum of the two equations. Likewise, If FDS is required to be extended for 5.0 ≤ $T_{NSC}/T_{1\text{-}B}$ ≤10.0, the same approach as indicated for lower-rise buildings can be used.

The process of generating FDS for both low and medium-rise buildings according to the above equations was coded in the MATLAB program [30]. The extended code requires four inputs: the fundamental period of the building ($T_{1\text{-}B}$), its corresponding uniform hazard design spectral acceleration (UHS($T_{1\text{-}B}$)), the number of floors and their corresponding heights, and the category of the building (either low-rise or medium-rise).

6.8 **Results**

Here, the application of the proposed method is presented through generation of FDS for two RC buildings of the database: Building#4 as a low-rise example and Building#18 as a medium-rise. The proposed FDS for all floors of both buildings considering four different NSC damping ratios (2, 5, 10, and 20% of critical viscous damping) are generated using the MATLAB code [30] and compared with the corresponding PA-FRS derived from the dynamic analysis. A summary of the building information accompanied with the corresponding results are presented next.

6.8.1 Building#4 (Low-rise building)

Building#4 (label is useful if referring to the database described in [21, 22]) is a RCMF low-rise building with three stories above ground. The general information of the building, typical plan view, elevation view, and the AVM results for the first three modes are summarized in Table 6-2. The mode shapes are illustrated schematically where the blue color shapes show the building at rest and the green color represents the deformed modal shape corresponding to the extracted natural frequency.

Table 6-2 - Structural information and AVM results of Building#4 (HA = Height above ground level [m], HB = Height below ground level [m], NA = Number of floors above ground level, NB= Number of floors below ground level, ξ = Modal viscous damping ratio (percentage))

Building # 4

LLRS type	RCMF	Construction year		1957	
H_A / H_B (m)	11.0 / 0.0	Typical plan dimension (m)			
N_A / N_B	3 / 0	L =	53.7	W =	11

Typical plan view

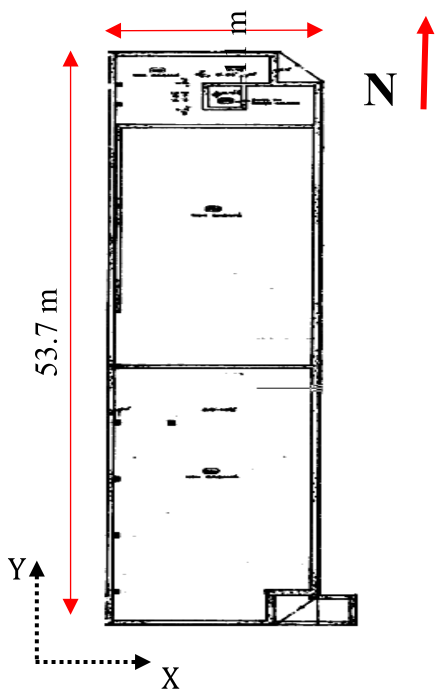

Elevation view

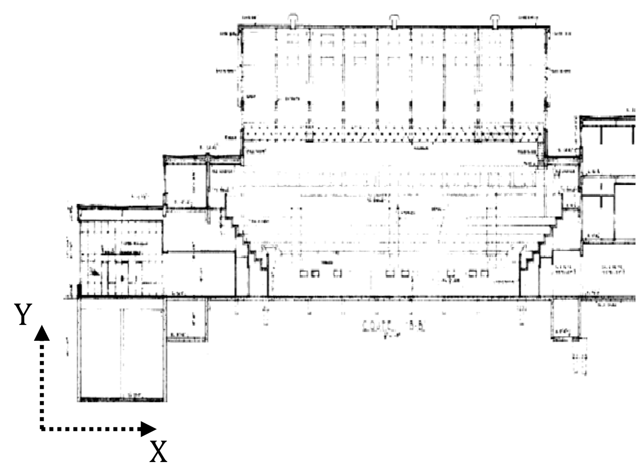

Modal properties extracted from AVM

Mode 1-Translation in X dir.		Mode 2-Translation in Y dir.		Mode 3-Torsion	
f = 5.42 Hz	ξ = 1.5 %	f = 5.69 Hz	ξ = 1.3 %	f = 10.0 Hz	ξ = 2.0 %

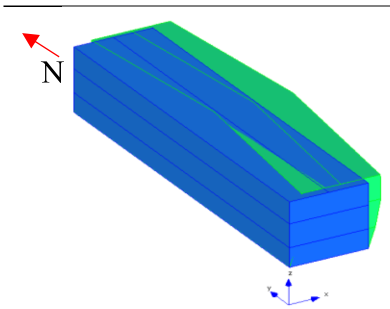

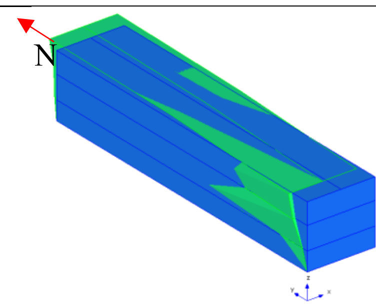

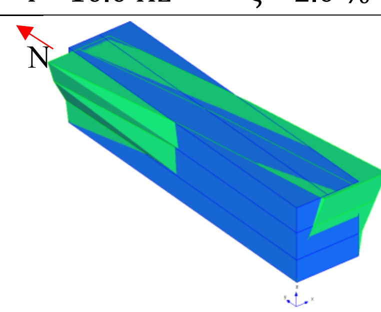

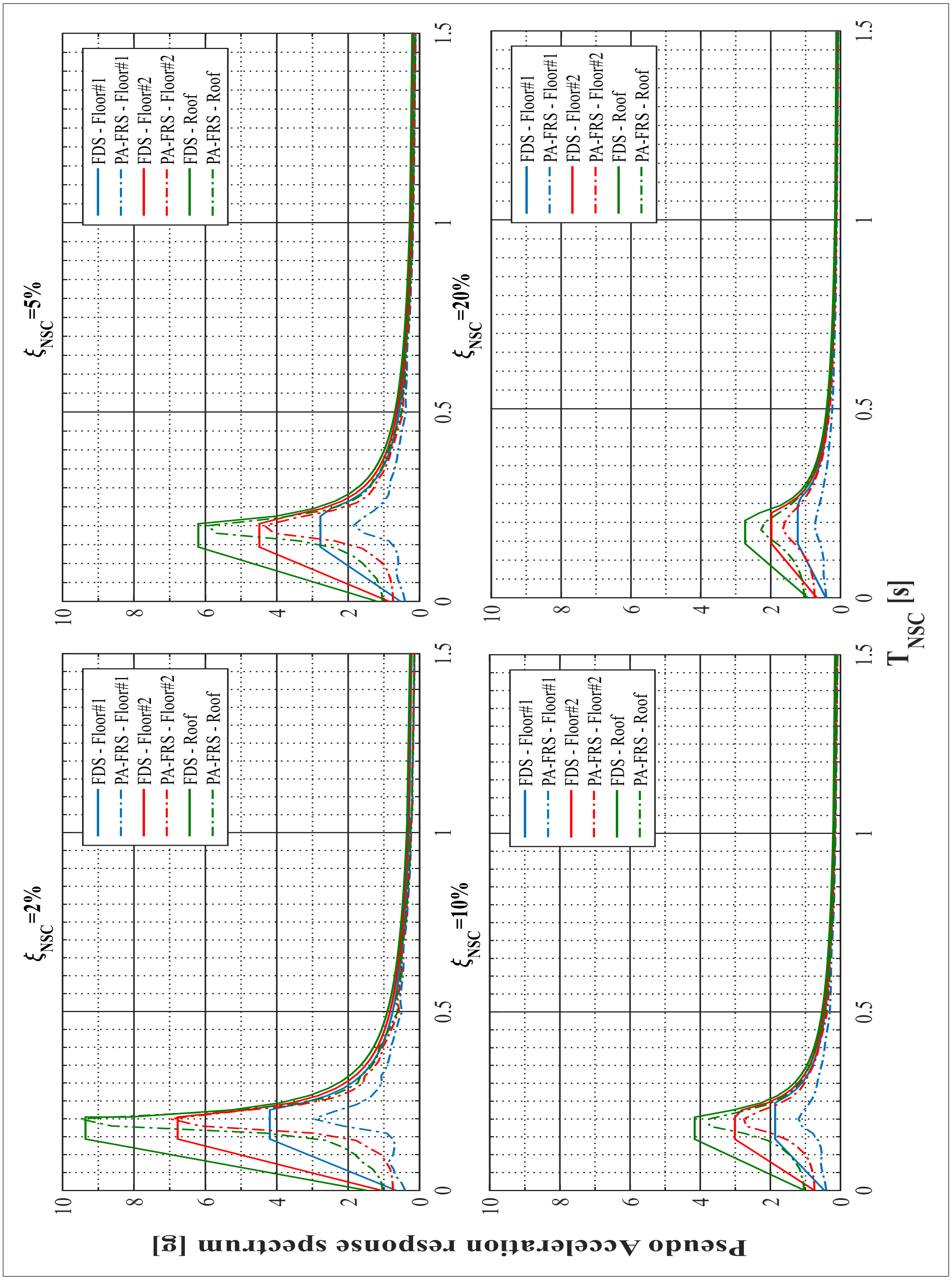

Figure 6.8 – Illustration and comparison of the proposed FDS and the real PA-FRS generated for all floors of Building#4 considering NSCs damping ratios of 2, 5, 10, and 20 %

Figure 6.8 shows the proposed FDS (Solid lines) for all three floors of Building#4 given four different NSC damping ratios compared with the corresponding PA-FRS (dashed lines) derived from the dynamic analysis of the building. The comparison shows that the proposed methodology is a reliable tool to estimate the seismic acceleration demand on NSCs with any damping ratio and located at any floor level.

6.8.2 Building#18 (Medium-rise building)

Building#18 (label is useful if referring to the database described in [21, 22]) is a RCSW medium-rise building with five stories above ground. The general information of the building, typical plan view, elevation view, and the AVM results for the first three modes are summarized in Table 6-3. The mode shapes are illustrated schematically where the blue color shapes show the building at rest and the green color represents the deformed modal shape corresponding to the extracted natural frequency.

Table 6-3 - Structural information and AVM results of Building#18 (Symbols are as described in Table 6-2)

<table>
<tr><th colspan="6">Building # 18</th></tr>
<tr><td>LLRS type</td><td>RCSW</td><td colspan="2">Construction year</td><td colspan="2">1988</td></tr>
<tr><td>H_A / H_B (m)</td><td>19.6 / 3.6</td><td colspan="4">Typical plan dimension (m)</td></tr>
<tr><td>N_A / N_B</td><td>5 / 1</td><td>L =</td><td>33.7</td><td>W =</td><td>24.6</td></tr>
<tr><th colspan="2">Typical plan view</th><th colspan="4">Elevation view</th></tr>
<tr><td colspan="2">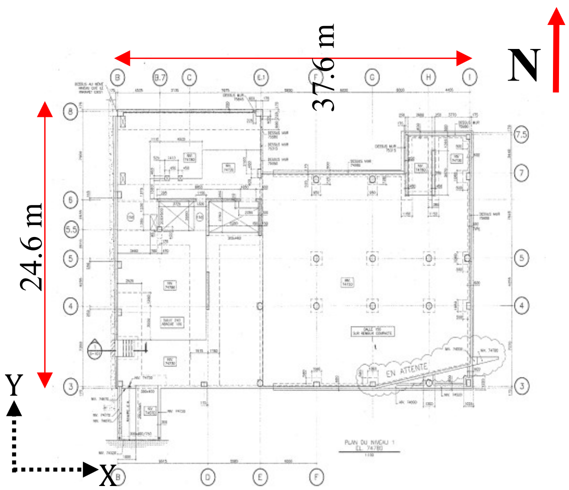
</td><td colspan="4">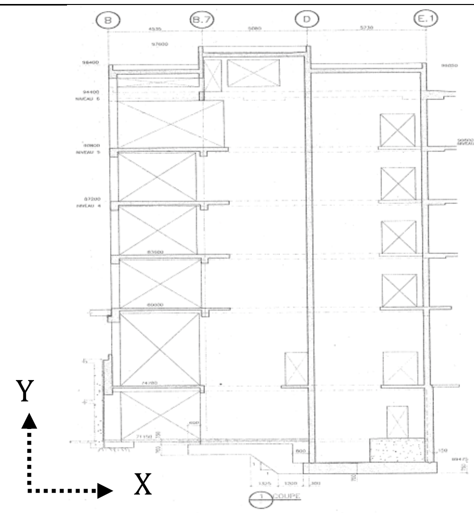
</td></tr>
</table>

<table>
<tr><th colspan="6">Modal properties extracted from AVM</th></tr>
<tr><td colspan="2">Mode 1-Translation in Y dir.</td><td colspan="2">Mode 2-Translation in X dir.</td><td colspan="2">Mode 3-Torsion</td></tr>
<tr><td>f = 2.52 Hz</td><td>ξ = 2.32 %</td><td>f = 2.76 Hz</td><td>ξ = 1.66 %</td><td>f = 3.56 Hz</td><td>ξ = 2.76 %</td></tr>
<tr><td colspan="2">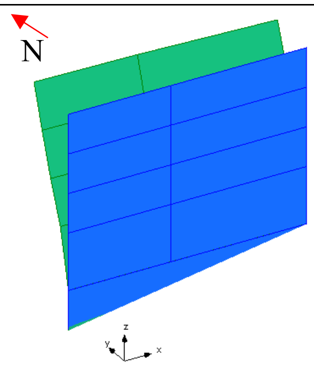
</td><td colspan="2">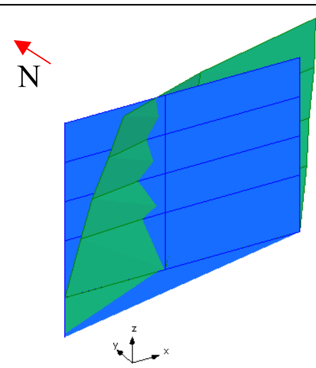
</td><td colspan="2">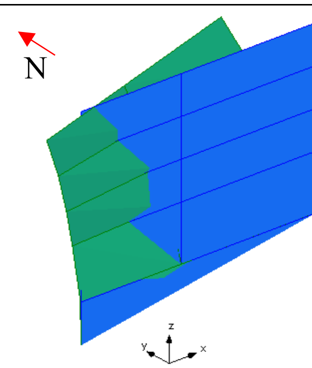
</td></tr>
</table>

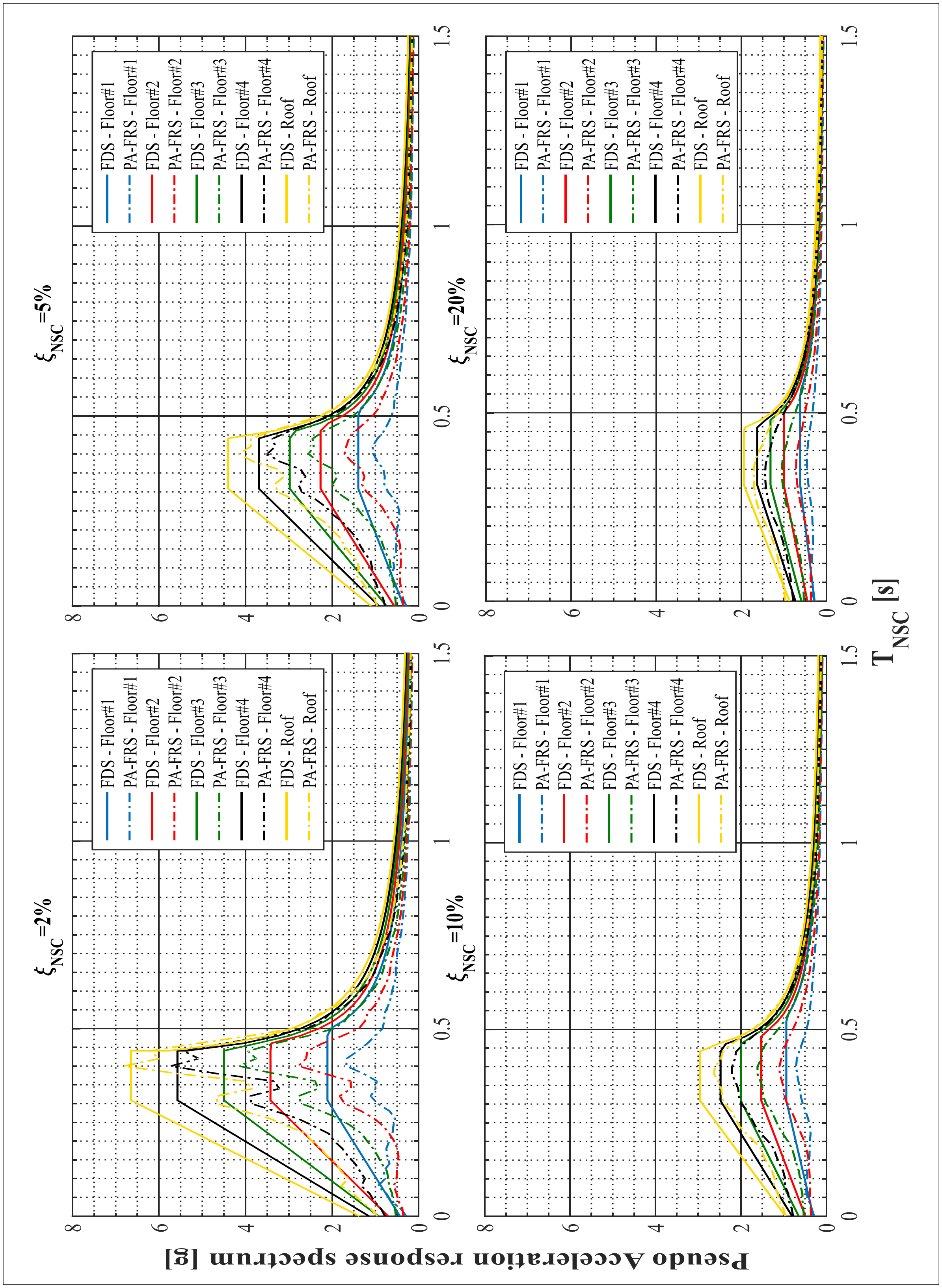

Figure 6.9 – Illustration and comparison of the proposed FDS and the real PA-FRS generated for all floors of Building#18 considering NSCs damping ratios of 2, 5, 10, and 20 %

Figure 6.9 shows the proposed FDS (Solid lines) for all five floors of Building#18 given four different NSC damping ratios compared with the corresponding PA-FRS (dashed lines) derived from the dynamic analysis of the building. Again, a good consistency can be seen between the proposed FDS and the PA-FRS obtained from analysis, which indicates that the proposed method is capable of reliably estimating the seismic acceleration demand on NSCs for the purpose of seismic assessment of NSCs particularly in existing post-critical buildings.

6.9 **Conclusion**

Previously, in a companion paper, an original approach has been proposed by the authors [22] to generate Floor Design Spectra (FDS) at roof level of Reinforced Concrete (RC) low and medium- rise buildings given 5% NSC internal damping. The recommendations were formulated for each building category (i.e. RC low and medium rises) to produce FDS directly from the 5% damped design response spectrum specified in building codes (Uniform Hazard Spectrum (UHS) of NBCC 2015 for Montreal to be specific). The FDS is produced for three distinct spectral regions (i.e. short, fundamental, and large period regions).

This study successfully extended the application of the previously proposed method to produce FDS for any selection of the floor level and NSCs damping ratio. To achieve this result, the Pseudo Acceleration Floor Response Spectrum (PA-FRS) have been derived for every floor of the buildings in the database (12 low-rise, 10 medium-rise, and 5 high-rise) considering four different NSC damping ratios (2, 5, 10, and 20 % viscous damping). Approximately 132,000 PA-FRS have been generated for statistical analysis. The effects of NSCs damping ratio (ξ_{NSC}) and their location along the building height (Z/H) on the derived PA-FRS have been quantified through statistical analysis and a height and a damping modification factors have been introduced. These factors are to modify the previously generated reference FDS at roof level (Z/H=1.0) and 5% NSCs damping (ξ_{NSC}=5%). These modification factors are incorporated into the previous recommendations and two sets of updated equations are recommended for RC low and medium rise buildings.

The recommended equations have been coded in the MATLAB program [30] and then applied over the entire database from which one low-rise (Building#4) and one medium-rise (Building#18) cases have been illustrated. The FDS were generated for every floor of the 27 selected buildings given four different NSC damping ratios and compared with the corresponding PA-FRS derived from the dynamic analysis. The comparison showed consistency between the results which attests the reliability of the proposed approach. Compared to the conventional analytical FRS approach and current building code recommendations, the proposed method offers several advantages and improvements, namely including capturing the effects of: 1- dynamic interaction between the supporting system and NSCs, 2- higher frequency and torsional modes of the supporting system, 3- NSCs internal damping ratios, and the generation of an exclusive FDS for each individual building, taking into account its dynamic characteristics (i.e. its fundamental period and its UHS design spectral accelerations). The generated FDS is a practical, accurate, and fast tool for seismic assessment and design of acceleration-sensitive NSCs particularly in post-critical existing buildings.

6.10 **References**

1. Adham, S.A. and B. Ballif, *The Borah Peak, Idaho earthquake of October 28, 1983—buildings and schools.* Earthquake spectra, 1985. **2**(1): p. 169-182.

2. Taly, N., *The Whittier Narrows, California Earthquake of October 1, 1987-Performance of Buildings at California State University, Los Angeles.* Earthquake Spectra, 1988. **4**(2): p. 277-317.
3. Reitherman, B., et al., *Nonstructural damage.* Earthquake Spectra, 1995. **11**(S2): p. 453-514.
4. Miranda, E., et al., *Performance of nonstructural components during the 27 February 2010 Chile earthquake.* Earthquake Spectra, 2012. **28**(S1): p. S453-S471.
5. Filiatrault, A., et al., *Reconnaissance report of the February 28, 2001 nisqually (seattle-olympia) earthquake.* SSRP, 2001: p. 67.
6. Ding, D., et al., *Architecture, building contents, and building systems.* Earthquake Spectra, 1990. **6**(S1): p. 339-377.
7. FEMA E-74, *Reducing the Risks of Nonstructural Earthquake Damage – A Practical Guide*. 2011, FEDERAL EMERGENCY MANAGEMENT AGENCY: Washington, D.C.
8. Priestley, M.N., *Myths and fallacies in earthquake engineering—conflicts between design and reality.* Bulletin of the New Zealand National Society for Earthquake Engineering, 1993. **26**(3): p. 329-341.
9. Priestley, M., G. Calvi, and M. Kowalsky. *Direct displacement-based seismic design of structures*. in *2007 NZSEE conference*. 2007.
10. Sullivan, T.J., *An energy-factor method for the displacement-based seismic design of RC wall structures.* Journal of Earthquake Engineering, 2011. **15**(7): p. 1083-1116.
11. Calvi, P.M., *Relative displacement floor spectra for seismic design of non structural elements.* Journal of Earthquake Engineering, 2014. **18**(7): p. 1037-1059.
12. Welch, D., T. Sullivan, and A. Filiatrault. *Equivalent Structural Damping of Drift Sensitive Nonstructural Building Components*. in *Proceedings of the 10th US National Conference on Earthquake Engineering*. 2014.
13. MONDAL, G. and S.K. JAIN, *Design of non-structural elements for buildings: A review of codal provisions.* Indian concrete journal, 2005. **79**(8): p. 22-28.
14. Sullivan, T.J., P.M. Calvi, and R. Nascimbene, *Towards improved floor spectra estimates for seismic design.* Earthquake and Structures, 2013. **4**(1): p. 109-132.
15. Wieser, J., et al., *Floor accelerations in yielding special moment resisting frame structures.* Earthquake Spectra, 2013. **29**(3): p. 987-1002.
16. C. Petrone, et al., *Evaluation of the seismic demand on acceleration sensitive nonstructural components in RC frame structures*, in *Second European conference on earthquake engineering and seismology*. August,25-29,2014: Instanbul, Turkey.
17. Biggs, J.M., *Seismic response spectra for equipment design in nuclear power plants*, in *Proceedings of the First International Conference on Structural Mechanics in Reactor Technology*. 1972: Berlin, Germany. p. 329-343.
18. Singh, M.P., *Seismic design input for secondary systems.* Journal of the Structural Division, 1980. **106**(2): p. 505-517.
19. Villaverde, R., *Seismic Analysis and Design of Nonstructural Elements*, in *Earthquake engineering: From engineering seismology to performance-based engineering*. 2004, CRC Press.
20. Calvi, P.M. and T.J. Sullivan, *Estimating floor spectra in multiple degree of freedom systems.* Earthquakes and Structures, 2014. **7**(1): p. 17-38.

21. A. Asgarian and G. McClure, *Generation of experimental floor response spectra for seismic assessment of Non-Structural Components (NSCs) based on ambient vibration measurements.* Manuscript submitted for publication, 2017: p. 22.
22. Asgarian, A. and G. McClure, *Direct generation of Floor Design Spectra (FDS) from Uniform Hazard Spectra (UHS) - Part I: Formulation of the method.* Manuscript submitted for publication, 2017: p. 19.
23. National Research Council of Canada (NRC), Institute for Research in Construction (IRC), *National Building Code of Canada (NBCC)*. 2015: Ottawa, ON, Canada.
24. American Society of Civil Engineers, *ASCE Standard 7-16: Minimum Design Loads for Buildings and Other Structures*. 2016, American Society of Civil Engineers: Reston, VA.
25. Comite Europeen de Normalization, *Eurocode 8–Design of Structures for earthquake resistance–Part 1: General rules, seismic actions and rules for buildings*, in *EN-1998-1*. 2004: Brussels, Belgium.
26. Mirshafiei, F., M. Mirshafiei, and G. McClure, *A new three-dimensional seismic assessment method (3D-SAM) for buildings based on experimental modal analysis.* Computers & Structures, 2017. **180**: p. 125-137.
27. Atkinson, G.M. and I.A. Beresnev, *Compatible ground-motion time histories for new national seismic hazard maps.* Canadian Journal of Civil Engineering, 1998. **25**(2): p. 305-318.
28. Atkinson, G.M., *Earthquake time histories compatible with the 2005 National building code of Canada uniform hazard spectrum.* Canadian Journal of Civil Engineering, 2009. **36**(6): p. 991-1000.
29. Adams, J. and G. Atkinson, *Development of seismic hazard maps for the proposed 2005 edition of the National Building Code of Canada.* Canadian Journal of Civil Engineering, 2003. **30**(2): p. 255-271.
30. The MathWorks Inc., *MATLAB*. 2014: Natick, MA.
31. A. Asgarian, F. Mirshafiei, and G. McClure, *Experimental floor response spectra for seismic evaluation of operational and functional components of building*, in *CSCE 2014, 4th International Structural Specialty Conference*. 2014: Halifax, NS, May 28 to 31. p. 10.

7 Conclusions and future works

7.1 Conclusions

In this research, an original methodology is introduced to generate Floor Design Spectra (FDS) directly from Uniform Hazard Spectra (UHS). The method is capable of generating FDS for any selected floor level and any NSC damping ratios of interest. The method was developed using a database of 27 existing RC buildings in Montreal, Canada, in which floor AVM testing had been conducted. The derived FDS plays the same role for the seismic design of NSCs and their restraints as UHS does for structural building components. It can be used as a fast, reliable, and practical tool for seismic assessment and analysis of NSCs particularly in post-critical existing buildings. The detailed conclusions and achievements of the research can be summarized as follow:

1- Initially an original approach was developed to generate experimental floor response spectra (FRS) and inter-story drift curves for NSCs based on building modal properties extracted from ambient vibration measurements (AVM). The method has been validated through the detailed linear finite element modeling of a hospital building located in Montreal, Canada and comparing the numerical results with the experimental ones derived by the proposed approach. The comparison showed a very good consistency assuring the reliability of the proposed approach.

2- Compared to the conventional analytical FRS approach and current building code recommendations, the proposed method offers several advantages and improvements including: 1- It is capable of capturing the dynamic interactions between the NSCs and the supporting buildings, if present, as it is based on AVM conducted during the normal operation of the building when NSCs are all in place. Hence, if there is any interaction between primary and secondary systems, its effect are captured in AVM and, subsequently, reflected in the extracted modal properties of the building; 2- The effects of higher frequency building modes and torsional behaviour of the supporting system on the response of NSCs are taken into account. These effects become considerable particularly in high-rise and irregular buildings; 3- The cross-correlation in floor motions is considered in the inter-story drift curves that serve to assess the seismic response of drift-sensitive components; and 4- FRS are generated using the real dynamic properties of the building (frequencies and damping ratios) as extracted from AVM and adjusted for stronger base motion. As the dynamic properties of buildings are altered by the time and loading history, such changes cannot be foreseen by numerical simulations but can be captured in AVM tests; and finally, 5- the NSC-building tuning effect is taken into account by the method while it is disregarded in the code provisions.

3- The data recorded in 56 permanently-instrumented buildings that have experienced moderate to strong earthquakes but suffered no significant (visible) structural damage have been collected and studied. This was done to adjust the modal building properties measured by AVM to stronger shaking levels. This study has led to the following conclusions: 1- For the <u>fundamental mode of vibration</u>: a) natural frequencies at strong shaking are decreased by [1-41] % and damping ratios are increased by a factor of [1.6-10.2] for the set of weak-to-strong ground motions considered, b) the average decrease in fundamental frequencies is 24 %, and c) building damping ratios are increased by a factor of 4.0 on average; 2- For the <u>Second</u>

mode of vibration: a) a decrease of [0-36] % in the natural frequencies and an increase by a factor of [1.7-6.4] in damping ratios are observed, b) on average, the natural frequencies are decreased by 19% and the damping ratios increased by a factor of 3.3; and 3- The mode shapes are not significantly changed from ambient to strong vibration levels contingent upon the occurrence of no significant localized damage in the structure. As a result, an appropriate set of modification factors were proposed to modify AVM-extracted building modal properties for higher-amplitude ground motions.

4- The proposed method has been employed over the entire database of the collected 27 RC buildings subjected to 20 synthetic ground accelerograms compatible with UHS of NBC 2015 for Montreal. Given four different damping ratios for NSCs, an approximate number of 132,000 Pseudo Acceleration Floor Response Spectra (PA-FRS) have been generated and used to statistically study the effects of key parameters such as the NSC-building tuning effect, the location of NSCs along building height, and the internal NSC damping, on the acceleration response of NSCs. Comparing the results of the proposed method with the recommendations of three modern building codes (Canada NBCC 2015, United States ASCE-SEI-07, and Eurocode 8) showed that: a) The NSCs response can be directly correlated to the fundamental building mode response assumed in the empirical method adopted by all three codes in low and medium-rise buildings. However, this assumption is no longer valid and safe for high-rise buildings where the effect of higher frequency modes is significant; b) The building codes underestimate the amplification of the NSC acceleration with respect to the acceleration of the supporting floor (i.e. PCA/PFA ratio); c) NSCs internal damping has considerable effect on the component acceleration response, which is disregarded by the current building code provisions.

5- The experimentally-derived PA-FRS have been studied statistically and a methodology proposed to generate the roof FDS for components with 5% damping directly from the 5% damped building UHS prescribed by building codes. One set of equations is recommended for low and medium-rise buildings, separately. The proposed approach uses the dynamic properties of the building (i.e. T_{1-B} and UHS(T_{1-B})) as input variables, meaning that for each building an exclusive FDS is produced which accounts for its specific modal characteristics extracted from AVM records. This is another significant improvement of this method compared to the conventional FRS approach and code provisions.

6- Finally, the effects of NSCs damping ratio (ξ_{NSC}) and their location along the building height (Z/H) on the derived PA-FRS have been quantified through statistical analysis and, as a result, height and damping modification factors are introduced and incorporated into the previously recommended equations. In its final form, the extended methodology can generate FDS directly from UHS exclusively for each building given any floor level and any NSC damping ratio. The generated FDS is a practical, accurate, and fast tool to assess the seismic behaviour and performance of acceleration-sensitive NSCs in existing buildings undergoing low to moderate structural damage during design-level earthquakes.

7.2 Future research

Considering the applications of the method developed in this study as well as its limitations, the following opportunities remain to be investigated in more depth:

1- It is understood that although the recommendations of the study are derived only for RC low and medium rise buildings, the proposed methodology can be employed to different structural materials (i.e. steel structures) and building types (i.e. low, medium, and high rise), as long as sufficient AVM data are available to validate the model. This research study was initially intended to cover different types of lateral load resisting systems (LLRS) (i.e. Reinforced Concrete (RC) buildings and steel structures) but as most of the measured buildings in the database comprised RC structures, the focus was narrowed down to address only RC buildings. Similar studies can be conducted on steel structures and more high-rises using the proposed methodology.

2- The results of the proposed method (experimentally derived PA-FRS and generated FDS) could be compared with the FRS obtained from floor accelerations recorded during earthquake shaking provided that the building under study has been tested by AVM before the earthquake event. This comparison would serve for better understanding the applicability of the proposed method as well as assessing the adequacy of the proposed modification factors to account for shaking levels vs. AVM amplitudes of floor motion.

3- The data recorded in permanently-instrumented buildings (both RC and steel structures) during earthquakes has been collected in this study but only RC building were addressed. The data of the steel structures can be studied as a future work to recommend similar set of modification factors for this type of building. Upon the availability of more data from permanently instrumented buildings, the collected database can be updated to see if the modification factors can be refined any further.

4- A similar study can be done on buildings located in other cities and areas of different seismicity to evaluate the applicability of the method in different seismic zones.

5- This study was mainly focused on acceleration-sensitive NSCs. A future study can be conducted on the experimentally generated inter-story drift curves to evaluate the effect of key factors on this demand parameter and to introduce a similar tool for seismic assessment and design of displacement/drift sensitive components.

8 Appendix A: Information of the earthquake events recorded in permanently instrumented buildings

The information of the earthquake events recorded in the permanently instrumented buildings as well as the geographical distribution of the buildings compared to the epicenter of the seismic motion are briefly described in this appendix. The information are separated based on each studies in the same order as referred in Chapter 3.

1. Çelebi *et al.* (1993), Çelebi (1996, 2007, and 2009) [1-4]:

The recorded responses of the five buildings to the Loma Prieta earthquake [LPE] October 17, 1989 (M_s = 7.1). The general location map of the five buildings relative to the epicenter of the LPE is shown in Figure 8.1.

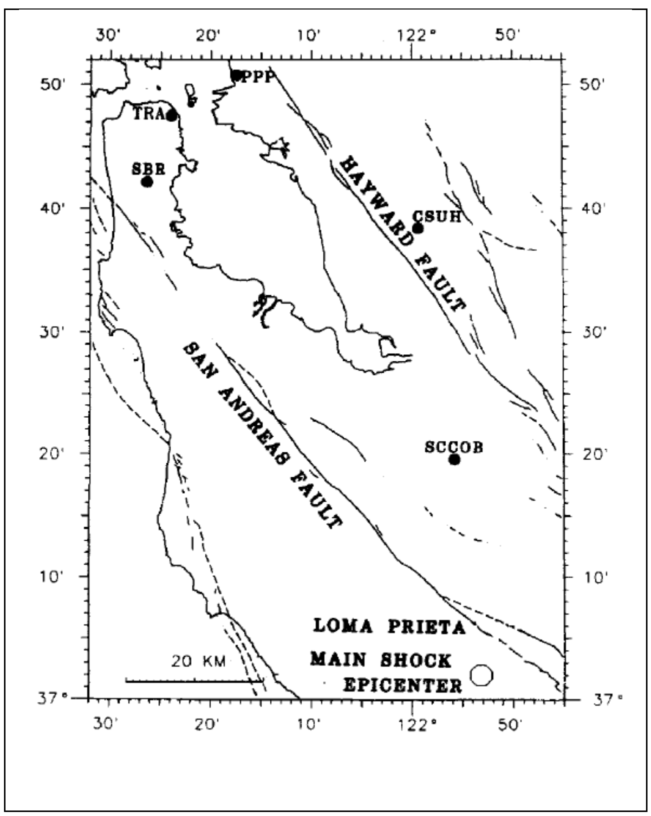

Figure 8.1 - General location map of the five buildings relative to the epicenter of the Lorna Prieta earthquake.

2. Trifunac *et al.* (2001) [5]:

The information of the nine seismic events recorded in Hollywood Storage Building and their geographical distribution compared to the location of the building are shown in Figure 8.2.

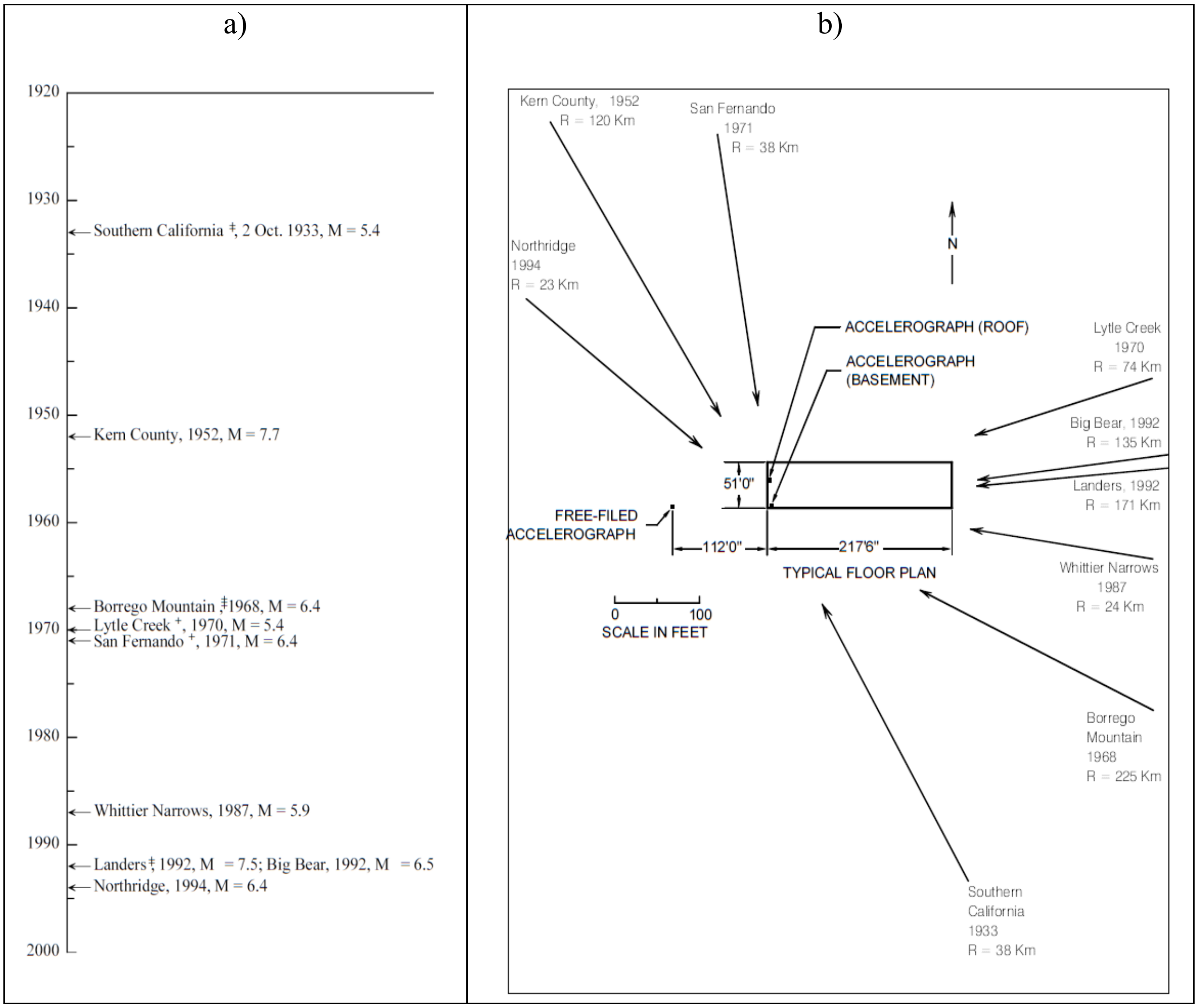

Figure 8.2 - a)- Chronical summary of nine earthquakes for which strong motion data was available for the Hollywood Storage Building (HSB), b) Direction of wave arrival from nine earthquakes recorded in HSB

3. Hao *et al.* (2004) [6]:

The information about the earthquakes recorded by the instrumented building in this study are summarized below:

San Fernando, 9 Feb. 1971, M=6.6
Whittier-Narrows, 1 Oct. 1987, M=5.9
Whittier-Narrows 1st aftershock, 1 Oct. 1987, M=3.8
Whittier-Narrows 3rd aftershock, 1 Oct. 1987, M=4.4
Whittier-Narrows 4th aftershock, 1 Oct. 1987, M=3.5
Whittier-Narrows 5th aftershock, 1 Oct. 1987, M=3.9
Whittier-Narrows 6th aftershock, 1 Oct. 1987, M=3.1
Whittier-Narrows 7th aftershock, 1 Oct. 1987, M=4.0
Whittier-Narrows 9th aftershock, 1 Oct. 1987, M=3.8
Whittier-Narrows 12th aftershock, 4 Oct. 1987, M=5.3
Whittier-Narrows 13th aftershock, 2 Nov. 1987, M=4.7
Sierra Madre, 28 June 1992, M=5.8
Landers, 28 June 1992, M=7.5
Big Bear, 28 June 1992, M=6.5
Northridge 1st aftershock, 17 Jan. 1994, M=5.9
Northridge 392th aftershock, 20 Mar. 1994, M=5.2

4. Todorovska *et al.* (2004 and 2006) [7, 8]:

The information of the seismic events used in this study are as follows:

Event	Date	Time	M_L	Latitude	Longitude	Depth (km)
San Fernando	02/09/1971	06:00	6.6	34 24 42N	118 24 00W	--
Whittier-Narrows	10/01/1987	14:42	5.9	34 03 10N	118 04 34W	14.5
Whittier-Narrows, 12th Aft.	10/04/1987	10:59	5.3	34 04 01N	118 06 19W	13.0
Whittier-Narrows, 13th Aft.	02/03/1988	15:25	4.7	34 05 13N	118 02 52W	16.7
Pasadena	12/03/1988	11:38	4.9	34 08 56N	118 08 05W	13.3
Malibu	01/19/1989	06:53	5.0	33 55 07N	118 37 38W	11.8
Montebello	06/12/1989	16:57	4.4	34 01 39N	118 10 47W	15.6
Upland	02/28/1990	23:43	5.2	34 08 17N	117 42 10W	5.3
Sierra Madre	06/28/1991	14:43	5.8	34 15 45N	117 59 52W	12.0
Landers	06/28/1992	11:57	7.5	34 12 06N	116 26 06W	5.0
Big Bear	06/28/1992	15:05	6.5	34 12 06N	116 49 36W	5.0
Northridge	01/17/1994	12:30	6.7	34 12 48N	118 32 13W	18.4
Northridge, Aft. #1	01/17/1994	12:31	5.9	34 16 45N	118 28 25W	0.0
Northridge, Aft. #7	01/17/1994	12:39	4.9	34 15 39N	118 32 01W	14.8
Northridge, Aft. #9	01/17/1994	12:40	5.2	34 20 29N	118 36 05W	0.0
Northridge, Aft. #100	01/17/1994	17:56	4.6	34 13 39N	118 34 20W	19.2
Northridge, Aft. #129	01/17/1994	20:46	4.9	34 18 04N	118 33 55W	9.5
Northridge, Aft. #142	01/17/1994	23:33	5.6	34 19 34N	118 41 54W	9.8
Northridge, Aft. #151	01/18/1994	00:43	5.2	34 22 35N	118 41 53W	11.3
Northridge, Aft. #253	01/19/1994	21:09	5.1	34 22 43N	118 42 42W	14.4
Northridge, Aft. #254	01/19/1994	21:11	5.1	34 22 40N	118 37 10W	11.4
Northridge, Aft. #336	01/29/1994	11:20	5.1	34 18 21N	118 34 43W	1.1
Northridge, Aft. #392	03/20/1994	21:20	5.2	34 13 52N	118 28 30W	13.1
Hector Mine	10/16/1999	09:46	7.1	34 36 00N	116 16 12W	3.0
West Hollywood	09/09/2001	23:59	4.2	34 04 30N	118 22 44W	3.7

5. Dunand *et al.* (2004, 2005, and 2006) [9-11]:

The information of the seismic events used in this study are as follows:

Event Date	Event Name	Lat. (deg)	Long. (deg)	M	Dist. (km)	Peak Base A (g)	Peak Roof A (g)
09-Feb-71	San Fernando**	34.40	-118.41	6.6	42	0.12	0.18
21-Feb-73	Point Mugu	34.065	-119.035	5.9	82	0.02	0.02
01-Oct-87	Whittier Narrows	34.06	-118.08	6.1	7	0.29	0.27
04-Oct-87	Whittier Narrows Aftershock	34.07	-118.10	5.3*	5	0.14	0.18
11-Feb-88	Whittier Narrows Aftershock	34.08	-118.05	5.0*	10	0.04	0.03
28-Feb-90	Upland	34.14	-117.70	5.2	42	0.02	0.03
28-Jun-91	Sierra Madre	34.26	-118.00	5.8	24	0.13	0.15
28-Jun-92	Landers	34.20	-116.44	7.3	158	0.03	0.12
28-Jun-92	Big Bear	34.20	-116.83	6.5	123	0.02	0.06
17-Jan-94	Northridge	34.21	-118.54	6.7	38	0.16	0.14
20-Mar-94	Northridge Aftershock	34.23	-118.47	5.2*	34	0.03	0.02
16-Oct-99	Hector Mine	34.59	-116.27	7.1	182	0.04	0.10
09-Sep-01	West Hollywood	34.075	-118.379	4.2*	21	0.02	0.008
28-Oct-01	Compton	33.922	-118.270	4.0*	20	0.008	0.003
22-Feb-03	Big Bear City	34.310	-116.848	5.2*	122	0.004	0.006
22-Dec-03	San Simeon	35.71	-121.10	6.5	324	0.004	0.03
01-Oct-87	Whittier Narrows**	34.06	-118.08	6.1	10	0.62	0.53
17-Jan-94	Northridge	34.21	-118.54	6.7	53	0.153	0.241
18-Oct-89	Loma Prieta	37.04	-121.88	6.9	99	0.117	0.233
18-Oct-89	Loma Prieta	37.04	-121.88	6.9	100	0.225	0.341
18-Oct-89	Loma Prieta	37.04	-121.88	6.9	67	0.057	0.148
18-Oct-89	Loma Prieta	37.04	-121.88	6.9	97	0.123	0.312
18-Oct-89	Loma Prieta	37.04	-121.88	6.9	97	0.232	0.49
02-Feb-03	Dublin	34.740	-121.937	3.6*	34	0.005	0.008
17-Jan-94	Northridge	34.21	-118.54	6.7	62	0.06	0.209
17-Jan-94	Northridge	34.21	-118.54	6.7	120	0.061	0.165
17-Jan-94	Northridge	34.21	-118.54	6.7	55	0.061	0.148
28-Jun-92	Landers	34.20	-116.44	7.3	79	0.09	0.36
17-Jan-94	Northridge	34.21	-118.54	6.7	116	0.045	0.243
17-Jan-94	Northridge	34.21	-118.54	6.7	88	0.063	0.188
12-Sep-70	Lytle Creek**	34.27	-117.54	5.2*	56	0.019	0.055
09-Feb-71	San Fernando**	34.40	-118.41	6.6	39	0.20	0.35
03-Sep-02	Yorba Linda	33.917	-117.776	4.8*	40	0.006	0.009
22-Feb-03	Big Bear City	34.310	-116.848	5.2*	119	n/a	0.008
22-Dec-03	San Simeon	35.71	-121.10	6.5	323	0.002	0.008

6. Clinton *et al.* (2006) [12]:

The information of the seismic events used in this study are as follows:

Event/Test
Forced vibrations, 1967
Lytle Creek, 1970, M 6.3, Δ = 57 km
San Fernando, 1971, M 6.6, Δ = 31 km
Forced vibrations, 1974
Whittier Narrows, 1987, M 6.1, Δ = 19 km
Forced vibrations, 1988
Sierra Madre, 1991, M 5.8, Δ = 18 km
Forced vibrations, 1993
Northridge, 1994, M 6.7, Δ = 34 km
Forced vibrations, 1994
Forced vibrations, 1995
Beverly Hills, 2001, M 4.2, Δ = 26 km
Forced vibrations, 2002, full weights
Forced vibrations, 2002, half weights
Big Bear, 2003, M 5.4, Δ = 119 km
Continuous data average, May 2001–Nov. 2003
San Simeon, 2003, M 6.5, Δ = 323 km

7. Boroschek and Lazcano (2008), and Carreño and Boroschek (2011) [13, 14]:

The information of the seismic events used in this study are as follows:

Earthquake Events					
Event	**Mag. Richter**	**Latitude**	**Longitude**	**Peak Ground Acceleration (g)**	**Max Structural Acceleration (g)**
Jan24, 1997	5.3	33°28.1' S	70°47.1' W	0.064	0.140
April 20, 1997	5.3	33°59.7' S	70°28.0' W	0.022	0.050
Jun 19, 1997	5.1	33°09.4' S	70°18.1' W	0.013	0.040
Oct 14, 1997	6.8	30°44.5' S	71°19.7' W	0.024	0.080
Jan 12, 1998	5.9	31°18.8' S	71°25.1' W	0.009	0.046

8.1 Refrences

1. Çelebi, M. *On the variation of fundamental frequency (period) of an undamaged building–a continuing discussion*. in *Proceedings of International conference on Experimental Vibration Analysis for Civil Engineering Structures (EVACES07)*. 2007. Porto, Portugal, October 24-27.
2. Çelebi, M., *Comparison of recorded dynamic characteristics of structures and ground during strong and weak shaking*, in *Increasing Seismic Safety by Combining Engineering Technologies and Seismological Data*. 2009, Springer. p. 99-115.
3. Çelebi, M., L. Phan, and R. Marshall, *Dynamic characteristics of five tall buildings during strong and low-amplitude motions.* The structural design of tall buildings, 1993. **2**(1): p. 1-15.
4. Çelebi, M., *Comparison of damping in buildings under low-amplitude and strong motions.* Journal of wind engineering and industrial aerodynamics, 1996. **59**(2): p. 309-323.
5. Trifunac, M.D., T. Hao, and M. Todorovska, *Response of a 14-story reinforced concrete structure to nine earthquakes: 61 years of observation in the Hollywood storage building*, in *Report CE01-02*. 2001: Department of Civil Engineering, University of Southern California, Los Angeles, California,.
6. Hao, T., M. Trifunac, and M. Todorovska, *Instrumented buildings of University of Southern California—strong motion data, metadata and soil-structure system frequencies*, in *Report CE04-01*. 2004: Department of Civil Engineering, University of Southern California, Los Angeles, California,.
7. Todorovska, M., T. Hao, and M. Trifunac, *Building periods for use in earthquake resistant design codes earthquake response data compilation and analysis of time and amplitude variations*, in *Report CE 04-02*. 2004: Department of Civil Engineering, University of Southern California, Los Angeles, California,.
8. Todorovska, M., M. Trifunac, and T.-Y. Hao, *Variations of apparent building frequencies-lessons from full-scale earthquake observations*, in *1st European conference of earthquake engineering and seismology*. 2006: Geneva, Switzerland, September 3-8.
9. Dunand, F., *Pertinence du bruit de fond sismique pour la caractérisation dynamique et l'aide au diagnostic sismique des structures de génie civil*. 2005, Université Joseph-Fourier-Grenoble: Grenoble, France.
10. Dunand, F., P.-y. Bard, and J. Rodgers, *Comparison of the dynamic parameters extracted from weak, moderate and strong motion recorded in buildings*, in *1st European conference of earthquake engineering and seismology*. 2006: Geneva, Switzerland, September 3-8.
11. Dunand, F., et al., *Ambient vibration and earthquake strong-motion data sets for selected USGS extensively instrumented buildings*. 2004: In USGS Open-File Report 2004-1375.
12. Clinton, J.F., et al., *The observed wander of the natural frequencies in a structure.* Bulletin of the Seismological Society of America, 2006. **96**(1): p. 237-257.

13. Boroschek, R. and P. Lazcano. *Non-damage modal parameter variations on a 22 story reinforced concrete building*. in *International Modal Analysis Conference, IMAC XXVI*. 2008. Orlando, FL.
14. Carreño, R.P. and R.L. Boroschek, *Modal parameter variations due to earthquakes of different intensities*, in *Civil Engineering Topics, Volume 4*. 2011, Springer. p. 321-333.